2014 CNMS USER MEETING
Agenda and Abstracts

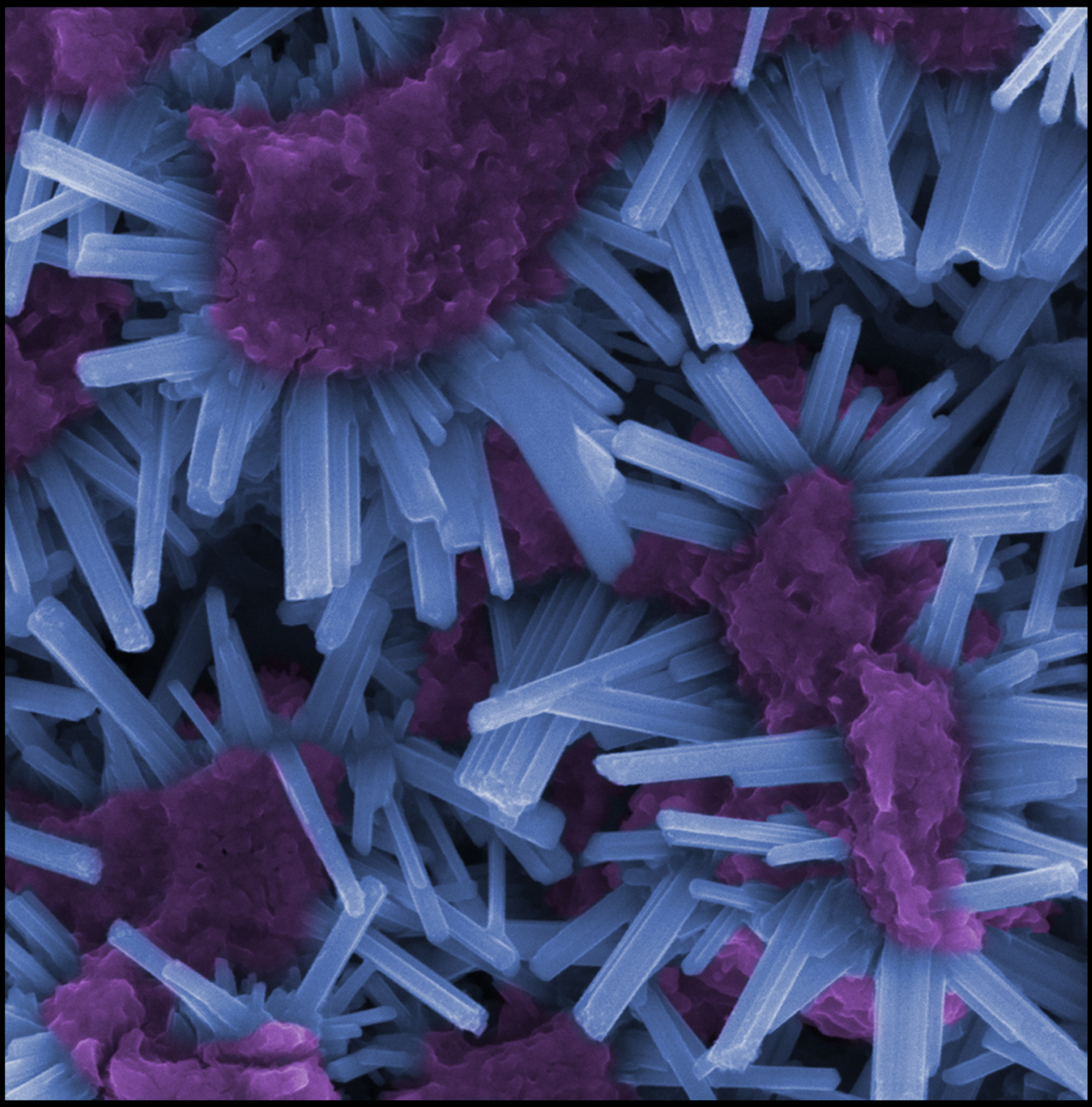

OAK RIDGE National Laboratory | CENTER FOR NANOPHASE MATERIALS SCIENCES

Table of Contents

Denotes Student Poster

Cover Image

by Raymond R. Unocic

SEM image of a Na-Mn Oxide thin film electrode material synthesized using radio frequency magnetron sputtering.

This material is being evaluated as an electrode material for sodium ion battery applications.

NOTE:
The Abstract Book is available online only. A printed copy will not be included in the handout material.

OAK RIDGE National Laboratory
CENTER FOR NANOPHASE MATERIALS SCIENCES

Agenda

2014 CNMS User Meeting
Oak Ridge National Laboratory
Oak Ridge, Tennessee

4:00p	**Tuesday, September 16**	**Poster Session and Student Poster Competition** - SNS Atrium and C-152
5:45	The 8th edition of ***RidgeDance NanoScience Film Festival*** – SNS Auditorium	
7:30a	**Wednesday, September 17**	**Registration Opens** - Posters available for viewing
	PLENARY SESSION *Iran Thomas Auditorium, SNS* **Chair**: Hans Christen, CNMS Director	
8:00	**Welcome and Announcements**	
8:20	"Hierarchical 3-D Nano-Architectures for Biomimetics, Batteries, and Lightweight Structural Materials" **Julia Greer,** *California Institute of Technology*	
9:05	"Accelerated Materials Discovery by Combining High-Throughput Computation and Experiments" **Gerbrand Ceder**, Mas*sachusetts Institute of Technology*	
9:50	**Break**	
	New Capabilities for Users at CNMS	**Chair**: Vivek Prabhu, NIST
10:10	"Analysis and Visualization Strategies for Large Data Sets," **Alex Belianinov**	
10:25	"Probing Magnetism with an Electron Microscope," **Juan Carlos Idrobo**	
10:40	"Advanced Atom Probe Tomography for Nanoscience Applications," **Jonathan Poplawsky**	
10:55	"Beam-Induced Direct Writing of Nanostructures using the CNMS Helium-Ion Microscope," **Adam Rondinone**	
11:10	**Panel Session: Q&A with CNMS Senior Staff**	
11:30	**User Group Town Hall Meeting** *including announcement of Student Poster Award winners*	
12:00p	**Lunch on your own; Posters available for viewing**	

	Track A (CLO, C-156) **Chairs:** Martyn McLachlan and Megan Robertson	**Track B (Auditorium)** **Chairs:** Anthony Hmelo and Ray Unocic
1:30	**INVITED:** "Tuning Interactions at Melt/Brush Interfaces for Functional Polymer Films," **Gila Stein** (U. Houston)	**INVITED:** "Characterizing Interfacial Effects in Ferro-Electric Thin Films using Aberration-Corrected STEM," **Robert Klie** (U. Illinois, Chicago)
2:00	"*In-Situ* Study of Phase Transitions and Morphological Evolution in Solution-Processed Bilayer Organometal Halide Perovskite Photovoltaic Cells," **Bin Yang** (CNMS)	"Studies on Multiferroic and Magnetoelectric Properties of Pb(Fe0.5Nb0.5)O3 and Pb(Fe0.5Nb0.5)O3/ Ni0.65Zn0.35Fe2O4 Heterostructures," **Dhiren Pradhan** (U. Puerto Rico)
2:20	"Rapid and Sensitive Detection/Diagnosis of Pathogens," **Cheng Cheng** (U. Tennessee)	"Dielectric Meta-Reflectarray for Broadband Linear Polarization Conversion and Optical Vortex Generation," **Yuanmu Yang** (Vanderbilt U.)
2:40	"A Bridge Between DNA Nanotechnology and Inorganic Nanotechnology," **Liqian Wang** (U. Rome Tor Vergata)	"Air-Stable, Lithium Superionic Conductors," **Gayatri Sahu** (CNMS)
3:00	**Break**	
3:20	**INVITED:** "Crafting Functional Nanocrystals by Capitalizing on Nonlinear Block Copolymers as Nanoreactors," **Zhiqun Lin** (Georgia Tech)	**INVITED:** "Controllable Complex Oxide Heterointerface," **Ying-hao (Eddie) Chu** (National Tsing-Hua U.)
3:50	"Detection of Aflatoxin B1 by Aptamer-Based Biosensor using PAMAM Dendrimers as Immobilization Platform," **Katia Spinella** (U. Rome Tor Vergata)	"Electronic Properties of Bilayer Graphenes Strongly Coupled to Interlayer Stacking and the External Field," **Changwon Park** (CNMS)
4:10	"Symbiotic Relation in Bimetallic Ag Nanoparticles," **Abhinav Malasi** (U. Tennessee)	"Electronic Properties of Rhenium Doped Tungsten Disulfide Monolayers," **Eduardo Cruz-Silva** (Pennsylvania State U.)
4:30	"Line-focused Femtosecond Laser Machining of Fused Silica," **Brian Canfield** (U. Tennessee Space Institute)	"Controlled Vapor-Phase Growth of Photoresponsive Two-Dimensional GaSe Crystals and Van der Waals Heterostructures," **Xufan Li** (CNMS)
4:50	"Volumetric Durable Superhydrophobic Coatings," **John Simpson** (U. Tennessee)	"Origins of Electromechanical Strain Ascertained from in situ X-ray and Neutron Diffraction," **Jacob Jones** (North Carolina State U.)
5:10	**Adjourn**	

Center for Nanophase Materials Sciences
2014 User Meeting
Poster Session

**denotes Student Poster*

Tuesday, September 16, 2014
4:00 – 5:00p

Poster Locations
Main Hallway: 01-46, and
Room C152: 47-54

Posters will also be available for viewing on Wednesday, September 17

01. *Wicking nanopillar arrays with dual roughness for selective transport and fluorescence measurements
Jennifer J. Charlton,[1, 2] Nickolay Lavrik,[3], James A. Bradshaw,[2,1] Michael J. Sepaniak[1*]
[1]The University of Tennessee Knoxville, Department of Chemistry, Knoxville, Tennessee 37996
[2]Y-12 National Security Complex, Analytical Chemistry Organization, Oak Ridge, Tennessee 37830
[3]Center for Nanophase Material Sciences, Oak Ridge National Laboratory, Oak Ridge, Tennessee 37830

02. *Fabrication of microfluidic chips with a pressure actuation system for *in vivo* studies of cellular organization
Da Yang,[1] Ryan Hefti,[1] Scott Retterer,[2] Jaan Männik[1]
[1]Department of Physics and Astronomy, University of Tennessee, Knoxville, TN
[2]Center for Nanophase Materials Sciences, Oak Ridge National Laboratory

03. *Capillary driven transport and dispersion in hierarchically porous phases formed by conformal deposition of petal like carbon on silicon pillar arrays
Danielle Lincoln
M. J. Sepaniak's Group, Department of Chemistry, University of Tennessee, Knoxville, TN

04. *Highly Sensitive Dopamine Sensor Based on Vertically-aligned Pristine Carbon Nanotube Sheathed Niobium Microelectrodes
Cheng Yang and B. Jill Venton
University of Virginia

05. *Vertically Aligned Carbon Nanofiber Embedded Biosensor Platform for Electric Cell Impedance Measurement System
Khandaker A. Mamun,[1] Yongchao Yu,[1] Dale Hensle,[2] Ivan Kravchenco,[2] Nicole McFarlane[1]
[1]Department of Electrical Engineering and Computer Science, University of Tennessee, Knoxville, TN 37996
[2]Center for Nanophase Materials Sciences, Oak Ridge National Laboratory

06. *Noise Analysis of Confined Cell-free Protein Production
Patrick Caveney,[1] Liz Norred,[2] Jonathan Boreyko,[2] Charles Chin,[2] Jason Fowlkes,[3] Pat Collier,[3] Mitch Doktycz,[2,3] Mike Simpson[3]
[1]Bredesen Center, University of Tennessee, Knoxville, TN 37996
[2]Biosciences Division, University of Tennessee, Knoxville, TN 37996
[3]Center for Nanophase Materials Sciences, Oak Ridge National Laboratory

07. *Silicon Photonics for Biosensing and Reconfigurable Photonics Applications
Petr Markov
Vanderbilt University

08. *Surface Polarization Enhanced Seebeck Effects in Vertical Multi-layer Metal/Dielectric/Polymer/Metal thin-film devices

Qing Liu,[1] Hongfeng Wang,[1] Yu-Che Hsiao,[1] Xsin Wang,[2] Bin Hu[1*]
[1]Department of Materials Science and Engineering, University of Tennessee, Knoxville, Tennessee, 37996
[2]Oak Ridge National Laboratory, Oak Ridge, TN 37831, USA

09. *Laser Induced Instabilities and Pattern Formation in Ultrathin Metal films under Water-Glycerol Solutions

S. Yadavali,[1] R. Kalyanaraman[1,2]
[1]Department of Chemical and Biomolecular Engineering, University of Tennessee, Knoxville, Tennessee, 37996
[2]Department of Materials Science and Engineering, University of Tennessee, Knoxville, Tennessee, 37996

10. *Realization of All-Dielectric Metamaterial Perfect Reflector

Parikshit Moitra,[1] Brian A. Slovick,[2] Zhi Gang Yu,[2] S. Krishnamurthy,[2] and Jason Valentine[3*]
[1]Interdisciplinary Materials Science Program, Vanderbilt University, Nashville, Tennessee 37212, USA
[2]Applied Optics Laboratory, SRI International, Menlo Park, CA 94015
[3]Department of Mechanical Engineering, Vanderbilt University, Nashville, Tennessee 37212, USA

11. *EELS Imaging for Quantitative Phase Fraction Mapping in OPV Materials

Ondrej Dyck,[1] Sheng Hu,[2] Bamin Khomami,[2] and Gerd Duscher[1]
[1]Materials Science and Engineering, University of Tennessee, Knoxville, Tennessee, 37996
[2]Chemical and Biomolecular Engineering, University of Tennessee, Knoxville, Tennessee, 37996

12. *Controlling Solar Cell Active Layers via Surface Modification and Gas Expanded Polymer Annealing

Sarah Russell,[†‡] Holly Stretz,[*†] Mark Dadmun,[I∆] S. Michael Kilbey II,[I§] and Zach Seibers[J]
[†]Department of Chemical Engineering, Tennessee Technological University, Cookeville, Tennessee, 38505
[‡]Center for Manufacturing Research, Tennessee Technological University, Cookeville, Tennessee 38505
[I]Department of Chemistry, University of Tennessee, Knoxville, Tennessee 37996, United States
[J]Department of Energy Science and Engineering, University of Tennessee, Knoxville, TN 37996
[∆]Chemical Sciences Division, Oak Ridge National Laboratory, Oak Ridge, Tennessee 37831
[§]Department of Chemical and Bimolecular Engineering, University of Tennessee, Knoxville, TN 37996

13. *Underlying Mechanism of the Enhanced Power Conversion Efficiency of Organic Inverted Solar Cell

Sanjib Das,[1] Jong K. Keum,[2,3] James F. Browning,[3] Jihua Chen,[2] Changwoo Do,[3] Gong Gu,[1] Pooran C. Joshi,[4] Adam J. Rondinone,[2] Kunlun Hong,[2] David B. Geohegan,[2] Kai Xiao[2]
[1]Department of Electrical Engineering and Computer Science, University of Tennessee, Knoxville, TN, 37996, USA.
[2]Center for Nanophase Materials Sciences, Oak Ridge National Laboratory, Oak Ridge, TN, 37831, USA.
[3]Neutron Scattering Science Divisions, Oak Ridge National Laboratory, Oak Ridge, TN, 37831, USA.
[4]Material Sciences and Technology Division, Oak Ridge National Laboratory, Oak Ridge, TN, 37831, USA

14. *Experimental Studies on Properties of Photoexcited Excitons and Charge Dissociation Processes in $CH_3NH_3PbI_{3-x}Cl_x$ Perovskite Solar Cells

Yu-Che Hsiao, Ting Wu, Mingxing Li, Ilia Ivanov, Bin Hu
Department of Materials Science and Engineering, University of Tennessee, Knoxville, Tennessee, 37996

15. *Unravelling the Spin-Dependent Excited States in Organo-Metal Halide Perovskite

Ting Wu,[1] Yu-Che Hsiao,[1] Mingxing Li,[1] Nam-Goo Kang,[2] Jimmy W. Mays,[2] Bin Hu[1*]
[1]Department of Materials Science and Engineering, University of Tennessee, Knoxville, Tennessee, 37996
[2]Department of Chemistry, University of Tennessee, Knoxville, Tennessee, 37996

16. *In-situ High Temperature X-ray Diffraction Study of Formation of the Thin Film PV Absorbers $(Cu_xAg_{1-x})(In_xGa_{1-x})Se_2$ and Cu_2ZnSnS_4

H. Tong,[1] C. Muzzillo,[1] S. Wilson,[1] J. Keum,[2] A. Rondinone,[2] K. More[3], L. Pogue,[4] A. Rockett,[4] S. Soltanmohommad,[5] W. N. Shafarman,[5] T. J. Anderson,[1]

[1]Department of Chemical Engineering, University of Florida, Gainesville, FL 32611

[2]Center for Nanophase Materials Sciences, Oak Ridge National Laboratory, Oak Ridge, TN, 37831

[3]Materials Sciences and Technology Division, Oak Ridge National Laboratory, Oak Ridge, TN, 37831

[4]Department of Materials and Engineering, University of Illinois at Urbana-Champaign,61801

[5]Institute of Energy Conversion, University of Delaware, Newark, DE, 19716

17. *In-situ investigation of chemical bath deposition of CdS via localized surface plasmon resonance (LSPR) spectroscopy

H. Taz,[1] R. Ruther,[2] A. Malasi,[3] S. Yadavali,[3] C. Carr,[4] J. Nanda,[2] R. Kalyanaraman[3,4]

[1]Bredesen Center, University of Tennessee, Knoxville, TN 37996

[2]Materials Science and Technology Division, Oak Ridge National Laboratory , Oak Ridge, TN 37831

[3]Department of Chemical and Biomolecular Engineering, University of Tennessee, Knoxville, TN 37996

[4]Department of Materials Science and Engineering, University of Tennessee, Knoxville, TN 37996

18. *Junction size dependence of tunneling electroresistance effect in e-beam patterned $BaTiO_3$ ferroelectric tunnel junctions

Amit V. Singh,[1] M. Althammer,[1] K. Rott,[2] G. Reiss,[2] A. Gupta[1]

[1]Center for Nanophase Materials Sciences, Oak Ridge National Laboratory, Oak Ridge, TN, 37831

[2]Thin Films and Physics of Nanostructures, Department of Physics and Center for Spinelectronic Materials and Devices, Bielefeld University, 33615 Germany

19. *Skyrmionic MnSi nanowires on Si: SiO2 layer as a catalyst assistant for the CVD growth

Siwei Tang,[1,2] Ivan Kravchenko,[1] Jieyu Yi,[1,2] Guixin Cao,[1,2] Jane Howe,[1] David Mandrus,[2] and Zheng Gai[1]

[1]Center for Nanophase Materials Sciences, Oak Ridge National Laboratory, Oak Ridge, TN 37831

[2]Department of Materials Science and Engineering, University of Tennessee, TN 37996

20. *Oscillatory local density of states on $Cr_{1/3}NbS_2$ surface

Jieyu Yi,[1,2] Siwei Tang,[1,2] Ling li,[1] Guixin Cao,[2] David Mandrus,[1] and Zheng Gai[2]

[1]Department of Materials Science and Engineering, University of Tennessee, TN 37996

[2]Center for Nanophase Materials Sciences, Oak Ridge National Laboratory, Oak Ridge, TN 37831

21. *A Study of Formation Mechanism of Mn Containing Precipitates during Homogenization in 6xxx Series Aluminum Alloys

Gongwang Zhang,[1] Yi Han,[2] Yi Xu,[2] Hiromi Nagaumi,[2] Sha Gang,[3] Chad M. Parish,[4] Donovan N. Leonard,[4] and Tongguang Zhai[1]

[1]Department of Chemical and Materials Engineering, University of Kentucky, Lexington, KY 40506, USA

[2]Suzhou Research Institute for Nonferrous Metals, Suzhou, Jiangsu 215026, China

[3]School of Materials Science and Engineering, Nanjing University of Science and Technology, Nanjing, Jiangsu, 210094, China

[4]Microscopy Group, Materials Science & Technology Division, Oak Ridge National Laboratory, Oak Ridge, TN 37831, USA

22. *Quantitative Understanding 3-D Effects of Constituent Particles on Fatigue Crack Initiation in High Strength Aluminum Alloys by FIB

Yan Jin,[1] Pei Cai,[1] Wei Wen,[1] Chad M Parish,[2] Donovan N. Leonard,[2] and Tongguang Zhai[1]

[1]Chemical and Materials Engineering Department, University of Kentucky, Lexington, KY 40506

[2]Center for Nanophase Materials Sciences, Oak Ridge National Laboratory, Oak Ridge, TN 37831

23. *Entropic Softening of Graphene

Ryan Nicholl

Vanderbilt University

24. *Structure modification of TiO_2 nanoparticles for photocatalysis

Mengkun Tian

University of Tennessee, TN 37996

25. *Phase Stability and Ultrafast Response of Vanadium Dioxide Nanoparticles

R. E. Marvel,[1] C. L. McGahan,[1] A. Boulesbaa,[2] S. T. Retterer,[2] and R. F. Haglund, Jr.[1]
[1]Department of Physics and Astronomy, Vanderbilt University, Nashville, TN
[2]Center for Nanophase Materials Sciences, Oak Ridge National Laboratory, Oak Ridge, TN 37831

26. *Spontaneous pillar-matrix nanostructure and interface strain in epitaxial $La_{2/3}Sr_{1/2}MnO_3$: ZrO_2 thin films

Yuze Gao,[1,2] Guixin Cao,[3,4] Kepeng Song,[5] Kui Du,[5] Jincang Zhang[1]
[1]Department of Physics, Shanghai University, Shanghai 200444, PR China
[2]Max Planck Institute for Solid State Research, Heisenbergstrasse 1, Stuttgart D-70569, Germany
[3]Center for Nanophase Materials Sciences, Oak Ridge National Laboratory, Oak Ridge, TN 37831, USA
[4]Department of Materials Science and Engineering, University of Tennessee, Knoxville, TN 37996, USA
[5]Shenyang National Laboratory for Materials Science, Institute of Metal Research, Chinese Academy of Science, Shenyang 110016, Liaoning, PR China

27. *Direct Deposition of Ferroelectric PZT Films on Glass and Polymer Substrates

S. J. Brewer,[1] T. C. Field,[1] P. C. Joshi,[2] and N. Bassiri-Gharb[1,3]

[1]G.W. Woodruff School of Mechanical Engineering, Georgia Institute of Technology Atlanta, GA 30332-0405, USA
[2]Materials Science and Technology Division, Oak Ridge National Laboratory Oak Ridge, TN 37831-6083, USA
[3]School of Materials Science and Engineering, Georgia Institute of Technology Atlanta, GA 30332-0245, USA

28. *Study of Ionic Dynamics in Nanostructured Ceria through Lateral Electrochemical Measurements and Finite Element Modeling

J. Ding,[1] E. Strelcov,[2] S. Kalinin,[2] and N. Bassiri-Gharb[1,3]
[1]Department of Materials Science and Engineering, Georgia Institute of Technology, Atlanta, GA, 30332
[2]Institute for Functional Imaging of Materials and Center for Nanophase Materials Science, Oak Ridge National Laboratory, Oak Ridge, TN, 37831
[3]G. W. Woodruff School of Mechanical Engineering, Georgia Institute of Technology, Atlanta, GA, 30332

29. *Non-Volatile Ferroelectric Memories from CdS Nanoparticles-P(VDF-TrFE) Nanocomposite Films

Saman Salemizadeh Parizi, Daniela Caruntu, and Gabriel Caruntu
Department of Chemistry and Science of Advanced Materials Program, Central Michigan University, Mt. Pleasant, MI 48858, USA

30. Quantum transport simulations in carbon nanoring devices with low-energy phonon scattering

Mark A. Jack
Florida A&M University, Physics Department, Tallahassee, FL 32307

31. Modeling of a pH responsive weak polyelectrolyte brush using SCFT

Jyoti Prakash Mahalik, Rajeev Kumar and Bobby Sumpter
Center for Nanophase Materials Sciences, Oak Ridge National Laboratory, Oak Ridge, TN 37831, USA

32. Controlling the Topology of Polymers to Tune Their Properties

Mi Zhou,[1,2] Heng Wang,[1] Xiaolong Jiang,[1] Kunlun Hong,[2] Xin Qian[1]
[1]College of Materials Science and Engineering, Zhejiang University of Technology, Hangzhou, Zhejiang 310012
[2]Center for Nanophase Materials Sciences, Oak Ridge National Laboratory, Oak Ridge, TN 37831, USA

33. New CO_2 Responsive Macromolecular Nanomaterials

Balaka Barkakaty
Center for Nanophase and Materials Sciences, Oak Ridge National Laboratory, Oak Ridge, TN 37831

34. Synthesizing Deuterated Soft Materials

Peter V. Bonnesen, Kunlun Hong, Jun Yang
Center for Nanophase and Materials Sciences, Oak Ridge National Laboratory, Oak Ridge, TN 37831

35. Temperature Gradient Interaction Chromatography: An inside look at the heterogeneity of multigraft polymers

Chelsea N. Widener,[1] Deanna L. Pickel[2] and David W. Uhrig[2]
[1]Wesleyan College, Macon, GA 30467
[2]Center for Nanophase and Materials Sciences, Oak Ridge National Laboratory, Oak Ridge, TN 37831

36. Manipulating Nanoscale Morphology by P3HT/PLA Molecular Bottlebrushes: Synthesis, Aggregation and Self-Assembly

Suk-kyun Ahn
Center for Nanophase and Materials Sciences, Oak Ridge National Laboratory, Oak Ridge, TN 37831

37. Dynamics of Confined Flexible and Unentangled Polymer Melts in Highly Adsorbing Cylindrical Pores

Jan-Michael Carrillo[1] and Bobby Sumpter[2,3]
[1]National Center for Computational Sciences, Oak Ridge National Laboratory, Oak Ridge, Tennessee 37831, USA
[2]Center for Nanophase Materials Sciences, Oak Ridge National Laboratory, Oak Ridge, Tennessee 37831, USA
[3]Computer Science and Mathematics Division, Oak Ridge National Laboratory, Oak Ridge, Tennessee 37831, USA

38. Molecular Engineering of 3-Alkylthiophene Polymers

Youjun He, Jihua Chen, Kai Xiao, Ming Shao, Jong Keum, Kunlun Hong
Center for Nanophase Materials Sciences, Oak Ridge National Laboratory, Oak Ridge, Tennessee 37831, USA

39. Overview of the CNMS User Proposal Process and Keys to Success

Tony Haynes and Viviane Schwartz
Center for Nanophase Materials Sciences, Oak Ridge National Laboratory, Oak Ridge, Tennessee 37831, USA

40. Optically Tunable Spin-exchange Energy at Donor:Acceptor Interfaces in Organic Solar Cells

Mingxing Li,[1] Hongfeng Wang,[1] Lei He,[1] Hengxing Xu,[1] Zheng Gai[2] and Bin Hu[1]
[1]Department of Materials Science and Engineering, University of Tennessee, Knoxville, TN 37996, USA
[2]Center for Nanophase Materials Sciences, Oak Ridge National Laboratory, Oak Ridge, Tennessee 37831, USA

41. Microfluidic Modules for Isolation of Recombinant Cytokine from Bacterial Lysates

Larry J. Millet,[1] Scott T. Retterer[2] and Mitchel J. Doktycz[1,2]
[1]Biosciences Division, Oak Ridge National Laboratory, Oak Ridge, Tennessee 37831, USA
[2]Center for Nanophase Materials Sciences, Oak Ridge National Laboratory, Oak Ridge, Tennessee 37831, USA

42. X-ray and neutron studies on hard $L1_0$ FePt(001)/soft CoFeB bilayers

Sin-Yong Jo,[1] Hyeok-Cheol Choi,[1] Chun-Yeol You,[1] Haile Ambaye,[2] Valeria Lauter,[2] Jong Kahk Keum,[2] Raymond R. Unocic,[2] Kyujoon Lee,[3] Myung-Hwa Jung,[3] J. Y. Gu,[4] Ki-Yeon Kim[5*]
[1]Department of Physics, Inha University, Incheon 402-751, Republic of Korea
[2]Oak-Ridge National Laboratory, Oak-Ridge, TN 37831, USA
[3]Department of Physics, Sogang University, Seoul 121-742, Republic of Korea
[4]Department of Physics and Astronomy, California State University-Long Beach, CA 90840, USA
[5]Neutron Science Division, KAERI, Daejeon 303-353, Republic of Korea

43. Electro-Optical Properties of Self-assembled Metal-Chalcogenide Nanoparticles

Christopher B. Jacobs,[1] Gyoung Gug Jang,[2] David E. Graham,[2] Pooran C. Joshi,[3] Ji-Won Moon,[2] Ilia N. Ivanov[1]
[1]Center for Nanophase Materials Sciences, Oak Ridge National Laboratory, Oak Ridge, TN, 37931
[2]Biosciences Division, Oak Ridge National Laboratory, Oak Ridge, TN, 37931
[3]Materials Science and Technology Division, Oak Ridge National Laboratory, Oak Ridge, TN, 3793

44. Tailoring of a metastable material: alpha-FeSi2 thin film

Guixin Cao,[1] D. J. Singh,[2] Xiaoguang Zhang,[1] German Samolyuk,[2] Liang Qiao,[1] G.M. Stocks,[2] and Zheng Gai,[1*]
[1]Center for Nanophase Materials Sciences, Oak Ridge National Laboratory, Oak Ridge, TN, 37931
[2]Materials Science and Technology Division, Oak Ridge National Laboratory, Oak Ridge, TN, 37931

45. Unusual strain-lattice behavior in Sr-doped La2CuO4 thin film

Jaekwang Lee,[1] Lu Jiang,[2] Tricia Meyer,[2] Ho Nyung Lee,[2] and Mina Yoon[1]
[1]Center for Nanophase Materials Sciences, Oak Ridge National Laboratory, Oak Ridge, TN, 37931
[2]Materials Science and Technology Division, Oak Ridge National Laboratory, Oak Ridge, TN, 37931

46. Discovery, Understanding and Validation of Functional Materials Using Novel Computational Methods

Panchapakesan Ganesh
Center for Nanophase Materials Sciences, Oak Ridge National Laboratory, Oak Ridge, TN, 37931

47. Controlled Molecular Growth via Metal-ion Induced Orbital Hybridization of Metal Phthalocyanine on Deactivated Si Surfaces

Bing Huang,[1] Changwon Park,[1] Sean Wagner,[2] Jiagui Feng,[2] Pengpeng Zhang,[2] and Mina Yoon[1]
[1]Center for Nanophase Materials Sciences, Oak Ridge National Laboratory, Oak Ridge, TN, 37931
[2]Department of Physics and Astronomy, Michigan State University, East Lansing, Michigan 48823, U.S.A

48. Understanding the Role of Ultrasmall Nanoparticles as Nanoscale Building Blocks for Mesoscale Architectures

M. Mahjouri-Samani,[1*] M. Tian,[3] K. Wang,[1] A. A. Puretzky,[1] C. M. Rouleau,[1] G. Eres,[2] M. Yoon,[1] K. L. More,[1] M. Chi,[1] G. Duscher,[2,3] D. B. Geohegan[1]
[1]Center for Nanophase Materials Sciences, Oak Ridge National Laboratory, Oak Ridge, TN
[2]Materials Science and Technology Division, Oak Ridge National Laboratory, Oak Ridge, TN
[3]Department of Materials Science and Engineering, University of Tennessee, Knoxville, TN

49. Two-dimensional Layered Materials of ZnX and CdX

Jia Zhou, Jingsong Huang, Bobby G. Sumpter
Center for Nanophase Materials Sciences, Oak Ridge National Laboratory, Oak Ridge, TN, 37931

50. Growth and Optical properties of Two-Dimensional Transition Metal Dichalcogenides: WS2 and WSe2 Monolayers

Kai Wang,[1] Masoud Mahjouri-Samani,[1] Ming-Wei Lin,[1] Mengkun Tian,[2] Abdelaziz Boulesbaa,[1] Alexander Puretzky,[1] Christopher Rouleau,[1] Gerd Duscher,[2] Kai Xiao,[1] David Geohegan[1]
[1]Center for Nanophase Materials Sciences, Oak Ridge National Laboratory, Oak Ridge, Tennessee 37831,USA
[2]Department of Materials Science and Engineering, University of Tennessee, Knoxville, Tennessee, 37996, USA

51. Theoretical discovery of two-dimensional SiP alloys for energy conversion applications

Bing Huang, Mina Yoon, and Bobby Sumpter
Center for Nanophase Materials Sciences, Oak Ridge National Laboratory, Oak Ridge, Tennessee 37831,USA

52. Ultrafast spectroscopy and microscopy of exciton dynamics in two-dimensional materials and heterostructures

Abdelaziz Boulesbaa*, Kai Wang, Masoud Mahjouri-Samani, Christopher Rouleau, Kai Xiao, Bing Huang, Mina Yoon, Bobby Sumpter, Alexander Puretzky, and David Geohegan
Center for Nanophase Materials Sciences, Oak Ridge National Laboratory, Oak Ridge, Tennessee 37831,USA

53. Adsorption of a Hydrogen Atom on a Graphene Flake Examined with a Quantum Trajectory/Electronic Structure Dynamics

Lei Wang,[1] Sophya Garashchuk,[1] Jacek Jakowski,[2] Bobby Sumpter[3,4]
[1]Department of Chemistry and Biochemistry, University of South Carolina, Columbia, SC 29208
[2]National Institute of Computational Sciences, University of Tennessee, Oak Ridge, TN 37831
[3]Center for Nanophase Materials Sciences, Oak Ridge, TN 37831
[4]Computer Science and Mathematics Division, Oak Ridge National Laboratory, Oak Ridge, TN 37831

54. Thickness Dependence of Electrical Transport in Few-Layer Two-Dimensional Crystals

Ming-Wei Lin,[1] Ivan Kravchenko,[1] Jason Fowlkes,[1] Jiaqiang Yan,[2] Xufan Li,[1] Alexander A. Puretzky,[1] Christopher M. Rouleau,[1] David Mandrus,[2] David Geohegan,[1] and Kai Xiao[1*]
[1]Center for Nanophase Materials Sciences, Oak Ridge National Laboratory, Oak Ridge, Tennessee 37831,USA
[2]Department of Materials Science and Engineering, University of Tennessee, Knoxville, Tennessee, 37996, USA

Plenary Session

2014 User Meeting

Hierarchical 3-D Nano-Architectures for Biomimetics, Batteries, and Lightweight Structural Materials

J.R. Greer
[1]*California Institute of Technology*

Creation of extremely strong yet ultra-light materials can be achieved by capitalizing on the hierarchical design of 3-dimensional nano-architectures. Such structural meta-materials exhibit superior thermomechanical properties at extremely low mass densities (lighter than aerogels), making these solid foams ideal for many scientific and technological applications. The dominant deformation mechanisms in such "meta-materials", where individual constituent size (nanometers to microns) is comparable to the characteristic microstructural length scale of the constituent solid, are essentially unknown. To harness the lucrative properties of 3-dimensional hierarchical nanostructures, it is critical to assess mechanical properties at each relevant scale while capturing the overall structural complexity.

We present the fabrication of 3-dimensional nano-lattices whose constituents vary in size from several nanometers to tens of microns to millimeters. We discuss the deformation and mechanical properties of a range of nano-sized solids with different microstructures deformed in an *in-situ* nanomechanical instrument. Attention is focused on the interplay between the internal critical microstructural length scale of materials and their external limitations in revealing the physical mechanisms which govern the mechanical deformation, where *competing material- and structure-induced size effects* drive overall properties.

We focus on the deformation and failure in metallic, ceramic, and glassy nano structures and discuss size effects in nanomaterials in the framework of mechanics and physics of defects. Specific discussion topics include: fabrication and characterization of hierarchical 3-dimensional architected meta-materials for applications in biomedical devices, ultra lightweight batteries, and damage-tolerant cellular solids, nano-mechanical experiments, flaw sensitivity in fracture of nano structures.

Accelerated Materials Discovery by Combining High-Throughput Computation and Experiments

Gerbrand Ceder

Massachusetts Institute of Technology

Abstract not yet available

New Capabilities for Users at CNMS

2014 User Meeting

Analysis and Visualization Strategies for Large Data Sets

Alex Belianinov
Center for Nanophase Materials Sciences, Oak Ridge National Laboratory

Multimodal measurements and collection of multidimensional data sets have opened new avenues in areas of STEM and SPM; where execution was typically hampered by software and hardware inadequacies. While collecting, transferring and storing the data is becoming relatively easy, processing the newly acquired information in a way to extract novel physical insight remains to be a challenge.

The underlying data processing principle - analysis of structure factors, or equivalently two point correlation function averaged over probing volume – remained invariant since the early days of Braggs, but the direct use of these methods is too constricting to accommodate additional information afforded by Big Data.

We demonstrate an approach based on the multivariate statistical analysis of the coordination spheres of individual atoms to reveal preferential structures and symmetries. Our method takes advantage of the high veracity imaging afforded by latest generation of instrumentation, as well as tailored, scalable algorithms capable of handling multidimensional data sets. The underlying mechanism for this analysis is for each atom, *i*, laying on the lattice site with indices (*l, m*), we construct a near coordination sphere as a vector $\mathbf{N}_i = (x_1,..,x_8)$, where (x_j, y_{j+1}) is the radius-vector to *j/2*-th nearest neighbor. Once the set of $\mathbf{N}_i$ vectors is assembled, its statistical properties are analyzed though cluster analysis and other various multivariate methods. Both, main and secondary lattices can be analyzed individually or in unison. Our findings map out underlying phase separation, lattice irregularities, coordination number changes and other surface properties for large families of materials including $La_{0.7}Sr_{0.3}MnO_3$, $BiFeO_3$ and $LaCoO_3$. Furthermore breakdown analysis of different lattice distortions sheds insight into surface physics.

Probing magnetism with an electron microscope

Juan Carlos Idrobo
Center for Nanophase Materials Sciences
Oak Ridge National Laboratory

In this talk I will present direct experimental measurements that show that aberrated probes, in aberration-corrected scanning transmission electron microscopes (STEM), can have tails with a phase distribution that plays an analogous role as polarization in X-rays synchrotrons. These novel electron probes can be utilized to filter out chiral dichroic signals in materials via electron energy-loss spectroscopy (EELS). In particular, I will show that an aberrated electron probe with a customized phase distribution can reveal, with atomic resolution, the checkerboard antiferromagnetic ordering of Mn moments in LaMnAsO. The novel experimental setup presented here, which is now available in CNMS' Nion UltraSTEM^{TM} 100 aberration-corrected STEM, opens new paths for probing dichroic signals in materials with unprecedented spatial resolution.

Advanced Atom Probe Tomography for Nanoscience Applications

Jon Poplawsky
Center for Nanophase Materials Sciences, Oak Ridge National Laboratory

Atom probe tomography (APT) is currently the highest resolution technique capable of identifying the atomic composition of all elements in a material with a sensitivity that can exceed 10 ppm. Since the inception of the three dimensional atom probe (3DAP) in 1986, APT has been primarily used for studying metals due to the conductivity of these specimens. The introduction of state-of-the-art local electrode atom probes (LEAP) with laser pulsing capabilities in 2005 has revolutionized the ability to study materials beyond metallic alloys, e.g., semiconductors and insulating materials, whereby the position and elemental identity of atoms within a given volume of a solid can be determined. The LEAP at ORNL has recently been acquired by the Center for Nanophase Material Sciences, creating opportunities for new and exciting research possibilities within the CNMS. A brief overview of the capabilities, operation, and limitations of the LEAP technique will be discussed. Also, an example application involving the identification of elemental segregation within CdTe grain boundaries and the CdS/CdTe pn-junction of CdTe solar cell devices using APT will be presented, as shown in Figure 1.

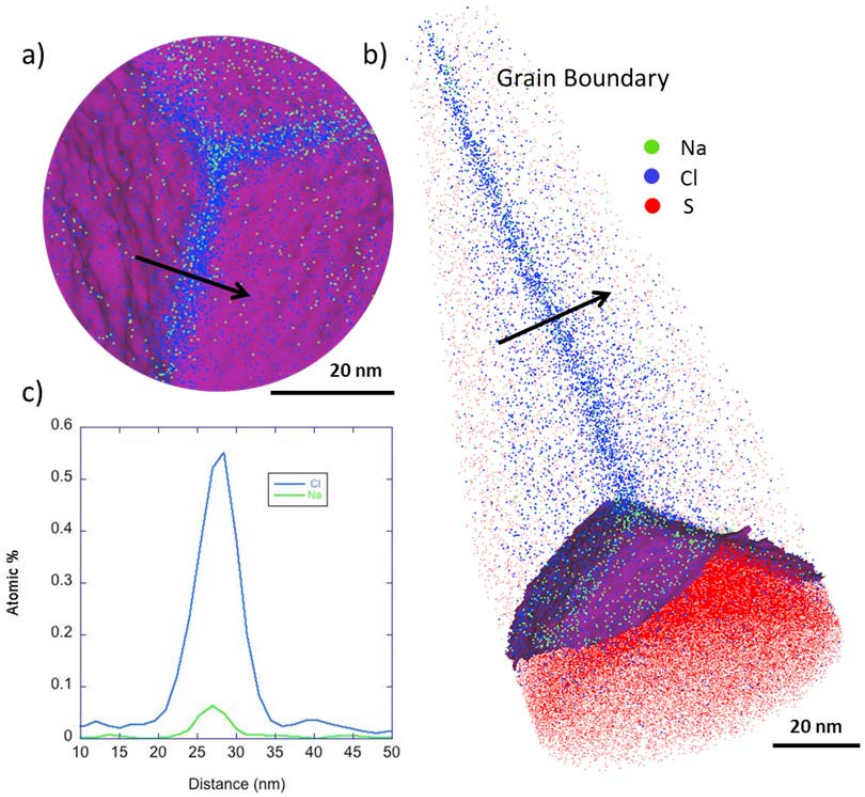

Figure 1. A three dimensional APT reconstruction shown from the top (a) and side (b) of a triple CdTe grain boundary (GB) meeting the CdS/CdTe interface within a CdTe solar cell device. Each colored sphere in the APT map indicates the position and type of atom detected (only Na, Cl, and S atoms are display for clarity). An 18% sulfur isoconcentration surface (displayed as a magenta surface) was drawn to separate the CdTe and CdS layers. The images clearly show Cl segregation within the CdTe GBs and Na segregation at the CdS/CdTe interface. A 1D concentration profile (c) across a CdTe GB reveals that Na segregation of <0.1 atomic percent can be detected by this technique. Na segregation at the CdS/CdTe interface and within CdTe or CdS GBs is below the detection limit of analytical STEM, and therefore, has never been detected using those techniques.

Beam-induced direct writing of nanostructures using the CNMS helium-ion microscope

Adam Rondinone

Center for Nanophase Materials Sciences, Oak Ridge National Laboratory

The CNMS helium-ion microscope (HIM) is a premier imaging and nanofabrication tool, capable of ion-milling to nanometer resolutions using either He^+ or Ne^+, with less adjacent damage and no doping compared to other ion-milling techniques. The CNMS HIM is now being modified with an OmniGIS system, which allows beam-induced, direct deposition of metals and oxides through the interaction of the ion beam with volatile precursors. The injectors maintain a small cloud of precursor molecules in the vicinity of the ion beam/sample surface, which are lysed by the ion beam, subsequently depositing metals ions and atoms resulting in structures as small as 30 nm. This technique allows for the direct write of lines, pads, and 3D structures on the sample without the need for lithographic resists or removal of the sample. Direct-deposited structures may be annealed in situ using a 915nm pulsed laser which improves crystallinity and conductivity of deposited structures.

Oral Presentations

Track A

2014 User Meeting

Tuning Interactions at Melt/Brush Interfaces for Functional Polymer Films

Gila E. Stein
University of Houston

Wetting at the interface of a linear polymer melt and a brushy surface can be tuned with changes in linear chain length, brush chain length, and brush grafting density. We exploit these physics to control the structure and function in two materials systems. First, we examine the thin film ordering of lamellar block copolymers on brushed substrates, where the brush grafting density (Σ) was systematically varied to control the interfacial energy. The lamellar domains are expected to orient normal to the substrate, forming an in-plane pattern of nanolines. However, using a combination of high resolution microscopy and grazing-incidence small angle X-ray scattering, we demonstrate that lamellar domains will bend to create a more favorable interface with the brushed substrate, and the severity of these deformations is controlled by Σ. These outcomes will be discussed in the context of materials design for block copolymer lithography. Second, we examine the thin film phase behavior of athermal bottlebrush/linear polymer melts. The length of linear chains was systematically varied to control wetting at the bottlebrush interface. Using dynamic secondary ion mass spectroscopy, we demonstrate that short linear chains can disperse the bottlebrushes throughout the film thickness, while long linear chains drive the bottlebrushes to segregate at the free surface and substrate. This spontaneous, entropy-driven de-mixing process provides a simple route to generate brush-like surfaces in any engineering thermoplastic.

In-Situ Study of Phase Transitions and Morphological Evolution in Solution-Processed Bilayer Organometal Halide Perovskite Photovoltaic Cells

Bin Yang,[1] Jong Keum,[1,2] Sanjib Das,[3] Ondrej Dyck,[4] Ilia Ivanov,[1] Suk-Kyun Ahn,[1] Gong Gu,[3] Pooran Joshi,[5] Christopher Rouleau,[1] Gerd Duscher,[4] David Geohegan,[1] Kai Xiao[1]

[1]Center for Nanophase Materials Sciences, Oak Ridge National Laboratory, Oak Ridge, TN, 37831, USA. [2]Neutron Scattering Science Division, Oak Ridge National Laboratory, Oak Ridge, TN, 37831, USA. [3]Department of Electrical Engineering and Computer Science, University of Tennessee, Knoxville, TN, 37996, USA. [4]Department of Materials Science and Engineering, University of Tennessee, Knoxville, TN, 37996, USA. [5]Materials Science and Technology Division, Oak Ridge National Laboratory, Oak Ridge, TN, 37831, USA.

The recent emergence of organometal halide perovskite materials for high-efficiency (>15%) and low-cost photovoltaics have focused interest on improving material processing control and advanced optical management[1-2], toward even higher efficiencies of 25%. In addition, understanding how to extend the long term stability of these materials is another key challenge.[1] Both device efficiency and stability in perovskite absorbers (e.g., $CH_3NH_3PbI_{3-x}Cl_x$, $CH_3NH_3PbI_3$) are believed to be significantly affected by the evolution of phase transition and morphology during synthesis and environmental exposure, where fundamental systematic studies are needed. Here, we apply multiple in-situ techniques including X-ray diffraction, differential scanning calorimetry (DSC), and ultraviolet–visible spectroscopy to identify the structural phase transitions of spin-coated organometal halide perovskite films as temperature is increased from room temperature to 250 ^oC in inert gas environment, such as argon, or directly in air. As-grown perovskites (e.g., $CH_3NH_3PbI_3$) were shown to experience a tetragonal-cubic phase transition at about 55 ^oC, and start decomposing to lead iodide (PbI_2) at temperatures above 135 ^oC, eventually completing the decomposition at about 185 ^oC. Time-resolved in-situ x-ray diffraction measurements were also applied to understand the kinetics of crystal growth and evolution of crystalline order. The cross sectional TEM measurements were applied to understand the materials structure and vertical phase morphology of the perovskite films. The electrical and photovoltaic performance of the perovskite solar cells was found to be closely related to the phase transition, crystal growth, and phase morphology. The best device performance was obtained by annealing the $CH_3NH_3PbI_3$ perovskite films at 70 ^oC for tetragonal phase. Process improvements to address control over phase transitions and film morphology as a result of these studies will be discussed.

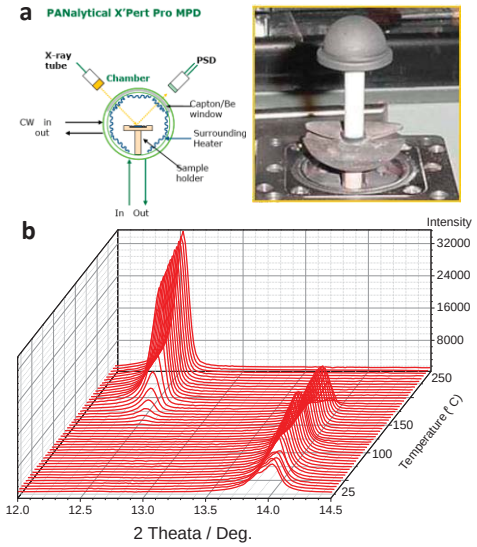

Figure 1 (**a**) The schematic drawing (top left) to show the in-situ XRD measurement setup in the Anton Paar XRK900 reaction chamber (top right). (**b**) In-situ XRD patterns as a function of temperature.

This research was conducted at the Center for Nanophase Materials Sciences (CNMS) and the Spallation Neutron Source (SNS) which are sponsored at Oak Ridge National Laboratory by the Scientific User Facilities Division, Office of Basic Energy Sciences, U.S. Department of Energy.

References:

1. R. F. Service, Science, 2014, 344 , 458
2. M. D. McGehee, Nature, 2013, 501, 323

RAPID AND SENSITIVE DETECTION/DIAGNNOSIS OF PATHOGENS

Cheng Cheng[a], Haochen Cui[a], Jayne Wu[a], Shigetoshi Eda[b]
[a]*Department of Electrical Engineering and Computer Science*
[b]*Department of Forestry, Wildlife and Fisheries, The University of Tennessee, Knoxville, TN 37996, USA*

Introduction

This work presents a label-free capacitive immunosensor, which capitalizes on dielectrophoresis (DEP) to achieve rapid, sensitive and easy-to-handle specific assay. In our current work, avian influenza virus detection has been used as an example. Experiments show that DEP helps speed up the binding process occurred on the electrode surface by trapping target virus towards the binding sites and therefore the testing time for an assay could be as low as 20s. With this rapid immunosensing technique, the limit of detection could reach to 1 ng/ml. Clinical swab sample tests and blind tests were also conducted. By comparing with ELISA results, the accuracy of our capacitive immunosensor has been validated.

Materials and Methods

In this work, the interfacial capacitance, or C_{int}, is sensed. By interpreting the change rate of C_{int}, whether the samples have been infected can be diagnosed. This interfacial capacitance can be defined as $C_{int} = \varepsilon_r S/(4\pi kd)$ where ε_r is the relative permittivity of the media in between, S is the surface area, k is the electrostatic constant, and d is the thickness of the media. With binding process continues, the thickness of double layer d keeps increasing which results to a decreasing change on C_{int}. The normalized change rate dC_{int}/dt, which is the slope of the lease squares fit line of the data set collected in one assay, is used to indicate the occurrence of binding on the electrode surface.

Results and Discussion

Figure 1(a) shows the proof of concept tests on swab samples, and the results for positive, negative and control samples are as expected. Capacitance changes after 20 seconds become more gradual, which is probably due to the saturation of the available binding sites on the electrode. This phenomenon indicates that 1:100 dilution is too high. To find an optimal dilution, samples were diluted from 1:10 to 1:100,000 and tested, as shown in Figure 1(b). 1:10,000 dilution was determined to be the optimal dilution. Subsequently, a test of 6 swab samples was conducted. In Figure 1(c), 3 positive and 3 negative clinical swab samples are clearly differentiated by the -1.2%/s threshold line.

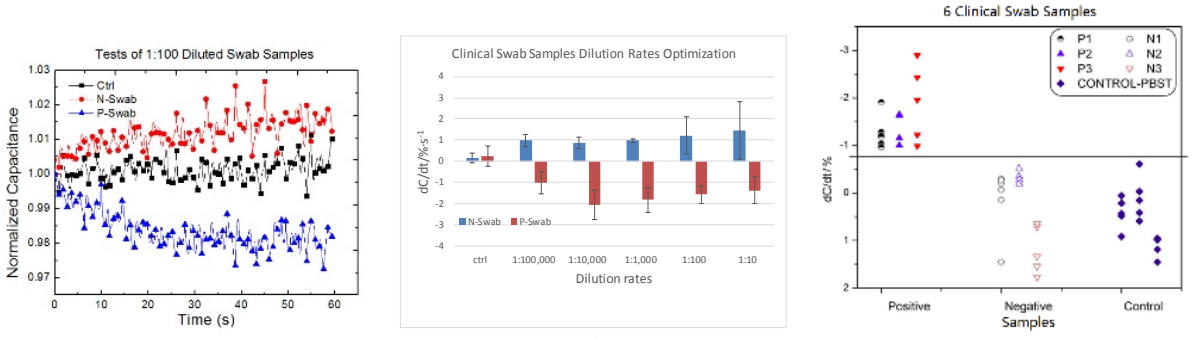

(a) (b) (c)

Figure 1. (a) Proof of concept on swab samples; (b) Clinical samples dilution rate optimization; (c) Tests of six swab samples.

Conclusions

We have developed an immunosensor that is rapid (20 seconds), simple (minimum pretreatment and no wash), and sensitive with the limit of detection reaching 1 ng/ml. In this work, all six clinical swab samples can be clearly differentiated and the results are confirmed by ELISA and PCR results.

A bridge between DNA nanotechnology and inorganic nanotechnology

Liqian Wang[1] [2] [3], Claudia Dalmastri[1] and Piero Morales[1] [3]

[1] ENEA, Italian National Agency for New Technologies, Energy and the Environment, Via Anguillarese 301 00123, Rome, Italy

[2] Università di Roma TorVergata, Dipartimento di Scienze e Tecnologie Chimiche, via della Ricerca Scientifica 1, 00133 Rome, Italy

[3] NAST center,via della Ricerca Scientifica 1, 00133 Rome, Italy

Abstract:

What DNA nanotechnology has achieved in recent 30 years is remarkable. The reason, apart from the size of nucleic acid double helices are about 2 nm wide, is its ability of chemical information contained in the sequences of programmed DNA to organize matter, DNA itself and other chemical species. To immobilize these Bottum-up synthesized DNA nanostructures onto inorganic Top-down fabricated nano patterns could broaden the application field of DNA nanotechnology to a new level. The concept of our project is to demonstrate the "DNA motherboards", which is sketched in Fig 1. Suitably designed DNA origami flat structures will self-assembled; these, in turn spontaneously assemble "plug-in" protein-based components on designated sites. Furthermore, the DNA "motherboards" will be anchored to nanopads of four different inorganic materials that are fabricated in the desired location of a planar chip by e-beam lithography.

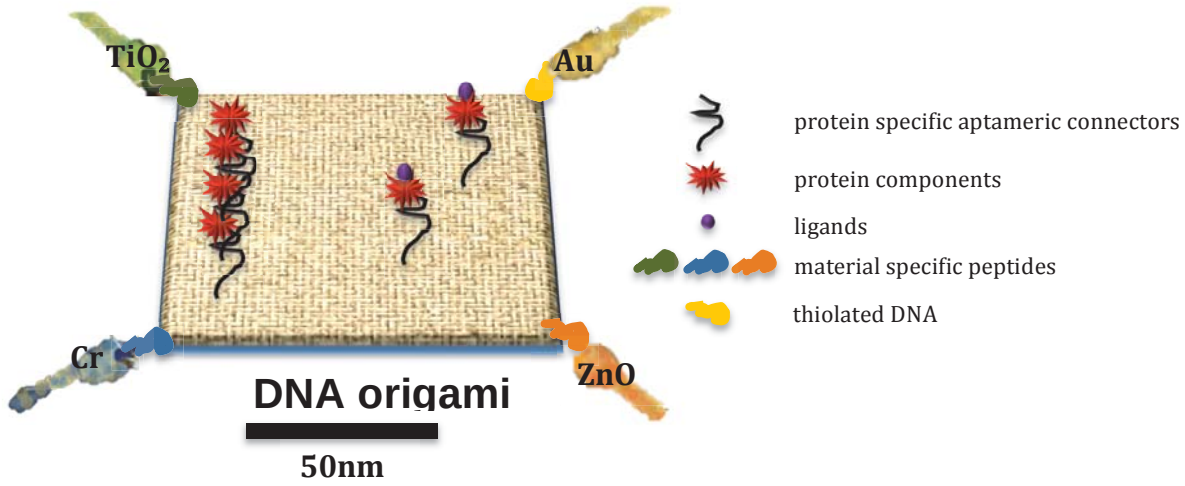

Sketch 1. Concept of DNA "motherboard" based on DNA origami structure.

Crafting Functional Nanocrystals by Capitalizing on Nonlinear Block Copolymers as Nanoreactors

Zhiqun Lin

Professor

School of Materials Science and Engineering, Georgia Institute of Technology, Atlanta, GA 30332, USA

Email: Zhiqun.lin@mse.gatech.edu

Colloidal nanocrystals exhibit a wide range of size and shape dependent properties and have found application in a myriad of fields such as optics, electronics, mechanics, drug delivery and catalysis to name but a few. Synthetic protocols that enable simple and convenient production of colloidal nanocrystals with controlled size, shape and composition are therefore of key general importance. Current strategies, however, often require stringent experimental conditions, are difficult to generalize, or require tedious multi-step reactions and purification. Recently, linear amphiphilic block copolymer micelles have been used as template for the synthesis of functional nanocrystals, but the thermodynamic instability of these micelles limits the scope of this approach. In this talk, I will elaborate a general strategy for synthesizing a large variety of functional nanocrystals with precisely controlled dimensions, compositions and architectures by using star-like block copolymers as templates. This new class of copolymers forms unimolecular micelles that are structurally stable under various experimental conditions and therefore overcomes the intrinsic instability of linear block copolymer micelles. Our approach enables the facile synthesis of organic solvent- and water-soluble nearly monodisperse nanocrystals with desired composition and architecture, including core/shell and hollow nanostructures. To demonstrate the generality of our approach we describe, as examples, the synthesis of various sizes and architectures of metallic, semiconductor, ferroelectric, magnetic, thermoelectric, upconversion, and luminescent colloidal nanocrystals.

Detection of aflatoxin B_1 by aptamer-based biosensor using PAMAM dendrimers as immobilization platform

Katia Spinella[1,2], Gabriela Castillo[3], Alexandra Poturnayová[3, 4], Maja Šnejdárková[4], Lucia Mosiello[3], Tibor Hianik[3]

[1] *ENEA, Italian National Agency for New Technologies, Energy and the Environment, Via Anguillarese 301 00123, Rome, Italy*

[2] *Università di Roma TorVergata, Dipartimento di Scienze e Tecnologie Chimiche, via della Ricerca Scientifica 1, 00133 Rome, Italy*

[3] *Faculty of Mathematics, Physics and Informatics, Comenius University, Mlynska dolina F1, 842 48 Bratislava, Slovakia*

[4] *Institute of Biochemistry and Animal Genetics, Slovak Academy of Sciences, Moyzesova 61, 900 28 Ivanka pri Dunaji, Slovakia*

We report an aptamer-based biosensor for detection of aflatoxin B_1 (AFB_1), a mycotoxin identified as contaminant in food. The sensor is assembled in a multilayer framework that utilizes cyclic voltammetry (CV) and electrochemical impedance spectroscopy (EIS) for acquiring the signal response by means of redox indicators: $K[Fe(CN)_6]^{-3/-4}$. Poly(amido-amine) dendrimers of fourth generation (PAMAM G4) immobilized on gold electrode covered by cystamine, were employed for attachment of single stranded amino-modified DNA aptamers specific to AFB_1. The cystamine-PAMAM (Cys-PAMAM) substrate was prepared on a previously cleaned gold electrode which was immersed in 0.1 M aqueous solution of cysteamine dihydrocloride during 2 h, followed by carefully washing in deionised water. Next, 5% glutaraldehyde (GA) was incubated for 1h and the modified electrode was rinsed in PBS buffer. After that, the electrode was incubated in 70 µM PAMAM G4 dendrimers for about 5 h. In order to block unreactive groups of GA and prevent non-specific interactions, 5 mM $NaBH_4$ was reacted with the modified electrode during 30 min. After rinsing in PBS buffer, the electrode was again incubated with 5% GA for 1h, washed in PBS and subsequently incubated with 1 µM aptamers for 16 h. Blocking with 5 mM $NaBH_4$ was applied again to the surface and after PBS washing, the sensor was ready for electrochemical detection of AFB_1. AFB_1 in the range 0.1-10 nM was added to the sensing surface, each concentration was incubated for 40 min and the surface was rinsed thoroughly in PBS buffer before measurements. The range of AFB_1 concentrations was selected as target interval for further utilization of the biosensor in food samples. The sensor was validated in certified contaminated peanuts extract as well as in spiked samples of peanuts demonstrating optimal response. Non specific interactions were analyzed by testing the sensor in other mycotoxins such as aflatoxin B_2 (AFB_2) and ochratoxin A (OTA) with negligible response. Sensor achieved a limit of detection LOD = 0.4 ± 0.03 nM, it was regenerable in 0.2 M glycine-HCl and did not lose its stability up to 60 h storing at 4 ºC (Fig1). Atomic Force Microscopy (AFM) studies were also performed for illustrating individual steps of biosensor assembly.

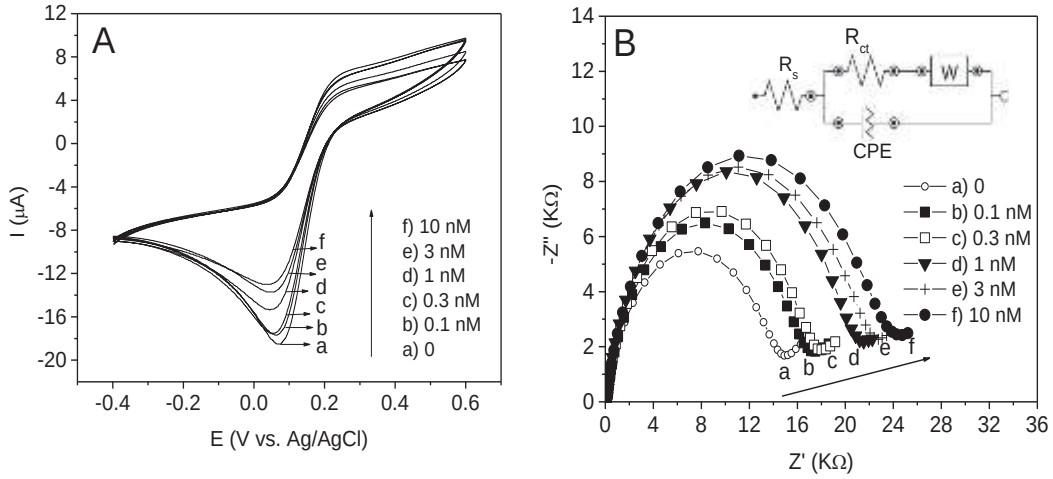

Fig. 1. A) Cyclic voltammograms for detection of AFB_1 varying from 0.1 to 10 nM. B) Corresponding Nyquist plots for the same AFB_1 range of concentrations. Closed symbols: real data, lines: data fit performed according to Randle's equivalent circuit (inset). CV and EIS performed in 5 mM $K[Fe(CN)_6]^{-3/-4}$ (1:1) containing 0.1 M KCl.

Symbiotic relation in bimetallic Ag nanoparticles

[1]A. Malasi, [2]R. Sachan, [2]J. Xe, [2]V. Ramos, [1]S. Yadavali, [3]H. Krishna, [3]A. Gangopadhyay, [4]H. Garcia, [2,5*]G. Duscher and [1,2†]R. Kalyanaraman

[1]Department of Chemical and Biomolecular Engineering, University of Tennessee, Knoxville, Tennessee, 37996, USA
[2]Department of Material Science and Engineering, University of Tennessee, Knoxville, Tennessee 37996, USA
[3]Department of Physics, Washington University, St. Louis, Missouri, 63130, USA
[4]Department of Physics, Southern Illinois University, Edwardsville, Illinois, 62026, USA
[5]Material Science and Technology Division, Oak Ridge National Laboratory, Oak Ridge, TN 37831, USA

Abstract

Here, we report a symbiotic relation which is a well-known biological phenomenon, in plasmonic nanomaterials. For this study, we chose CoAg as a model bimetallic system which has important applications in the biological and chemical sensing area and consists of a well-known plasmonic material Ag and Co with damped plasmonic characteristics. These bimetallic nanoparticles were synthesized using pulsed laser dewetting technique. The near-field and far-field plasmonic properties of the bimetallic Ag nanoparticles were analyzed by using the broad band optical spectroscopy and electron energy-loss spectroscopy (EELS). The whole study is divided into two parts. In the first, the oxidation study of different bimetallic Ag nanoparticles was done by studying their localized surface plasmon resonance behavior. It was observed that the oxidation of Ag in ambient conditions was suppressed by contacting Ag with Co in a nanoparticle due to galvanic effect where Co behaved as a sacrificial anode. As a consequence, plasmonic stability in bimetallic CoAg NPs increased in comparison to that of pure Ag NPs. The morphology of the nanoparticles played a crucial role on the oxidation lifetime and it was seen that the oxide free Ag of CoAg nanoparticles was 12 times more stable than the literature values and had a shelf life of $\sim$3 folds more than that of pure Ag nanoparticles. As the presence of Co helped stabilize the Ag NPs, this study was extended to other bimetallic systems: FeAg and NiAg which are also thermodynamically immiscible systems similar to Co-Ag. The study showed Fe when in contact with Ag stabilize the NPs even further.

In the second study, low loss EELS technique was used to analyze surface plasmon excitation with high spatial resolution in a monochromated STEM. Here, we observed the discovery of intense localized surface plasmon resonance in ferromagnetic Co and CoFe (8% alloy) part of the bimetallic Ag nanoparticle. The morphology and elemental analysis of the CoAg nanoparticle was done using high angle annular dark field (HAADF) imaging and core-loss EELS mapping. The plasmons on the Co side of the bimetallic nanoparticles are termed as *Ferroplasmons* as these plasmons are in the visible range and are comparable in bandwidth and intensity with the plasmons on the Ag side of the nanoparticle. In general, the plasmons on Co nanoparticles are in the UV range and are highly damped. The existence of these sharp plasmons which have been seen for the first time could be due to the plasmon interaction between the Co and Ag sides of the nanoparticle. The effect of nanoparticle size and substrate was also studied and was seen that the existence of the ferroplasmon was independent of either of them. In contrast to the first study, this study shows that Co when in contact with Ag in a nanoparticle excites intense localized surface plasmon like Ag which suggest a mutually beneficial symbiotic relationship between Ag and Co metals in a bimetallic nanoparticle which potentially opens the route to synthesize new plasmonic materials for various plasmon related sensing applications.

*gduscher@utk.edu
†ramki@utk.edu

Line-focused Femtosecond Laser Machining of Fused Silica

Brian K. Canfield, Trevor S. Bowman, and Lloyd M. Davis
Center for Laser Applications, University of Tennessee Space Institute,
411 B. H. Goethert Parkway, MS 35, Tullahoma, TN 37388

Direct writing of nanoscale features, which can be used for a range of micro-optical and fluidic devices, may be achieved with single, tightly focused femtosecond laser pulses. Such pulses induce extreme but strongly localized physical conditions on sub-picosecond time-scales, limiting thermal damage while also generating plasma that alters material properties. Plasma/pulse interactions are typically believed to restrict the depth of material modification. However, near a surface material in the form of nano/microparticles, which have many potential nanotechnology applications, may also be ejected even if the modification region is shallow. In this work we examine the formation within fused silica (SiO_2) substrates of extraordinarily deep, high aspect ratio microchannels by single, line-focused fs laser pulses. We also study line-focused surface ablation and material propagation in ambient atmosphere.

Controlled through a custom LabVIEW program, single 40 fs, 800 nm laser pulses of up to 1.2 mJ were provided on-demand by the amplified Mira fs laser at CNMS and shaped into a tight line focus using a cylindrical lens and a 0.68 numeric aperture molded glass asphere with a 1.7 mm working distance. The optical layout was optimized in Zemax ray-tracing software to yield a near-diffraction-limited focus at the back surface of a 200 μm-thick SiO_2 substrate, with ~2 μm width × 700 μm length and a Gaussian intensity profile along the line.

Exceptionally high aspect ratio line features could be formed by single fs pulses, as shown in the cross-sectional image of Fig. 1(a) for a series of pulses focused at successive levels within the substrate. Depths of material modification exceeding 60 μm can be observed. In addition, unusual formations such as discontinuities and bifurcations of the beam path are also visible. The depth and complexity of the features is attributed to the extreme conditions occurring near the focus, with pulse/plasma interaction causing highly nonlinear optical phenomena such as nonlinear refraction and filamentation.

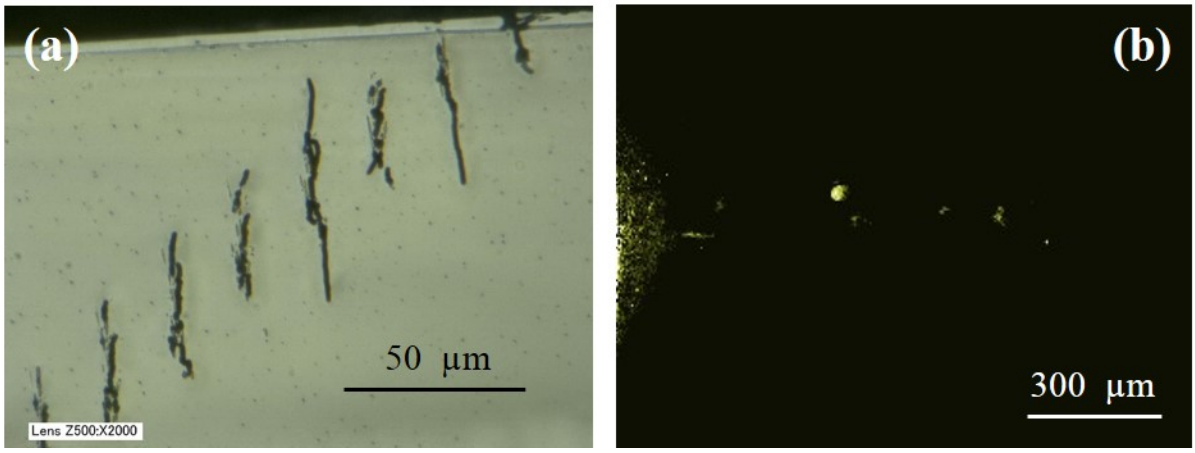

Figure 1. (a) Optical image of a cross-section through high aspect ratio line features formed in SiO_2. (b) False-color time-gated optical image of SiO_2 particles ejected in ambient atmosphere by a line-focused fs laser pulse.

In addition, we have studied the propagation of ablated particles in ambient atmosphere. Fig. 1(b) depicts a time-gated optical image (gate delay 45 μs, gate width 10 μs) of SiO_2 particles ejected from the surface of a SiO_2 substrate (just off left, in the plane of the image). Illumination was provided by a continuous-wave green diode laser coincident with the fs pulse. Although the majority of the focus produces some particulates (the cloud at left edge), the central region, where the intensity is the highest, ejects particles at high speeds that can travel long distances (>1 mm) in air (the blobs distributed across the image).

Volumetric Durable Superhydrophobic Coatings

Dr. John T Simpson
University of Tennessee
Material Science and Engineering Department

Abstract:

Over the past couple years the coating industry has seen the introduction of oxide/polymer-based superhydrophobic coatings with exceptional water repellency. YouTube videos have caught the public's imagination by showing people walking through mud without getting their tennis shoes muddy and water literally flying off coated surfaces. One might rightfully ask, why isn't this technology more common and being used everywhere water repellency is needed. A big reason is the lack of durability of these coatings. Up to this point all superhydrophobic coatings have been strictly a surface effect. And worse yet, the superhydrophobic nanostructured particles had to be weakly bonded to the coated material because too much binder would cover or engulf the nanostructure required for superhydrophobic behavior. Thus, any significant abrasion quickly destroyed the coating's superhydrophobic behavior.

This talk will describe a recent breakthrough in superhydrophobic coating technology that allows nanotextured amorphous silica-based superhydrophobic coatings to, not only be superhydrophobic on the coating's outer surface, but to also be superhydrophobic throughout the entire volume of the coating. No other superhydrophobic coating can make such a claim. As a result of this breakthrough, durable superhydrophobic paints, epoxies, silicone, and other such coatings are possible and have, in fact, been demonstrated. These breakthroughs in superhydrophobic coating technology will likely lead to the rapid and wide spread commercialization of superhydrophobic paints and epoxies, including superhydrophobic water-based latex paints.

Oral Presentations

Track B

2014 User Meeting

Characterizing interfacial effects in ferro-electric thin films using aberration-corrected STEM

P. Phillips, Q. Qiao and R.F. Klie
Dept. of Physics, University of Illinois at Chicago, Chicago, IL, USA 60607

Crystalline complex oxide thin films on semiconductor substrates have emerged as an alternative to SiO_2-based technologies in fabricating the metal-oxide-semiconductor field-effect transistors. Moreover, the integration of functional oxide thin-films on compound semiconductors can lead to a new class of reconfigurable spin-based optoelectronic devices if defect-free, fully reversible active layers are stabilized. $BaTiO_3$ (BTO) has been studied as a prototypical oxide exhibiting ferroelectricity, piezoelectricity, and pyroelectricity. Growth of epitaxial single-crystalline BTO film has been successfully conducted on both polar and non-polar semiconductors, and can lead to the production of switchable optical emitters or a tunable 2-dimensional electron gas in the compound semiconductor, if the ferroelectricity is preserved in the oxide film. One path to achieving virtually defect-free, epitaxial single-crystal films is by minimizing the interfacial strain, using a 2-monolayer (ML) thick $SrTiO_3$ (STO) buffer between the BTO film and GaAs substrate. It was previously reported that epitaxial STO on GaAs exhibits Fermi level pinning, which can be relieved with the addition of 0.5 ML Ti pre-layer, which enables the development of functional oxides films, such as BTO, on compound semiconductors.

In my talk, I will present an atomic-resolution investigation of the fundamental mechanism behind ferroelectric-oxide thin films on GaAs substrates to develop an atomic-scale model of the oxide-semiconductor hetero-interfaces. Using aberration-corrected scanning transmission electron microscopy (STEM) imaging and electron energy-loss spectroscopy (EELS) in combination with first-principles density functional theory (DFT) modeling, I will show that the single-domain polarization of a 8 nm thick BTO film on GaAs with a 2 monolayer thick STO buffer layer (see Figure 1) is pinned in the out-of-plane polarization with respect to the heterointerface. This pinning is further enhanced by the presence of an oxygen-deficient SrO layer at the GaAs-oxide interface, which would result in a non-switchable $BaTiO_3$ film. However, by introducing surface oxygen vacancies, I will demonstrate that the polarization in the BTO layer can be reversed and turn the oxide layer into a fully switchable ferroelectric, in agreement with prior piezo-force microscopy (PFM) measurements.

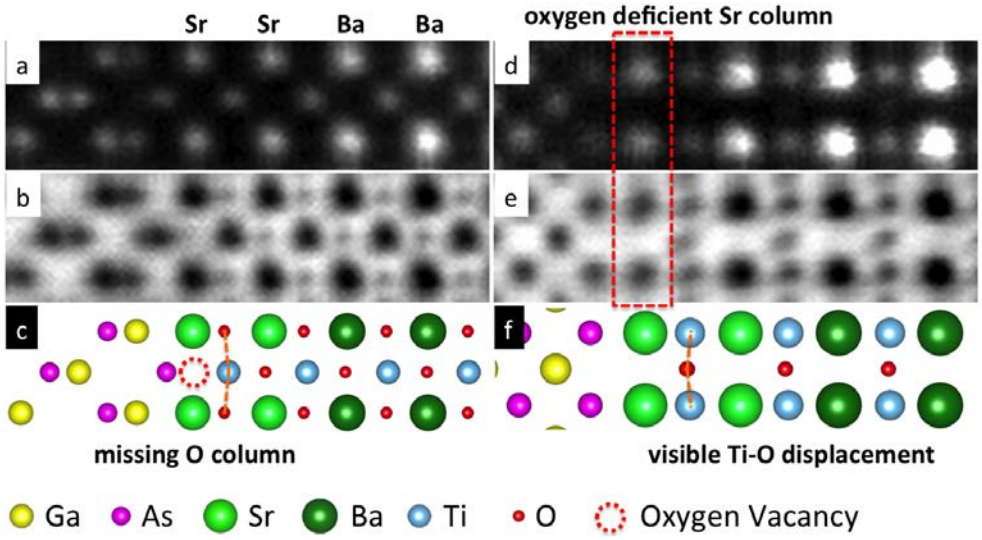

Figure 1. Averaged image of BTO/STO/GaAs interface. (a) HAADF and (b) ABF image, (c) atomic model of BTO[100]/STO[100]/GaAs[110], Sr and Ba can be distinguished by image intensity, oxygen column missing in first SrO layer is shown as a dashed circle; (d) HAADF and (e) ABF image, (f) atomic model of BTO[110]/STO[110]/GaAs[100], oxygen deficient Sr column is observed in both (d) and (e) as red rectangle shows, visible Ti-O displacement in (f) indicated by orange dashed lines.

Studies on Multiferroic and Magnetoelectric properties of $Pb(Fe_{0.5}Nb_{0.5})O_3$ and $Pb(Fe_{0.5}Nb_{0.5})O_3$/ $Ni_{0.65}Zn_{0.35}Fe_2O_4$ heterostructures

Dhiren K. Pradhan[1], Danilo Barrionuevo Diestra[1], Venkata S. Puli [2], Sergei V. Kalinin[3], Ram S. Katiyar[1]

[1]Department of Physics and Institute of Functional Nanomaterials, University of Puerto Rico, USA
[2]Department of Physics and Engineering Physics, Tulane University, New Orleans- LA 70118, USA
[3]Center for Nanophase Materials Sciences, Oak Ridge National Laboratory, Oak Ridge, Tennessee 37831, USA

Multiferroic magnetoelectric materials which exhibit simultaneous ferroelectric and ferromagnetic behavior and control the magnetic order parameter via electric field in a switchable manner and vice versa have drawn significant interest in recent years because of their intriguing physical origin and great potential for multifunctional applications. Multiferroic composites/ heterostructures, showing magnetostrictive and piezoelectric (ferroelectric) properties, are very attractive as compared to single-phase magnetoelectric materials due to their combined robust electric and magnetic polarizations at room temperature with effective magneto-electric coefficients. In the present work we have chosen $Pb(Fe_{0.5}Nb_{0.5})O_3$; lead iron niobate (PFN)/ $Ni_{0.65}Zn_{0.35}Fe_2O_4$ (NZFO) heterostructures to achieve enhanced multiferroic properties and magneto electric coupling at room temperature. PFN single layer and PFN/NZFO multilayer thin films were grown at 600^o C by pulsed laser deposition (PLD) using a KrF excimer laser (λ=248 nm) on $LaNiO_3$ buffered (001) oriented $(LaAlO_3)_{0.3}(Sr_2AlTaO_6)_{0.7}$ (LSAT) substrates under an oxygen pressure of 20 mTorr followed by annealing at 700^o C for 30 min in oxygen at a pressure of 300 Torr. The thickness of LNO was 60 nm for all films, while the thicknesses of the PFN thin films varied from 10 to 100 nm. The thicknesses of PFN/NZFO multilayers are found to be ~ 150 nm. The highly c-axis oriented growth containing only (00l) diffraction peaks of PFN and NZFO films along with in plane epitaxial relationship were confirmed by high resolution X-ray diffraction measurements. From the atomic force micrographs it was observed that all the films were densely packed, smooth, free from microcrack and particulates with uniform grain-size distributions. XPS measurements confirmed that in all films retain their same oxidation states. The existence of ferroelctricity and switching of polarization are confirmed from the Piezo Force Microscopy (PFM). PFM images showed clear and reversible out-of-plane phase contrast above ± 5 V, which indicates the ferroelectric character of those thin films. Detailed studies on dielectric, ferroelectric, magnetic and magnetoelectric properties of these above mentioned films will be discussed.

Dielectric Meta-Reflectarray for Broadband Linear Polarization Conversion and Optical Vortex Generation

Y. Yang[1], W. Wang[2], P. Moitra[1], I. I. Kravchenko[3], D. P. Briggs[3], J. Valentine[4]
[1]*Interdisciplinary Materials Science Program, Vanderbilt University, Nashville, Tennessee 37212, USA*
[2]*Department of Electrical Engineering and Computer Science, Vanderbilt University, Nashville, Tennessee 37212, USA*
[3]*Center for Nanophase Materials Sciences, Oak Ridge National Laboratory, Oak Ridge, Tennessee 37831, USA*
[4]*Department of Mechanical Engineering, Vanderbilt University, Nashville, Tennessee 37212, USA*
Email: yuanmu.yang@vanderbilt.edu

Plasmonic metasurfaces have recently attracted much attention due to their ability to abruptly change the phase of light, allowing sub-wavelength optical elements for polarization and wavefront control[1,2]. However, most previously demonstrated metasurface designs suffer from low coupling efficiency and are based on metallic resonators, leading to Ohmic loss. Here, we present an alternative approach to plasmonic metasurfaces by replacing the metallic resonators with high-refractive-index silicon cut-wires in combination with a silver ground plane. The meta-reflectarray utilizes Mie resonances in the Si resonators and multiple reflections from the silver mirror, allowing complete 2π phase control of light while maintaining high efficiency within a broadband range. We experimentally demonstrate that this meta-reflectarray can be used to realize linear polarization conversion with more than 98% conversion efficiency over a 200-nm-bandwidth in the short-wavelength infrared band. We also demonstrate optical vortex beam generation using a meta-reflectarray with an azimuthally varied phase profile. The vortex beam generation is shown to have high efficiency over a wavelength range from 1500 nm to 1600 nm. The use of dielectric resonators in place of their plasmonic counterparts could pave the way for ultra-efficient metasurface-based devices at high frequencies[3].

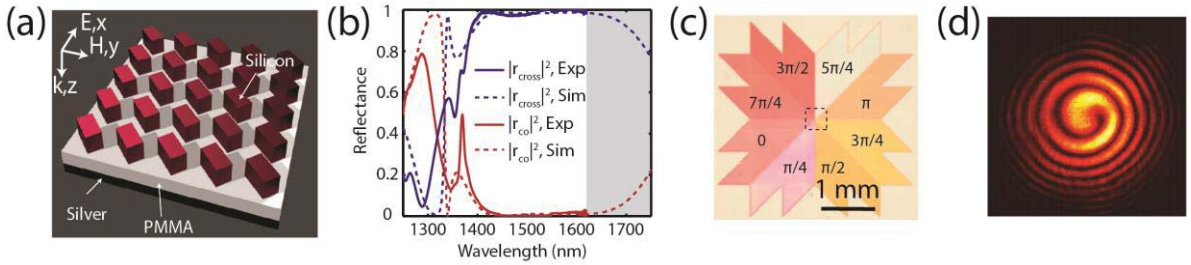

Figure1. (a) Schematic of the dielectric meta-reflectarray. (b) Broadband linear polarization conversion. (c) Optical microscope image of the spiral phase plate. (d) Interference pattern of the generated vortex beam and a co-propagating Gaussian beam.

References

1. Yu, N. *et al.* Light Propagation with Phase Discontinuities: Generalized Laws of Reflection and Refraction. *Science* **334,** 333–337 (2011).
2. Grady, N. K. *et al.* Terahertz metamaterials for linear polarization conversion and anomalous refraction. *Science* **340,** 1304–1307 (2013).
3. Yang, Y. *et al.* Dielectric meta-reflectarray for broadband linear polarization conversion and optical vortex generation. *Nano Lett.* **14,** 1394–1399 (2014).

Air-Stable, High-Conduction Solid Electrolytes of Arsenic-Substituted Li_4SnS_4

Gayatri Sahu[1], Zhan Lin[2], Juchuan Li[2], and Chengdu Liang[1*]

(1) Center for Nanophase Materials Sciences; (2) Material Science and Technology Division, Oak Ridge National Laboratory, Oak Ridge, TN 37831-6493, USA

Lithium-ion-conducting solid electrolytes show promise for enabling high-energy secondary battery chemistries and solving safety issues associated with conventional lithium batteries. Achieving the combination of high ionic conductivity and outstanding chemical stability in solid electrolytes is a grand challenge for the synthesis of solid electrolytes. Herein we report the design of aliovalent substitution of Li_4SnS_4 to achieve high conduction and excellent air stability based on the hard and soft acids and bases theory. The composition of $Li_{3.833}Sn_{0.833}As_{0.166}S_4$ has a high ionic conductivity of 1.39 mS/cm^{-1} at 25°C and a Li^+ transference number (t^+) of 0.9999. Considering the high Li^+ transference number, this phase conducts Li^+ as well as carbonate-based liquid electrolytes. This research also addresses the compatibility of the sulfide-based solid electrolytes through chemical passivation.

Acknowledgment:

This work was sponsored by the Division of Materials Science and Engineering, Office of Basic Energy Sciences (synthesis and characterization of solid electroltyes), and the Assistant Secretary for Energy Efficiency and Renewable Energy, Vehicle Technologies Office (VTO) of the U.S. Department of Energy (investigation of all-solid-state Li-S batteries). The synthesis was conducted at the Center for Nanophase Materials Sciences, which is sponsored at Oak Ridge National Laboratory by the Division of Scientific User Facilities, U.S. Department of Energy.

Controllable Complex Oxide Heterointerfaces

Ying-Hao Chu

Department of Materials Science and Engineering, National Chiao Tung University, Hsinchu, Taiwan 30010
Department of Electrophysics, National Chiao Tung University, Hsinchu, Taiwan 30010
Institute of Physics, Academia Sinica, Taipei 105, Taiwan

Interfaces have emerged as key focal points of current condensed matter science. In complex, correlated oxides, heterointerfaces provide a powerful route to create and manipulate the charge, spin, orbital, and lattice degrees of freedom. The most common interfaces have been explored are artificially constructed heterointerfaces. The interaction of degrees of freedom at the heterointerface has resulted in a number of exciting discoveries including the observation of a 2-D electron gas-like behavior at $LaAlO_3$-$SrTiO_3$ interfaces; the emergence of the ferromagnetism in a superconducting material at a $YBa_2Cu_3O_{7-x}$-$La_{0.7}Ca_{0.3}MnO_3$ interface and a induced ferromagnetic state in the heterointerface between $BiFeO_3$ and $La_{0.7}Sr_{0.3}MnO_3$ layer. Among them, the interface of the YBCO/LCMO heterostructures has been intensively studied to understand the proximity effect between the ferromagnets and superconductors. In order to shed more light into this topic, one key question is yet to be addressed in this prominent $YBa_2Cu_3O_{7-x}$-$La_{0.7}Ca_{0.3}MnO_3$ system: does termination type play an important role in determining the superconducting and magnetic properties? In this talk, $YBa_2Cu_3O_{7-x}$-$La_{0.7}Ca_{0.3}MnO_3$ heterostructures with two distinct types of interfacial termination are fabricated. Such a result suggests a control of thin film growth in nanocale. Their superconducting and magnetic properties are shown to exhibit different responses to the types of termination. Based on X-ray scattering, we have found the magnetic interaction only happens at particular termination. Cross-sectional scanning tunneling microscopy has bee used to study the proximity effect. Two different interfaces show different the competition of superconductor/ferromagnet. However, in the push for practical applications, it is desirable to have the ability to control the interface functionalities by an external stimulus. In this talk, the $LaAlO_3$-$SrTiO_3$ interface will be used as a model system. Two pathway including non-volatile ferroelectric control and visible-light control of the metal-insulator transition will be demonstrated. These recently studies open a new avenue to design and engineer new function oxide interfaces.

Electronic properties of bilayer graphenes strongly coupled to interlayer stacking and the external field

Changwon Park, Bobby Sumpter, Mina Yoon
Center for Nanophase Materials Sciences, Oak Ridge National Laboratory, Oak Ridge, TN, USA

Recent observations of the complex stacking structures of bilayer graphene [1,2] are expected to explain discrepancies between experiments and theories based on the ideal AB (Bernal)-stacking structure and also call for a theoretical guideline to their electronic structures. Especially in the design of switching devices exploiting the energy gap generated by an external electric field, the coexistence of various stacking regions can considerably alter their overall response. We systematically investigated the stacking-dependent evolution of electronic band structure and their response to the external electric field. Though the crossing band structure remains at any stacking (i.e., no energy gap opens), wavefunction characteristics around the Fermi level can be qualitatively different for different stackings, a phenomenon conveys to gap opening properties in the presence of an external electric field. We established a phase diagram summarizing stacking dependent critical field above which electronic gap opens and the structure transfer to a semiconductor.

This work was supported by theme research at the Center for Nanophase Materials Sciences, which is sponsored at Oak Ridge National Laboratory by the Scientific User Facilities Division, Office of Basic Energy Sciences, U.S. Department of Energy.

References

[1] “AC/AB Stacking Boundaries in Bilayer Graphene”, Junhao Lin et al., Nano Lett. 13, 3262-3268 (2013)
[2] “Strain solitons and topological defects in bilayer graphene1”, Jonathan S. Alden *et al.*, PNAS 110, 11256 (2013)

Electronic properties of rhenium doped tungsten disulfide monolayers

A.D. McCreary[1], E. Cruz-Silva[1], N. Perea-Lopez[1], A.L. Elias[1], H. Terrones[2], and M. Terrones[1,3,4,5]

[1] Department of Physics and Center for 2-Dimensional and Layered Materials, The Pennsylvania State University, University Park, Pennsylvania 16802
[2] Department of Physics, Applied Physics, and Astronomy, Rensselaer Polytechnic Institute, Troy, NY 12180
[3] Department of Chemistry, The Pennsylvania State University, University Park, Pennsylvania 16802
[4] Department of Materials Sciences and Engineering, The Pennsylvania State University, University Park, Pennsylvania 16802
[5] Carbon Institute of Science and Technology, Shinshu University, 4-17-1 Wakasato, Nagano 380-8553, Japan

Layered transition metal dichalcogenides (TMDs) have attracted the attention of numerous scientists due to their electronic and optical properties. In particular, MoS_2 and WS_2 show an indirect to direct electronic band gap transition when reduced to a monolayer, and display strong photoluminescence. While there are proposed applications for MoS_2 and WS_2 as electronic and optoelectronic devices, control of their electronic properties needs to be reached before these applications can be scaled up. In this context, chemical doping has been recently shown to allow the modification of the electronic properties of MoS_2 monolayers by substitution of either transition metals or the chalcogen. Here we present an experimental and theoretical study of the electronic and optical properties of doped WS_2 monolayers. Re-doped WS_2 monolayers have been produced by chemical vapor deposition (CVD) in which sulfur vapor reacts with a thin film of rhenium and tungsten oxides. Photoluminescence and Raman spectroscopy studies suggest that rhenium atoms have been successfully incorporated into WS_2 lattice. *Ab initio* calculations indicate that substitution of W atoms by Re results in the formation of new states in the vicinity of the Fermi energy that allows tailoring of the electronic band gaps, which also results in different optical properties.

Controlled Vapor-Phase Growth of Photoresponsive Two-Dimensional GaSe Crystals and Van der Waals Heterostructures

Xufan Li,[1] Ming-Wei Lin,[1] Alexander A. Puretzky,[1] Leonardo A. Basile Carrasco,[1] Cheng Ma,[1] Jaekwang Lee,[1] Ivan V. Vlassiouk,[2] Juan C. Idrobo,[1] Mina Yoon,[1] Miaofang Chi,[1] Christopher M. Rouleau,[1] Ivan I. Kravchenko,[1] David B. Geohegan,[1] Kai Xiao[1]*

[1]*Center for Nanophase Materials Sciences,* [2]*Energy & Transportation Science Division*

lix2@ornl.gov, xiaok@ornl.gov

I. INTRODUCTION

Two-dimensional (2D) nanosheets are very thin materials with only one or few atomic layers. Since the rise of graphene, recent years have seen a burst of 2D semiconductors with a variety of bandgaps compensating graphene in electronic and optoelectronic applications.[1] Moreover, the fabrication of 2D van der Waals (VDW) heterostructures allows combination of their properties and creation of artificial crystals with enhanced functionality.[2] Gallium selenide (GaSe) is a layered semiconductor widely studied and used in optoelectronics, nonlinear optics, and terahertz radiation. Few-layer GaSe nanosheets fabricated by mechanical exfoliation show good performance as photodetectors and transistors.[3] However, the growth of large-area, single-crystalline, uniform 2D GaSe nanosheets and GaSe-based VDW heterostructures, which is highly desired by device fabrication, is still a challenge.

II. MAIN RESULTS

In this work, large area, single-crystalline 2D GaSe monolayer and few-layer crystals were grown using a highly-controllable vapor-phase deposition method.[4] Large (up to ~60 μm in lateral size), uniform triangular monolayer GaSe crystals were obtained on SiO_2/Si substrate (Figure 1a, b, c). The honeycomb crystal structure of monolayer GaSe was observed using atomic resolution scanning transmission electron microscopy (STEM) (Figure 1d). Dark-field transmission electronic microscopy (DF-TEM) indicates the single crystal nature of individual triangles (Figure 1e) and grain boundary of merged flakes (Figure 1f). Few-layer GaSe nanosheets can be obtained in large amount by increasing the argon carrier gas flow rate. Two typical types of bi-layer crystals, with the second layer at the same orientation or rotated by 60 ° with respect to the first layer, show two different stacking modes. The 2D GaSe crystals show p-type semiconductor characteristics and high photoresponsivity (~1.7 A/W under white light illumination) comparable to exfoliated GaSe nanosheets. 2D GaSe-graphene VDW heterostructure was fabricated by growing GaSe nanosheets on graphene through VDW epitaxy (Figure 1g). The 2D GaSe preferentially nucleated on wrinkles of the graphene film and grew into irregularly-shaped islands (Figure 1g, h), in stark contrast with triangular flakes grown on SiO_2/Si. The epitaxially grown 2D GaSe generally shows a lattice orientation rotating within 10 ° with respect to that of the underneath graphene (Figure 1i) due to the large lattice mismatch between GaSe and graphene. The 2D GaSe-graphene VWD heterostructure show much enhanced photoresponse. These 2D GaSe crystals and GaSe-graphene VWD heterostructure are potentially useful for next-generation optoelectronic devices such as photodetectors.

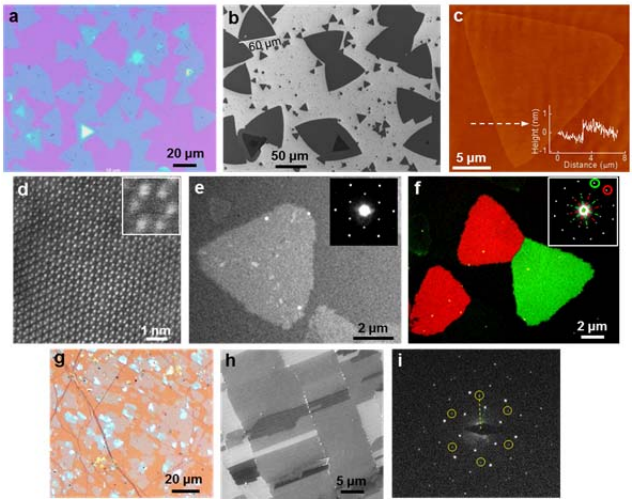

Fgure 1. (**a**–**d**) Optical micrograph, SEM, AFM, and atomic-resolution STEM images of monolayer GaSe crystals. (**e**–**f**) DF-TEM images of an individual monolayer triangular flake and two merged triangular flakes. (**g**–**i**) Optical micrograph, SEM image, and electron diffraction pattern of GaSe-graphene VDW heterostructures. The spots in yellow circles are from graphene.

Acknowledgment: Growth, synthesis, and theoretical studies sponsored by the Laboratory Directed Research and Development (LDRD) program at Oak Ridge National Laboratory. Materials and device characterization conducted at the Center for Nanophase Materials Sciences, which is sponsored at Oak Ridge National Laboratory by the Scientific User Facilities Division, Office of Basic Energy Sciences, U.S. Department of Energy. Synthesis science supported by the Materials Science and Energy Division, Office of Basic Energy Sciences, U.S. Department of Energy. Computing resources provided by the National Energy Research Scientific Computing Center, which is supported by the Office of Science of the U.S. Department of Energy under Contract No. DE-AC02-05CH11231.

REFERENCES

1. Bulter, S. Z. *et al*. Progress, challenges, and opportunities in two-dimensional materials beyond graphene. *ACS Nano* **7**, 2898−2926 (2013).
2. Britnell, L. *et al*. Stong light-matter interactions in heterostructures of atomically thin films. *Science* **340**, 1311−1314 (2013).
3. Hu, P. A. *et al*. Synthesis of few-layer GaSe nanosheets for high performance photodetectors. *ACS Nano* **6**, 5988−5994 (2012).
4. Li, X. F. et al. Controlled vapor phase growth of single crystalline, two-dimensional GaSe crystals with high photoresponse. *Sci. Rep.* **4**, 5497 (2014).

Origins of Electromechanical Strain Ascertained from *in situ* X-ray and Neutron Diffraction

Jacob L. Jones

Department of Materials Science and Engineering, North Carolina State University, Raleigh, NC

Dielectric and piezoelectric materials are used to store and convert electrical and mechanical energy, making them essential to a broad range of applications and devices including impact and displacement sensors, actuators, capacitors, microelectromechanical systems, vibrational energy harvesting, diesel fuel injectors, sonar, and ultrasound. In these applications, the dielectric and piezoelectric coefficients define the performance and the limits of device operation. However, the true origin of the material response, and thus the property coefficients, are not well understood because of the numerous and complex microstructural and crystallographic contributions to these properties (e.g., ionic and dipolar polarizability, ferroelastic domain wall motion, interphase boundary motion, the intrinsic piezoelectric effect, etc.) This talk will demonstrate our use of advanced *in situ* X-ray and neutron scattering methods to discern the underlying mechanics and physics at play in numerous ferroelectric and piezoelectric materials, ultimately revealing the contribution of these various mechanisms to their property coefficients. In all cases, direct measurements of the contribution from lattice deformation (e.g., piezoelectric) and the motion of intragranular interfaces (e.g., domain walls, interphase boundaries) are quantitatively related to the property coefficients using micromechanics-based formulations. It will be shown that domain wall motion, even during application of weak electric field amplitudes, dominates the electromechanical response of many ferroelectric materials.

Poster Abstracts

Denotes Student Posters

2014 User Meeting

Wicking nanopillar arrays with dual roughness for selective transport and fluorescence measurements

Jennifer J. Charlton[1, 2,] Nickolay Lavrik[3], James A. Bradshaw[2, 1], Michael J. Sepaniak[1]*

[1]The University of Tennessee Knoxville, Department of Chemistry, Knoxville, Tennessee 37996, United States [2]Y-12 National Security Complex, Analytical Chemistry Organization, Oak Ridge, Tennessee 37830, United States [3]The Center for Nanophase Material Sciences, Oak Ridge National Laboratory, Oak Ridge, Tennessee 37830, United States

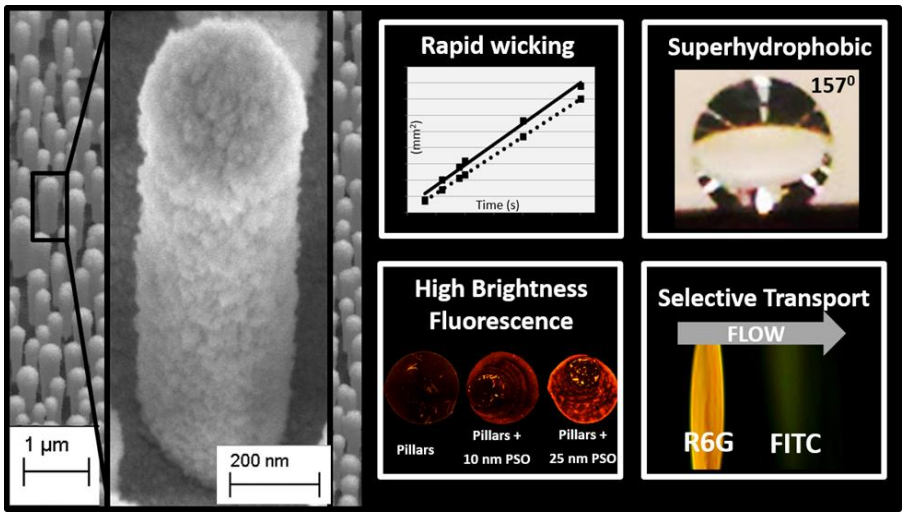

ABSTRACT: Silicon nanopillars are important building elements for innovative nanoscale systems with unique optical, wetting, and chemical separation functionalities. However, technologies for creating expansive pillars arrays on the submicron scale are often complex and with practical time, cost, and method limitations. Herein we demonstrate the rapid fabrication of nanopillar arrays using the thermal dewetting of Pt films with thicknesses in the range from 5 to 19 nm followed by anisotropic reactive ion etching (RIE) of the substrate materials. A second level of roughness on the sub-30 nm scale is added by over-coating the silicon nanopillars with a conformal layer of porous silicon oxide (PSO) using room temperature plasma enhanced chemical vapor deposition (PECVD). This technique produced environmentally conscious, economically feasible, expansive nanopillar arrays with a production pathway scalable to industrial demands. The arrays were systematically analyzed for size, density, and variability of the pillar dimensions. We show that these stochastic arrays exhibit rapid wicking of various fluids and, when functionalized with a physiosorbed layer of silicone oil, act as a superhydrophobic surface. We also demonstrate high brightness fluorescence and selective transport of model dye compounds on surfaces of the implemented nanopillar arrays with two-tier roughness. The demonstrated combination of functionalities creates a platform with attributes inherently important for advanced separations and chemical analysis.

Fabrication of microfluidic chips with a pressure actuation system for *in vivo* studies of cellular organization

Da Yang,[1] Ryan Hefti, [1] Scott Retterer, [2] Jaan Männik[1]
[1]*Department of Physics and Astronomy, University of Tennessee, Knoxville, TN*
[2]*Center for Nanophase Materials Sciences, Oak Ridge National Laboratory*

The common approach to understand how cellular organizations are maintained is by perturbing that organization, then observing the response from the cells. This task has been primarily carried out by cell biologists using genetic modifications, and chemical agents such as antibiotics. Both approaches may perturb, in addition to their intended targets, other cellular pathways in unexpected ways. Moreover, limited techniques are available for following cellular responses to those perturbations in real time. Here, we describe the development of a microfluidic platform which allows perturbations of cellular organization by mechanical forces, and enables real-time monitoring of cellular responses in a high resolution optical microscope. Our interest is to utilize this platform in studies of self-assembly processes of bacterial cell division machinery and organizations of bacterial chromosomes.

Our experimental design uses pressure actuated microfluidic valves to perturb the internal organization of a bacterium. The bacterium is placed under the valve when the valve is closed and observed in high resolution microscope. We implement this design in PDMS based microfluidic chips. Each chip consists of an unmodified glass cover slide, a PDMS elastomer layer of microfluidic flow channels, in which bacteria reside, and another PDMS elastomer layer of microfluidic control channels, which connects to pressure lines.

Our initial measurements show that considerable deformations of *Escherichia coli* bacteria and displacements of their chromosomes are achievable in these devices. However, bacteria tend to displace frequently as pressure is applied to control line or when culture media is flown. Moreover, the ceiling of flow channel tends to enclose the bacterium. We are currently fabricating and testing a new design where we “trim off” part of the material in the ceilings of the flow channels to ensure that the ceiling surfaces are under tension just before contacting bacteria. This modification should overcome aforementioned drawbacks and will enable us high throughput monitoring of bacteria as they undergo mechanical deformations.

Capillary driven transport and dispersion in hierarchically porous phases formed by conformal deposition of petal like carbon on silicon pillar arrays

Danielle Lincoln
M. J. Sepaniak's Group, Department of Chemistry, University of Tennessee, Knoxville, TN

Abstract:
Surface immobilized porous phases are associated with a variety of capillary phenomena, such as anomalous physisorption, capillary condensation, and capillary-driven flows. Capillary flow is of particular interest as it influences a great many mechanisms in biological and engineered systems. Our group has previously done work exhibiting separations in lithographically fabricated pillar array systems which use capillary flow as their primary mechanism. The work described here is a logical extension of this previous work, aiming to deposit new on-chip porous-phases with hierarchical porosity. These phases are created using plasma-enhanced vapor deposition (PECVD) of petal-like carbon (PLC). The distinctive nanoscale morphology of PLC is associated with high surface area, which is known to be a prerequisite for high performance stationary phases in analytical systems with high immunity to sample overloading. In addition, PLC, like other porous carbonaceous phases before it, may exhibit unique reversed-phase properties that allow it to be used as a retentive stationary phase without further surface modification. We are investigating the functionalities of PLC, including its solvent flow characteristics and porosity. We are also looking into its retentive capabilities as a stationary phase for our pillar array systems, as not only should its high surface area increase the efficiency of our separations, but its unique retention mechanisms may allow for the separation of highly polar analytes.

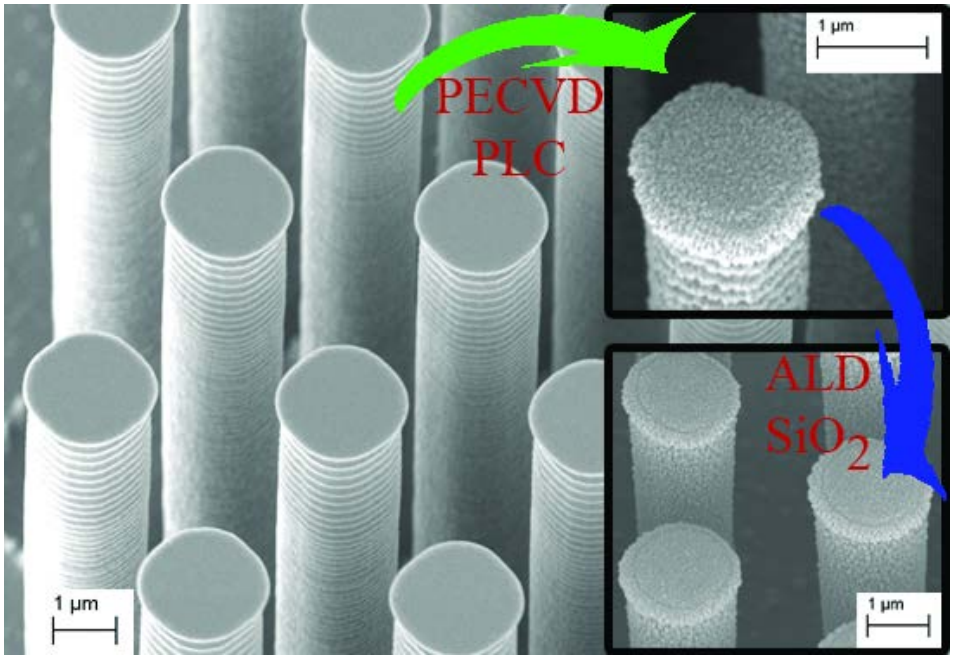

Figure 1: The deposition of petal like-carbon by plasma-enhanced vapor deposition, followed by atomic layer deposition of silicon dioxide, creates a marked increase in surface area in lithographically-created microscale pillar array systems.

Highly Sensitive Dopamine Sensor Based on Vertically-aligned Pristine Carbon Nanotube Sheathed Niobium Microelectrodes

Cheng Yang and B. Jill Venton
University of Virginia

Carbon nanotubes (CNTs) have been shown to enhance sensitivity and electron transfer kinetics attributing to their excellent electronic properties, large surface area and tendency to adsorb biomolecules to surface. The CNTs sheathed carbon fiber (CNTs-CF) microelectrodes have been reported to successfully detect dopamine. However, the intrinsic low conductivity of carbon fibers may limit the enhancement of electrochemical property comparing to the modification with CNTs. In this study, an as-synthesized vertically-aligned CNTs sheathed metal microelectrode is developed and used as a nano-molar level dopamine sensor. CNTs sheathed metal microelectrodes were fabricated by chemical vapor deposition at atmospheric pressure with ethylene as the precursor and characterized physically and electrochemically by scanning electron microscopy, transmission electron microscopy, Raman spectroscopy, and fast scan cyclic voltammetry. CNTs sheathed niobium (CNTs-Nb) microelectrodes were found to exhibit better electrochemical response to dopamine compared to carbon fibers as well as other metal substrates with CNTs sheathing. The enhanced detection limit of CNTs-Nb microelectrodes is 11±1 nM (S/N=3), which is approximately six times lower than CFMEs and five times lower than CNTs-CF. Additionally, the standard free energy for dopamine adsorption on carbon fibers as well as various metal substrates with CNTs sheathing was theoretically calculated and compared. This study demonstrates the analytical application of CNTs-Nb for highly sensitive dopamine monitoring, which may be applied for in vivo measurement in the future.

Vertically Aligned Carbon Nanofiber Embedded Biosensor Platform for Electric Cell Impedance Measurement System

Khandaker A. Mamun*, Yongchao Yu*, Dale Hensley, Ivan Kravchenco, Nicole McFarlane*
*Department of Electrical Engineering and Computer Science,
*The University of Tennessee, Knoxville, TN 37996, USA, kmamun@vols.utk.edu
Oak Ridge National Laboratory, Oak Ridge, TN 37831

Electric cell impedance measurement system is an attractive label-free technique to detect online cellular changes due to the presence, motility, morphology and viability of a cell [1]. Current state of the art uses co-planar electrodes. The use of VACNF based electrodes offers increased resolution and sensitivity. A VACNF embedded cell culture array is a promising tool in realizing a portable Integrated Cell Impedance Measurement system or Electric Cell Impedance Lab-on-a-Chip system.

The VACNF were grown on a quartz substrate according to the procedures established in [2]. A cell impedance measurement test system has been developed in our lab to test the functionality of the biosensor platform. A Lock-in-amplifier is used for producing the exciting signal and measuring the voltage across the VACNF electrodes. A Matlab program has been developed to control the amplifier over a frequency range (1~100kHz). Bovine Aortic Smooth Muscle cells were used in our preliminary experiments. The test was conducted for a range of frequencies over a period of 10~24 hours. During the test, the cells with cell culture medium, are placed into a well built around the VACNF electrodes, and the samples placed inside an incubator at 5% CO_2, and 37°C.

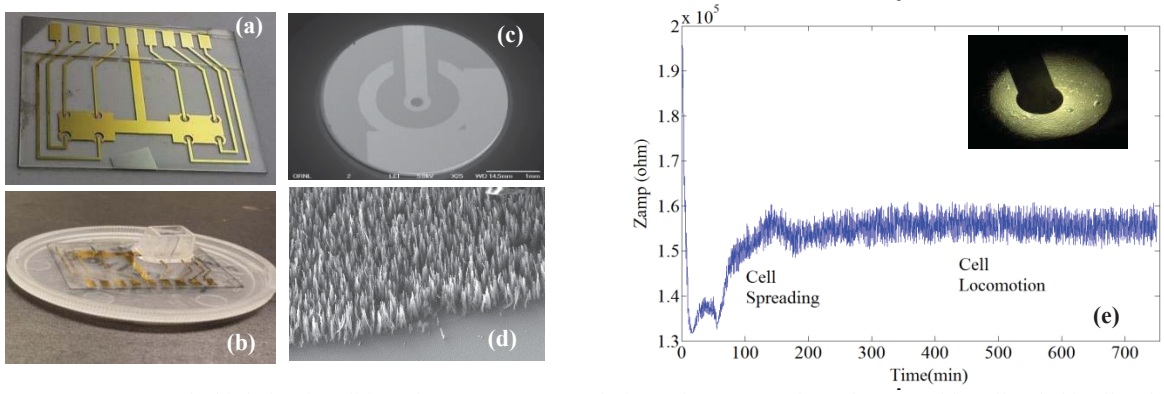

Fig. 1. (a) A VACNF embedded electric cell impedance measurement platform, (b) VACNF electrode array with well to hold cell and culture media, (c) a single well (d) VACNF forests on the electrode (e) Cell impedance variations over time (inset: cell spreading on the electrodes)

Preliminary results are shown in Fig.1. Fig. 1(a-d) shows the VACNF embedded cell impedance measurement chip. The chip contains 8 individual cell impedance measuring units. This allows for parallel measurements, and allows comparison with a reference solution. The plurality of such measurements also helps in the post processing of the real time data such as, averaging cell response, comparing responses of the different units, or cell growth rate. Fig.1 (e) shows a large change in impedance as cells adhere and spread-out on the VACNF electrodes surface. Currently additional experiments are underway which include the system long term measurements, quantifying the sensitivity and response time, increasing the sensitivity utilizing other electrode structures, and increasing the resolution using fibers at predetermined positions on chip.

References: [1]. C. R. Keese, I. Giaever, "A biosensor that monitors cell morphology with electrical fields", IEEE Engineering in Medicine and Biology Magazine, Vol. 13, no.3, pp. 402-408, 1994.
[2]. K.A. Mamun, F.S. Tulip, K.C. MacArthur, N. McFarlane, S.K. Islam, "Vertically aligned carbon nanofiber based biosensor platform for glucose sensor," International Journal on High Speed Electronics and Systems, Vol. 23, No. 01n02, March & June 2014.

Acknowledgements: This research was conducted at the Center for Nanophase Materials Sciences under the user program CNMS2014-094, which is sponsored at the Oak Ridge National Laboratory by the Office of Basic Energy Sciences, U.S. Department of Energy at the Center for Nanophase materials sciences (CNMS).

Noise Analysis of Confined Cell-free Protein Production

Patrick Caveney, Liz Norred, Jonathan Boreyko, Charles Chin, Jason Fowlkes, Pat Collier, Mitch Doktycz, Mike Simpson

Bredesen Center University of Tennessee, Biosciences Division, Center for Nanophase Material Sciences
pcaveney@vols.utk.edu, colliercp@ornl.gov, simpsonml1@ornl.gov

I. Introduction

Biological noise from episodic gene expression (bursting) has been observed in all kingdoms of life. The source of bursting is not known, but many sources have been proposed including confinement, crowding, gene looping, chromatin structure, and cellular life cycle[1]. In this paper, we use a cell free synthetic environment to isolate confinement from other potential sources of bursting. Previously, Karig et al. isolated and observed the intrinsic noise of gene circuits in cell-free environments[2]. In these experiments, EGFP was produced by cell-free protein synthesis (CFPS) with S30 *E. coli* extract inside confined femtoliter PDMS buckets. Here we follow a similar approach, but we look to find spatial correlations[3] that could lead to gene expression bursting. Fluorescence over time for each bucket was recorded during active transcription and translation, and the noise in these processes was isolated and characterized. This measured noise showed non-bursty (Poissonian) expression over the low expression regime, but we have found evidence that higher levels of expression are achieved through bursty processes that are heavily influenced by the degree of confinement.

II. Results

We measured expression noise (CV^2=variance in expression/mean expression level squared) in 137 different buckets with diameters of 2, 5, and 10 µm and equal heights of about 10 µm. We observe the transient for EGFP expression in each bucket is around one hour. In a Poissonian system, the mean and variance of the noise are equal. This leads to $CV^2 \propto 1$/protein abundance, where noise decreases as expression level increases. In the CFPS system, the burst size, number of protein produced from each mRNA transcript, factors into the noise as well. $CV^2 \propto$burst size/protein abundance. For all bucket sizes at the low end of expression, we observed the noise decreasing as expression level increased, as would be expected for Poissonian expression. However, the magnitude of the noise in this regime was smaller in the more confined buckets (**Fig. 1**), indicating that translational efficiency is affected by confinement.

Conversely at higher expression levels, there were strong deviations from Poissonian expression that we believe are caused by increased level of transcriptional bursting. These deviations from Poissonian behavior were found to be affected by bucket size (**Fig. 1**), and we hypothesize that greater levels of confinement lead to more pronounced expression burstiness.

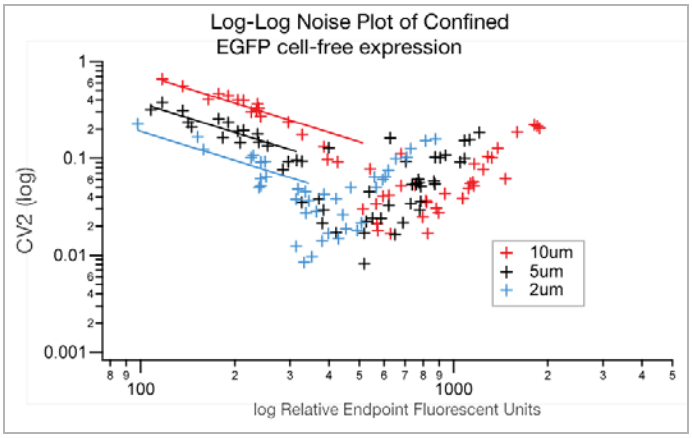

Figure 1. Noise plot for 10um, 5um, and 2um buckets.

III. Discussion

Our results indicate decreased translational efficiency and increased transcriptional burst rates in buckets with greater spatial confinement. Decreased translational bursting is indicated by the horizontal shifts of the curves to lower abundances with constant noise levels. Increased transcriptional bursting is indicated by the increase of noise at higher abundance levels. Confinement likely leads to spatial correlations between transcriptional machinery and the gene promoter, leading to repeated reinitiation of transcription. This hypothesis is being validated against computer models of the confined CFPS reaction.

References

[1] Hebenstreit, Daniel. "Are gene loops the cause of transcriptional noise?."*Trends in Genetics* 29.6 (2013): 333-338.

[2] Karig, David K., et al. "Probing cell-free gene expression noise in femtoliter volumes." *ACS synthetic biology* 2.9 (2013): 497-505.

[3] Fowlkes, Jason D., and C. Patrick Collier. "Single-molecule mobility in confined and crowded femtolitre chambers." *Lab on a Chip* 13.5 (2013): 877-885.

Silicon Photonics for Biosensing and Reconfigurable Photonics Applications

Petr Markov
Prof. Sharon Weiss Research Group, Vanderbilt University

The collaboration between CNMS and the Weiss group involves two themes: (1) Pushing the limits of on-chip, compact, label-free biosensors through the use of silicon-based photonics, and (2) Enabling ultra-fast, highly sensitive, power efficient devices for reconfigurable photonics.

1.) On-chip Compact Label-free Biosensors. Porous silicon (PSi) is an advantageous platform for biosensing due to its large surface area, ease of fabrication, and low cost. Block surface wave, waveguide, and optical ring resonator biosensors have been designed and experimentally realized for the capture of molecules of varying size and molecular weight (small molecules, nucleic acids, viruses, etc.). Highlighted below are PSi ring resonators with quality factors near 10^4 that exhibit detection sensitivities 3-fold greater than traditional ring resonator biosensors.

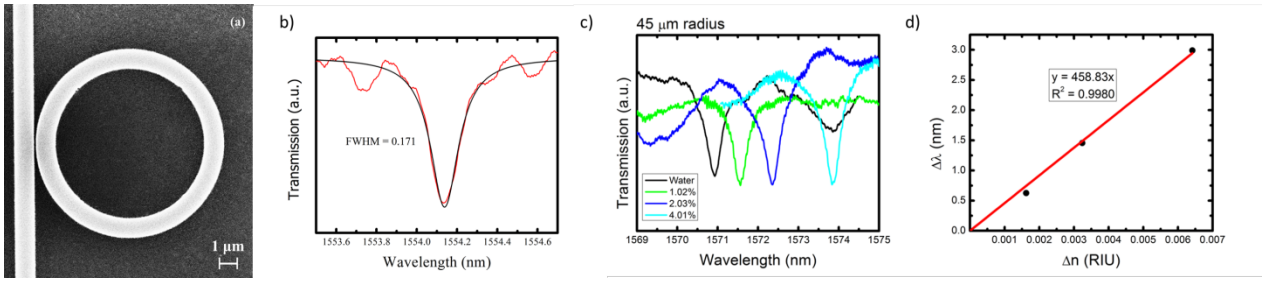

Fig 1. (a) Top view scanning electron microscope (SEM) image of a PSi ring resonator. (b) Transmission resonance of PSi ring resonator showing quality factor of 9000, as determined by a Lorentzian fit. (c) Transmission spectra of PSi ring resonator upon exposure to varying salt titrations. (d) Bulk detection sensitivity of 458 nm/RIU determined from (c).

2.) Hybrid Silicon / Vanadium Dioxide Electro-Optic Modulator. Motivated by the need for compact silicon-compatible optical switches operating near THz speeds, we demonstrate a hybrid Si/VO_2 electro-optic absorption modulator that is actuated using the electrically induced metal-insulator transition in VO_2. An ultra-small device footprint **(1μm × 500nm)** and competitive switching speed **(~2ns)** are realized. Furthermore, this device geometry enables determination of the spatial evolution of the VO_2 phase transition at nanosecond time-scales.

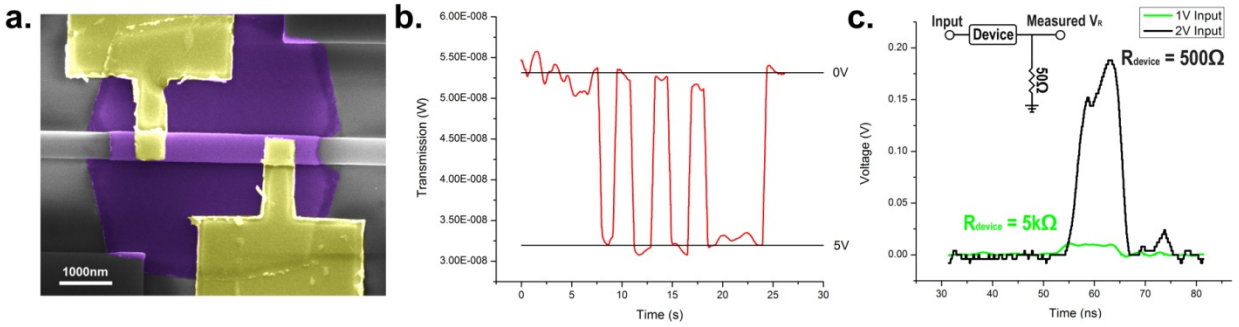

Fig 2. (a) SEM image of a hybrid Si-VO_2 linear absorption modulator. The lithographically placed VO_2 patch (purple) and gold contacts (yellow) are highlighted in false-color on the silicon waveguide. (b) Optical transmission of the hybrid linear absorption modulator as 5 V pulses are applied to the gold contacts. The demonstrated modulation depth is ~2 dB/μm. (c) Electrical response of the hybrid Si-VO_2 modulator to a 10ns voltage pulse below (green) and above (black) switching threshold. The inset shows the measurement setup schematic.

Surface Polarization Enhanced Seebeck Effects
in Vertical Multi-layer Metal/Dielectric/Polymer/Metal thin-film devices

Qing Liu[1], Hongfeng Wang[1], Yu-Che Hsiao[1], Xsin Wang[2], Bin Hu[1*]

[1] Department of Materials Science and Engineering, University of Tennessee, Knoxville, Tennessee, 37996

[2] Oak Ridge National Laboratory, Oak Ridge, TN 37831, USA

The entropy difference has been heavily used as the driving force to diffuse charge carriers between high and low temperature surfaces towards the development of Seebeck effects in thermoelectric devices. Specifically, the high and low temperature surfaces exhibit different internal energies of charge carriers in a medium, generating an entropy difference in internal energy of charge carriers. However, this driving force from entropy difference can cause an inverse relationship between Seebeck coefficient and electrical conductivity in the thermoelectric developments. Therefore, it is necessary to develop a new driving force, additional to entropy difference, for the diffusion of charge carriers to eliminate the negative effects caused by increased carrier concentration toward developing high Seebeck effects. In our work, we have explored temperature-dependent surface polarization, as an additional driving force, for developing Seebeck effects based on vertical metal/polymer/metal thin-film devices. In general, a hybrid metal/polymer interface can be used to restrict the thermal conduction but to allow the electric conduction. Here, the vertical thin-film design provides the possibility of developing temperature-dependent surface polarization for the development of Seebeck effects. The temperature-dependent surface-electrical polarization can come from the following two effects: (i) the coupling between local polarization ad thermal vibration on the polymer film surfaces through charge-phonon coupling mechanism and (ii) the interfacial dipoles modulated by the thermally activated Fermi electrons on the metal surfaces. These two effects combine to generate a difference in electrical polarization, namely temperature-dependent built-in electric field, across the polymer film between high and low-temperature metal surfaces. This temperature-dependent built-in electric field established by the surface polarization can drive the diffusion of charge carriers. To enhance the temperature-dependent surface polarization, a high dielectric layer can be inserted at the metal/polymer interface, increasing the built-in electrical field between high and low-temperature surfaces. The inserted dielectric interface can also allow the electrical conduction through transport but further hinder the thermal conduction through interface phonon scattering. In our study, the high dielectric film (MoO_3) was selected to enhance the temperature-dependent surface polarization in the vertical metal/dielectric/polymer/metal thin-film devices. We obtained enhanced Seebeck effects by using a high-dielectric MoO_3 layer through increasing the temperature-dependent polarization within the Al/MoO_3/P3HT:PCBM/Al thin-film device. Simultaneously, the electrical conductivity was also increased when the high-dielectric MoO_3 layer was used in the thin-film device. Therefore, using the high dielectric layer provides a possibility to cooperatively enhance the Seebeck coefficient and electrical conduction in organic materials.

Laser Induced Instabilities and Pattern Formation in Ultrathin Metal films under Water-Glycerol Solutions

S.Yadavali[1], R. Kalyanaraman[1,2]

July 30, 2014

[1]Department of Chemical and Biomolecular Engineering, University of Tennessee-Knoxville, TN 37996

[2]Department of Material Science and Engineering, University of Tennessee-Knoxville, TN 37996

Abstract

Spinodal dewetting of ultrathin metal films in air has been extensively studied with a view to manufacture self-assembled nanostructures for potential applications in plasmonic biosensing, chemical detection by surface enhanced raman scattering and soft-patterning. However, despite the scientific and technological promise of dewetting, one of its major limitations is that the length scales are limited by the surface tension (γ), strength of Hamaker forces, and film thicknes (h) as $\lambda = \sqrt{\frac{16\pi^3\gamma}{A}}h^2$. In this talk we show one possible way to overcome this limitation by dewetting metal thin films under liquid mixtures. The technique is demonstrated by fabricating metal nanoparticles of varying length scales and sizes from fixed initial film thickness of Au and Ag films under Water-Glycerol homogenous mixtures. The length scales and sizes of metal nanoparticles systematically varied with change in the composition of the mixture. This presentation will also provide a theoretical understanding of this novel liquid based dewetting process.

Realization of All-Dielectric Metamaterial Perfect Reflector

Parikshit Moitra[1], Brian A. Slovick[2], Zhi Gang Yu[2], S. Krishnamurthy[2], and Jason Valentine[3*]

[1]Interdisciplinary Materials Science Program, Vanderbilt University, Nashville, Tennessee 37212, USA
[2]Applied Optics Laboratory, SRI International, Menlo Park, CA 94015
[3]Department of Mechanical Engineering, Vanderbilt University, Nashville, Tennessee 37212, USA

Abstract:
Ohmic loss in metals at optical frequencies is a serious impediment to the application of plasmonic metamaterials at optical frequencies. Dielectric metamaterials utilize electric and magnetic Mie resonances in high index resonators and offer a potential lossless alternative to plasmonic metamaterials. Here, we present our work with all-dielectric metamaterials based on silicon cylinder unit cells. By controlling the height to diameter aspect ratio the spectral separation between the electric and magnetic dipole resonances has been maximized. The spectral separation of the resonances leads to the formation of a single negative metamaterial, i.e. either the real part of the effective permittivity, ε', or the effective permeability, μ', is negative. This leads to impedance mismatch to air ($z' = 0$), which in turn leads to broadband perfect reflection from a single layered metamaterial [1]. We experimentally demonstrated a 200 nm broad near-perfect reflectance band at optical frequencies with average reflectance over 98% and peak reflectance of 99% with single layer metamaterial [2]. The study is also extended to disordered metamaterials and it was found that near-unity reflection is preserved as long as resonator interaction is avoided. Due to their simple unit cell geometry and ability to tolerate disorder, all-dielectric metamaterial perfect reflectors are amenable to self-assembly based fabrication techniques and thus open the door to large scale implementations.

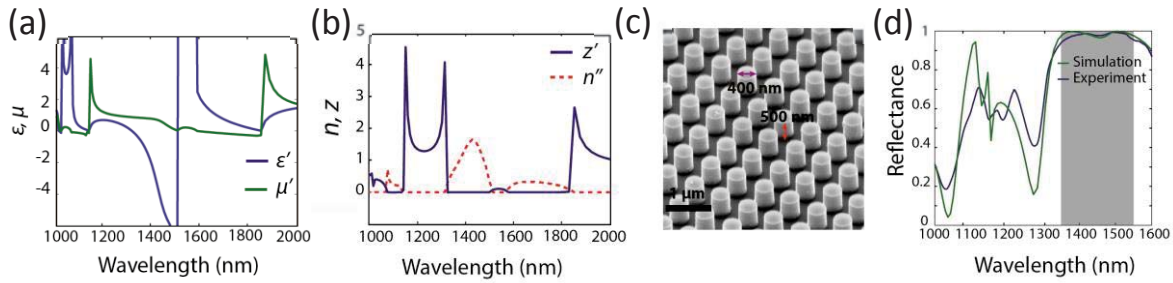

Fig. (a) Effective permittivity permeability of a periodic cylinder resonator-based metamaterial in an air background with a resonator geometry corresponding to D = 400 nm, H = 500 nm, and a periodicity of 660 nm. (b) Retrieved n'' and z' for the periodic metamaterial. (c) Isometric SEM images of periodic Si cylinder-based metamaterials. (d) Comparison between the numerically calculated and measured reflectance spectra of the metamaterials. The average reflectance between 1355 nm and 1555 nm (grey shaded region) is over 98.0%.

References:

[1] Slovick, B. *et al*. Perfect dielectric-metamaterial reflector. *Phys. Rev. B* **88**, 165116 (2013).
[2] Moitra, P., Slovick, B. A., Gang Yu, Z., Krishnamurthy, S. & Valentine, J. Experimental demonstration of a broadband all-dielectric metamaterial perfect reflector. *Appl. Phys. Lett.* **104,** 171102 (2014).

EELS Imaging for Quantitative Phase Fraction Mapping in OPV Materials

Ondrej Dyck[1], Sheng Hu[2], Bamin Khomami[2], and Gerd Duscher[1]

[1]Materials Science and Engineering, University of Tennessee, Knoxville, TN, USA
[2]Chemical and Biomolecular Engineering, University of Tennessee, Knoxville, TN, USA

Increasing interest in organic photovoltaics (OPV) [1] has resulted in a high scientific demand for microstructural device characterization. We introduce several techniques for studying OPV materials in a (scanning) transmission electron microscope (TEM/STEM) capable of electron energy-loss spectroscopy (EELS). We demonstrate detection capabilities for regio-regular poly(3-hexylthiophene) (P3HT) and [6,6]-phenyl C_{61}-butyric acid methyl ester (PCBM) which are the most commonly used donor/acceptor blend[1].

Commonly, energy filtered TEM (EFTEM) is used to generate contrast in OPV materials (fig. 1 left). This is performed by introducing a post-specimen energy window that only allows electrons of specific energies form the image [2-6]. This technique is only semi-quantitative at best. The plasmon energy shifts in the electron energy loss (EEL) spectrum are not quantitatively mapped across the sample neither can phase purity be determined. We present quantitatively mapped plasmon peak positions across a P3HT/PCBM bulk heterojunction (BHJ) (fig. 1 right) and, in conjunction, we also mapped absolute carbon density across the same area (fig. 2 left). P3HT is less carbon dense than PCBM and thus, the difference in carbon concentration is visible in the carbon density map [7]. Furthermore the carbon density map is reinterpreted as a quantitative phase ratio map that enables a clearer view into the BHJ structure (fig. 2 right).

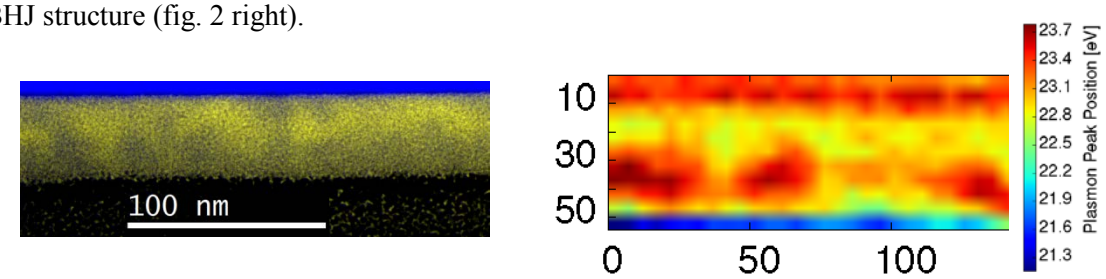

Figure 1. Left: EFTEM composite image showing contrast between P3HT (dark yellow) and PCBM (bright yellow). The Si substrate appears blue due to the strong plasmon in the lower energy range. Right: Plasmon peak position mapping (oriented 180 degrees compared to left image) shows similar features. Red indicates higher PCBM concentration.

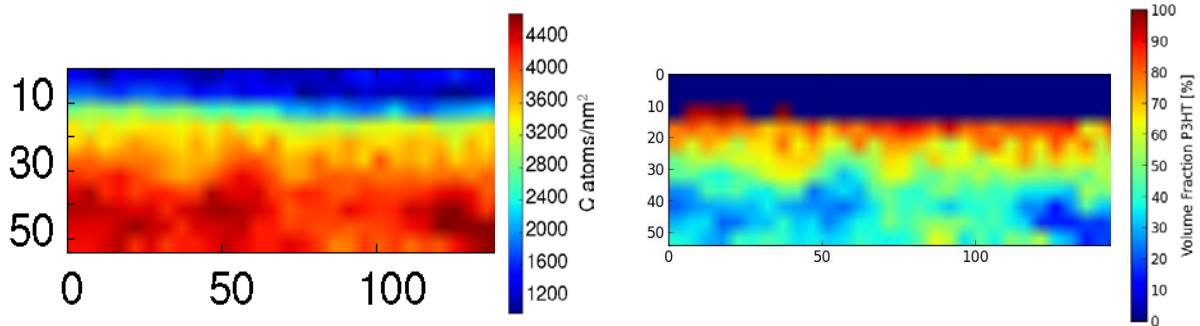

Figure 2. Left: Carbon density map shows features similar to the plasmon map (Fig. 1 right), indicating that carbon density may also be used to determine phase location. The data disagree at the top surface where a layer of Pt introduces anomalous results for the plasmon peak fitting routine. Lack of carbon conclusively shows no agglomeration of PCBM at the top surface. Right: Carbon density reinterpreted as phase ratio and displayed as % P3HT (volume fraction). We now have quantitative values for amount of P3HT and PCBM in the sample.

Controlling Solar Cell Active Layers via Surface Modification and Gas Expanded Polymer Annealing

Sarah Russell[†‡], Holly Stretz [†], Mark Dadmun [‖Δ], S. Michael Kilbey II [‖§], and Zach Seibers[⌋]*

[†]Department of Chemical Engineering, Tennessee Technological University, Cookeville, Tennessee 38505, United States
[‡]Center for Manufacturing Research, Tennessee Technological University, Cookeville, Tennessee 38505, United States
[‖]Department of Chemistry, University of Tennessee, Knoxville, Tennessee 37996, United States
[⌋]Department of Energy Science and Engineering, University of Tennessee, Knoxville, TN 37996, United States
[Δ]Chemical Sciences Division, Oak Ridge National Laboratory, Oak Ridge, Tennessee 37831, United States
[§]Department of Chemical and Bimolecular Engineering, University of Tennessee, Knoxville, TN 37996, United States

Controlling and characterizing the morphology of the active layer in organic photovoltaics (OPVs) is essential for improving sunlight-to-energy conversion. While the most widely used active layer is based on a blend of the donor-type polymer, poly(3-hexylthiophene) (P3HT) and the fullerene [6,6]-Phenyl-C_{61}-butyric acid methyl ester (PCBM), various thermal or solvent annealing protocols are required to achieve modest power conversions efficiencies of ~5%. Here the use of gas expanded polymer (GXP) annealing, which relies on varying pressure conditions by introducing and removing CO_2 gas at a constant flow rate, is investigated as a process to improve the dispersion of PCBM within a P3HT film. GXP annealing causes the thin film to swell and deswell which leads to a change in crystallinity of the polymer P3HT, as observed by X-ray diffraction, UV-Vis spectroscopy and contact angle measurements. The exact morphology of the active layer is difficult to characterize directly, due to limited nanoscale visualization techniques. Neutron reflectivity provides a way in which the dispersion of PCBM within the P3HT polymer film can be described. Neutron reflectivity, which is sensitive to the PCBM depth profile, suggests that pressure oscillation range of 875-900 psi causes PCBM to distribute more uniformly throughout the film compared to an as-cast sample. Modification of the film/substrate interface using a surface-grafted P3HT brush followed by GXP annealing can also be used to alter the active layer morphology. The efficacy of this surface modification will be described.

Underlying Mechanism of the Enhanced Power Conversion Efficiency of Organic Inverted Solar Cell

Sanjib Das,[1] Jong K. Keum,[2,3] James F. Browning,[3] Jihua Chen,[2] Changwoo Do,[3] Gong Gu,[1] Pooran C. Joshi,[4] Adam J. Rondinone,[2] Kunlun Hong,[2] David B. Geohegan,[2] Kai Xiao[2]

[1]Department of Electrical Engineering and Computer Science, University of Tennessee, Knoxville, TN, 37996, USA. [2]Center for Nanophase Materials Sciences, Oak Ridge National Laboratory, Oak Ridge, TN, 37831, USA. [3]Neutron Scattering Science Divisions, Oak Ridge National Laboratory, Oak Ridge, TN, 37831, USA. [4]Material Sciences and Technology Division, Oak Ridge National Laboratory, Oak Ridge, TN, 37831, USA.

Organic inverted solar cells (OISCs) have demonstrated long lifetime as well as high power conversion efficiencies (PCE) which have now exceeded 10%, the threshold for commercial application. While the increased lifetime as compared to regular organic solar cells (OSCs) is associated with the oxidation-free indium tin oxide cathode, the mechanism for the improved PCE has so far been unclear. In this project, we investigated the underlying mechanism of this improved PCE of OISCs and found that it is due to the diffusion of the electron acceptor (EA) material into the electron transporting layer, *poly [(9,9-bis(3'-(N,Ndimethylamino) propyl)-2,7- fluorene)-alt-2,7-(9,9–dioctylfluorene)]* (PFN). This diffusion increases the interfacial contact between the EA material and PFN, resulting in higher short circuit current density. Neutron reflectometry and cross sectional transmission electron microscopy clearly show the existence of diffused EA into the PFN layer. The diffusion of EA into the PFN layer is thought to occur when electron donor (ED)/EA solution is spun-cast on top of the PFN layer. Swelling of the PFN layer by the solvent appears to allow the nano-sized EA clusters to diffuse into the swollen PFN layer along with the solvent. When *1,8- diiodoctane* (DIO) is added to the casting solution as the solvent additive, more EA clusters diffuse into PFN layer resulting in higher device performance.

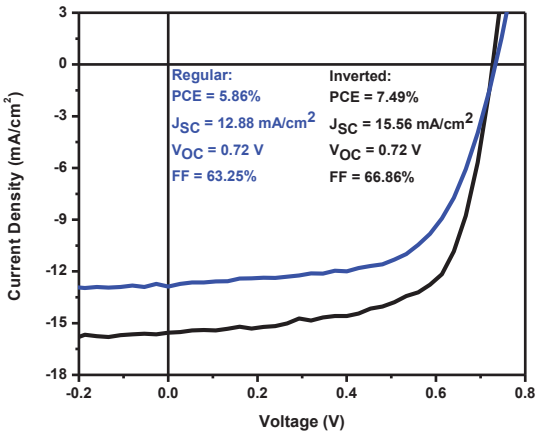

This research was conducted at the Center for Nanophase Materials Sciences (CNMS), High Flux Isotope Reactor (HFIR) and Spallation Neutron Source (SNS) which are sponsored at Oak Ridge National Laboratory by the Scientific User Facilities Division, U.S. Department of Energy.

Experimental Studies on Properties of Photoexcited Excitons and Charge Dissociation Processes in $CH_3NH_3PbI_{3-x}Cl_x$ Perovskite Solar Cells

Yu-Che Hsiao, Ting Wu, Mingxing Li, Ilia Ivanov, Bin Hu

Department of Materials Science and Engineering, University of Tennessee, Knoxville, Tennessee, 37996

Mixed lead halide perovskite materials ($CH_3NH_3PbI_{3-x}Cl_x$) have recently become extremely attractive photovoltaic candidates to develop high-efficiency organic solar cells. These recent developments bring a tremendous demand on revealing the properties of photoexcited states and the charge dissociation processes to further enhance the photovoltaic performance in mixed lead halide perovsikte solar cells. On the other hand, due to the low band-gap property that a large amount of separated electron-hole pairs with low binding energy, namely Wannier exciton, can be generated within perovskite crystalline domains under photoexcitation. Therefore, the low binding energy electron-hole pairs and internal spontaneous polarizations provide un-doubtable advantage to develop high-efficiency mixed lead halide perovskite based solar cells. For fully investigating the insight of photovoltaic response of mixed lead halide perovskite material, we introduce magnetic field effects of photocurrent (MFE_{PC}) and photoluminescence (MFE_{PL}) to study the properties of photoexcited excitons and the charge dissociation processes based on the planar-heterojuction ITO/PEDOT/$CH_3NH_3PbI_{3-x}Cl_x$/PCBM/TiOx/Al device. In general, magnetic field effects of photoluminescence can be conveniently developed when a magnetic field changes the density of light-emitting states by re-orientating the singlet-triplet ratio through spin mixing. It has been found that magnetic field effects of photoluminescence can be conveniently generated based on the following three processes. First, a photoexcitation is allowed to generate singlet excitons due to spin-selection rule. Second, the singlet excitons can partially convert into triplet excitons through singlet-triplet transitions governed mainly by spin flipping mechanisms through internal magnetic interactions from hyperfine or spin-orbital coupling which can be induced by heavy lead atoms. Third, a magnetic field can perturb the singlet-triplet transitions by contributing to the spin flipping and consequently changes the singlet/triplet density, leading to magnetic field effects of photoluminescence, namely magneto-photoluminescence. Therefore, magneto-photoluminescence can elucidate the properties of photoexcited excitons in lead halide perovskite materials. On one hand, the magnetic field effects of photocurrent can be observed when a magnetic field changes the singlet/triplet population by perturbing the singlet-triplet transitions in mixed lead halide perovskite solar cells. This is because the singlets and triplets excitons can exhibit different dissociation rates driven by either different energies or different polarizations towards the generation of free charge carriers. Clearly, magnetic field effects of photoluminescence and magnetic field effects of photocurrent can elucidate more insight of the properties of photoexcited excitons and the charge dissociation processes in the perovskite solar cells based on ITO/PEDOT/ $CH_3NH_3PbI_{3-x}Cl_x$ /PCBM/TiOx/Al device structure, and toward to higher photovoltaic efficiency.

Unravelling the Spin-Dependent Excited States in Organo-Metal Halide Perovskite

Ting Wu[1], Yu-Che Hsiao[1], Mingxing Li[1], Nam-Goo Kang[2], Jimmy W. Mays[2], Bin Hu[1]*

[1] Department of Materials Science and Engineering, University of Tennessee, Knoxville, Tennessee, 37996, USA

[2] Department of Chemistry, University of Tennessee, Knoxville, Tennessee, 37996, USA

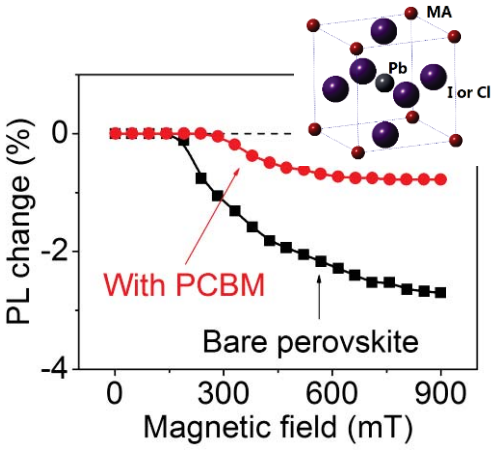

Magneto-photoluminescence from Perovskite

Organo-metal halide perovskite, as a new promising candidate for either photovoltaics or lasing applications, has been paid more and more attention during the past two years. Our work targets on an open question on the nature of photoexcited states in this type of materials with the aim of the magnetic and electric field-dependent photoluminescence. We observe, for the first time, that a magnetic field can decrease the photoluminescence intensity in perovskite under appropriate high excitation intensity and consequently generates a magneto-photoluminescence. This experimental result leads to a hypothesis that the excited states, either from photoexcitation or charge recombination, are populated in different spin states, forming light emitting and non-light emitting states, with an inter-conversions from high-energy states to low-energy states via exothermic process and spin flipping. Furthermore, we demonstrate that introducing the donor/acceptor (D/A) interface of perovskite/PCBM can affect both amplitude and line-shape in magneto-photoluminescence. This suggests that the D/A interface can dissociate the photoexcited excitons in bulk perovskite film and consequently changes the force-constant of inter-conversions. On the other hand, we show, by using electric field-dependent photoluminescence, that the D/A interface is formed with a local electric field under photoexcitation. This local electric field provides a driving force to dissociate the photoexcited excitons inside the perovskite film. Clearly, our magneto- and electro-photoluminescence studies provide a new understanding on the nature of spin-dependent excited states in perovskite materials from the perspective of spin.

In-situ High Temperature X-ray Diffraction Study of Formation of the Thin Film PV Absorbers $(Cu_xAg_{1-x})(In_xGa_{1-x})Se_2$ and Cu_2ZnSnS_4

H. Tong[1], C. Muzzillo[1], S. Wilson[1], J. Keum[2], A. Rondinone[2], K. More[3], L. Pogue[4], A. Rockett[4], S. Soltanmohommad[5], W. N. Shafarman[5], T. J. Anderson[1]

[1] Department of Chemical Engineering, University of Florida, Gainesville, FL 32611

[2] Nanomaterials Synthesis and Functional Assembly, Oak Ridge National Laboratory, Oak Ridge, TN, 37831

[3] Materials Science and Technology Devision, Oak Ridge National Laboratory, Oak Ridge, TN, 37831

[4]Department of Materials and Engineering, University of Illinois at Urbana-Champaign,61801

[5]Institute of Energy Conversion, University of Delaware, Newark, DE, 19716

High temperature XRD (HTXRD) experiments were performed at the CNMS to identify reaction pathways and to quantitatively determine kinetic parameters during selenization and sulfurization of chalcopyrite and kesterite materials used for absorbers in photovoltaic applications. A stainless-steel gas-tight reaction chamber equipped with x-Ray transparent windows, which were partially developed at CNMS, were used in these experiments. Recent improvement by carbon coating of these chambers using plasma enhanced chemical vapor deposition system at CNMS allowed for sulfurization experiment without corrosion of the chamber to a temperature of 450 °C.

The selenization of the chalcopyrite (Cu,Ag)(Ga,In)Se_2 (ACIGS) was of interest as improvement method to increase the bandgap energy of Cu(Ga,In)Se_2 (CIGS) to a more optimal value. The lower melting temperature of Ag compared to Cu produces a simpler phase diagram, which better avoids secondary phases during processing and potentially lowers the processing temperature and therefore lowers production costs. In particular, selenization of metal CIG precursors leads to large void fractions in the absorber near the substrate interface. The addition of Ag was demonstrated in this program to reduce the void fraction.

Previous HTXRD studies performed at CNMS showed that the activation energy for formation of $(Ag_yCu_{1-y})(In_xGa_{1-x})Se_2$ (ACIGS) during selenization of metal precursor structures with a 5 nm ("Ag-5") or 32 nm ("Ag-32") Ag interlayer is inversely related to Cu/(Cu+Ag) even with such small at.% of Ag. The effects of increasing the Ag content in the precursor was explored in this study using HTXRD. ACIGS PV devices were fabricated and characterized by at the University of Delaware in parallel with the HTXRD experiments at CNMS. SLG/Mo/Ag-Ga/In/CIG samples with Ag/(Cu+Ag) = 0.23, 0.50, and 0.73 were studied and compared to the SLG/Mo/CIG and the SLG/Mo/Ag-Ga/CIG samples from previous study. The general reaction pathway of $Ag(Ga_xIn_{1-x})_2 + \gamma - (Cu_yAg_{1-y})_9(Ga_zIn_{1-z})_4 + Se_{vapor} \rightarrow ACIGS$ was identified. Experiment and data analysis to extract kinetic parameters for ACIGS formation is currently underway.

The performance of thin film cells based on the kesterite material Cu_2ZnSnS_4 (CZTS) has shown rapid improvement in performance. The high earth abundance of the elements makes CZTS a more attractive system for large scale PV deployment. Initial HTXRD experiments on SLG/Mo/Cu-S/Sn-S precursors show significant reaction pathway differences with and without the addition of S to the reaction ambient. The large number possible compounds of similar crystal structures and lattice spacing shows several possible reaction pathways when using XRD alone. Additional characterization using Raman scattering is in progress to aid in pathway identification. .

In-situ investigation of chemical bath deposition of CdS via localized surface plasmon resonance (LSPR) spectroscopy

[1]H. Taz, [2]R. Ruther, [3]A. Malasi, [3]S. Yadavali, [4]C. Carr, [2]J. Nanda, [3, 4]R. Kalyanaraman
[1]Bredesen Center, University of Tennessee, Knoxville, TN 37996
[2]Materials Science and Technology Division, Oak Ridge National Laboratory , Oak Ridge, TN 37831
[3]Department of Chemical and Biomolecular Engineering, University of Tennessee, Knoxville, TN 37996
[4]Department of Materials Science and Engineering, University of Tennessee, Knoxville, TN 37996

Abstract:
Chemical bath deposition (CBD) of semiconductor materials is an excellent way to reduce the cost of manufacturing solar cells. An understanding of the CBD deposition technique, especially during early stages of deposition can lead to better control of morphology and eventually, photovoltaic properties. Here we have developed an in-situ technique based on dynamic measurements of the localized surface plasmon resonance (LSPR) from Ag nanoparticles to understand the deposition process of Cadmium Sulfide (CdS). By combining in-situ LSPR with ex-situ measurements by optical spectroscopy, Raman Spectroscopy, and Scanning electron microscopy, we have developed a plasmonics-based effective medium model to explain the deposition process of CdS by dynamic chemical bath deposition. In addition, SERS effect of the CdS observed due to the presence of the Ag NPs could prove very useful in the study of batteries or in signal sensing. Therefore this study and its results have implications in other energy-related research.

Junction size dependence of tunneling electroresistance effect in e-beam patterned $BaTiO_3$ ferroelectric tunnel junctions

Amit V. Singh[1], M. Althammer[1], K. Rott[2], G. Reiss[2], A. Gupta[1]
[1] Center for Materials for Information Technology, The University of Alabama, Tuscaloosa, Alabama, 35487, USA
[2] Thin Films and Physics of Nanostructures, Department of Physics and Center for Spinelectronic Materials and Devices, Bielefeld University, 33615 Germany

Abstract: A ferroelectric random access memory (FRAM) device compared to conventional RAMs or even magnetic tunnel junction based RAMs has several advantages, viz., one-two orders of lower power consumption and faster switching performance[1]. In recent years, due to technological advancements it has been possible to demonstrate functionality of such devices[2-8]. Two device geometries[9] are used for measurements reported in the literature. In the first, a conducting probe is used as the top electrode and in the second, it is used in contact with a metal or conducting metal oxide top electrode. The latter geometry has a closer resemblance with the actual device and is also used in this study. We use a multilayer stack (STO/$La_{0.7}Sr_{0.3}MnO_3$(~50nm)/$BaTiO_3$(2-2.5nm)/Ru(~10nm)) grown on strontium titanate (STO) substrate. We define circular patterns on the sample with diameters ranging from ~100 nm to 1 µm using e-beam lithography. The Ru top electrode is defined using (a) Ru deposition before pattering followed by ion-milling, and (b) Ru deposition after pattering and then lift-off. We do a systematic study of the area dependence of tunnel electroresistance (TER) effect with respect to the size of patterns. We also demonstrate switching behavior of STO/LSMO/BTO/Ru and compare it to that of STO/LSMO/BTO. Figure 1 shows I-V curves measured with Pt-coated AFM probe (diameter 30-50 nm) on BTO surface and on Ru patterns of sizes 180 and 225 nm, respectively. Figure 2 shows the difference in I-V characteristics for positive and negative poling voltages for 180 nm pattern.

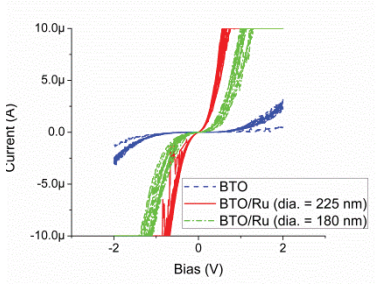

Figure 1: Comparison of I-V characteristics on BTO surface and 180, 225 nm Ru patterns.

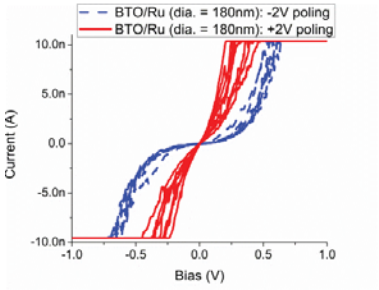

Figure 2: Comparison of I-V characteristics for opposite poling of 180 nm Ru pattern.

REFERENCES

1. X. Luo *et al.*, J. Appl. Phys. **111**, 074102 (2012).
2. A. Crassous *et al.*, Appl. Phys. Lett. **96**, 042901 (2010).
3. M. Gajek *et al.*, Nature Mater. **6**, 296 (2007).
4. V. Garcia *et al.*, Science **327**, 1106 (2010).
5. V. Garcia *et al.*, Nature (London) **460**, 81 (2009).
6. A. Gruverman *et al.*, Nano Lett. **9**, 3539 (2009).
7. G. Kim *et al.*, Appl. Phys. Lett., **102**, 052908 (2013).
8. P. Maksymovyc *et al.*, Science, **324**, 1421 (2009).
9. E.Y. Tsymbal *et al.*, MRS Bulletin 37.02 (2012): 138-143.

Skyrmionic MnSi nanowires on Si: SiO2 layer as a catalyst assistant for the CVD growth

Siwei Tang[1,2], Ivan Kravchenko[1], Jieyu Yi[1,2], Guixin Cao[1,2], Jane Howe[1], David Mandrus[2], and Zheng Gai[1]

[1]Center for Nanophase Materials Sciences, Oak Ridge National Laboratory, Oak Ridge, TN 37831, USA
[2]Department of Materials Science and Engineering, University of Tennessee, TN 37996, USA

Magnetic skyrmion, a vortex-like spin-swirling object recently observed in chiral-lattice magnets, are of great interest to future spin-electronic related data storage and other information technology applications. We report that single crystal helimagnetic MnSi nanowires could be synthesized in large amounts via SiO2 thin film assisted chemical vapor deposition comparing to previous reports, SiO2 plays an important role in controlling amount of diffusing Si to achieve relative low supersaturation ratio. Growth process is controlled so as to find the optimized parameters. Based on that, a temperature-time-distance growth phase diagram is plotted. The ac and DC magnetic properties of MnSi nanowires reveal the persistent of the helimagnetic and skyrmion magnetic ordering in the one-dimensional wires.

Oscillatory local density of states on $Cr_{1/3}NbS_2$ surface

Jieyu Yi [a,b], Siwei Tang [a,b], Ling li [a], Guixin Cao [b],
David Mandrus [a], and Zheng Gai [b]

[a] *Department of Materials Science and Engineering, University of Tennessee, Knoxville, TN 37996, USA*

[b] *Center for Nanophase Materials Sciences, Oak Ridge National Laboratory, Oak Ridge, TN 37831, USA*

Helimagnet has spins arranged in ferromagnetic planes, and the direction of the magnetism varies in a certain angel between adjacent planes, which makes it promising in spintronics application. $Cr_{1/3}NbS_2$ is a helimagnet with layered structure which has recently drawn a lot of attentions because of the structure similarity with skyrmion material. Non-center symmetry of the materials renders the helimagnetism and further skyrmion configuration if properly modified. While in some of helimagnets, Skyrmion configuration may appear, as a particle- like spin texture with spins aligned in a vortex shape, which was proven to be able to carry novel Hall effects and current driven with ultra low current density. In this work, we performed STM and STS studies on cleaved surface of $Cr_{1/3}NbS_2$ single crystal at variable temperature. Two different kinds of surface morphologies were observed on the terraces with atomically resolved resolution. Local density of state (LDOS) on the surface at various terminations has been studied across transition temperature. Oscillatory LDOS peaks were observed on one kind of terraces which is explained as the existence of a 2D electron gas on the surface.

A Study of Formation Mechanism of Mn Containing Precipitates during Homogenization in 6xxx Series Aluminum Alloys

Gongwang Zhang[a], Yi Han[b], Yi Xu[b], Hiromi Nagaumi[b], Sha Gang[c], Chad M. Parish[d], Donovan N. Leonard[d], Tongguang Zhai[a]

[a] Department of Chemical and Materials Engineering, University of Kentucky, Lexington, KY 40506, USA
[b] Suzhou Research Institute for Nonferrous Metals, Suzhou, Jiangsu 215026, China
[c] School of Materials Science and Engineering, Nanjing University of Science and Technology, Nanjing, Jiangsu, 210094, China
[d] Microscopy Group, Materials Science & Technology Division, Oak Ridge National Laboratory, Oak Ridge, TN 37831, USA

6xxx series Al alloys with addition of Mn and Cr were homogenized at temperatures ranging from 350 °C to 550 °C after casting. α-Al(MnCrFe)Si dispersoids were formed in the alloys, significantly retarding recrystallization by pinning dislocations during downstream thermomechanical processing (Fig. 1). The formation mechanism of these dispersoids has not been fully understood. In this work, it was found that during early annealing at 460 °C for 15 min, a lathe-shape Q-AlMgSiCu phase and Mn clusters were observed (Fig. 2) before the formation of these dispersoids in the alloys. 3D atom-probe experiments revealed that there was an early segregation of Mn and Cr at the Q and matrix interface before decomposition of Q phase. It appeared that the Q-phase was the precursor phase formed for the formation of α dispersoids. In the early stage of α-phase formation, Mn first segregated at the Q-phase/matrix interface, before decomposition of the Q-phase. After the Q-phase decomposition, Mn (Cr) formed clusters in place of the Q-phase, as shown in Fig. 2(a). Si subsequently participated to form α-dispersoids, as revealed by atom probe.

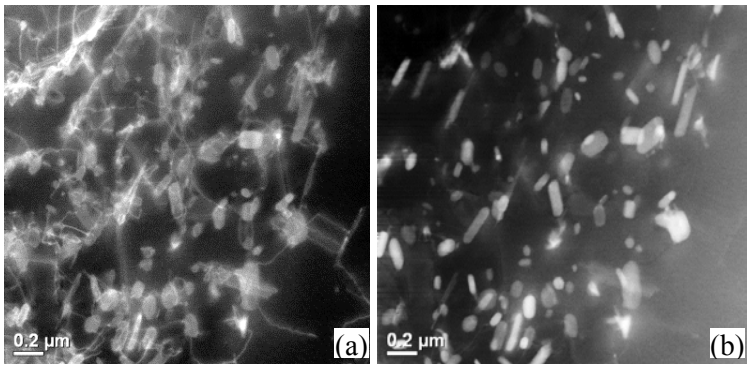

Fig. 1. (a) α-dispersoids interacting with dislocations in the 6xxx series Al alloy hot forged (80% forging ratio), ADF contrast; (b) HAADF (Z contrast) of α-dispersoids in the same area as in (a).

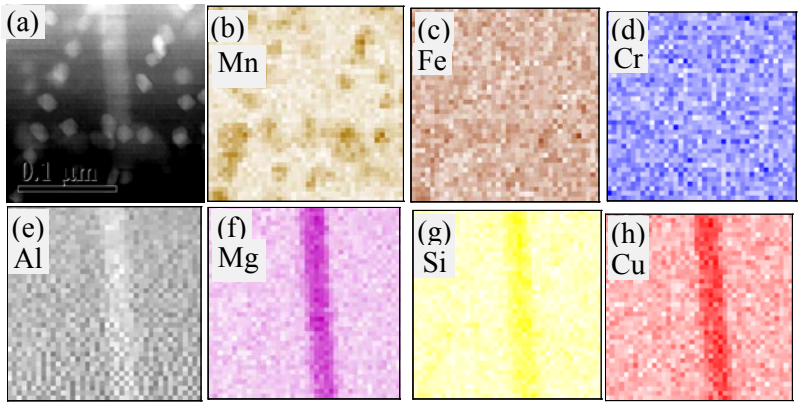

Fig. 2. (a) STEM micrograph of precipitates; (b-h) EDS elemental maps of Mn, Fe, Cr, Al, Mg, Si, and Cu, respectively, in the same area as in (a) in early stage of homogenization (homogenized for 15min at 460°C, direct heating). Lathe-shape precipitate is Q-phase, and dispersoids are Mn clusters.

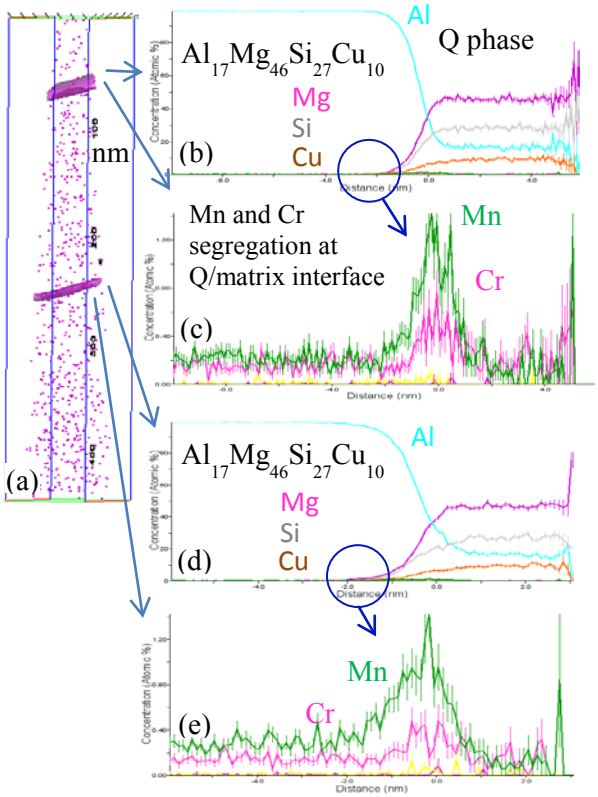

Fig. 3. (a) Atom-probe micrograph of Q-phase; (a) and (d) elemental distributions of the Q-phase particles; (c) and (e) segregation of Mn and Cr at the Q-phase and matrix interface (slow heating to 350°C, then quench).

Quantitative Understanding 3-D Effects of Constituent Particles on Fatigue Crack Initiation in High Strength Aluminum Alloys by FIB

Yan Jin*, Pei Cai*, Wei Wen*, Chad M Parish**, Donovan N Leonard** and Tongguang Zhai*
*Chemical and Materials Engineering Dept., University of Kentucky, Lexington, KY 40506
**Center for Nanophase Materials Sciences, Oak Ridge National Lab, Oak Ridge, TN 37831

Three types of fatigue cracks were found occurring at the Fe-bearing particles in AA2024 T351 and AA7075 T651 Al alloy plates (Fig. 1), type-1: micro-cracks never propagated into the matrix; type-2: cracks arrested just after propagating into the matrix; and type-3: propagating cracks. Cross-sectioning of these cracks using FIB revealed that types-1, 2 and 3 cracks were associated with the particles in thin, (<3 μm), medium (3 μm-6 μm) and thick (>6 μm) thickness, respectively. Cracks followed the 111 plane with the minimum twist angle at the particle/matrix interface, verified by FIB cross-sectioning (Fig. 2). The resistance to crack growth at the interface was measured to be a Weibull function of the twist angle of crack plane deflection at the interface (Fig. 3). A quantitative model was developed to simulate the growth behaviors of the micro-cracks from the particles in 3-D, by taking into account both driving force and resistance for the micro-cracks. The model could quantitatively explain why there were three-types of fatigue cracks formed at particles on the surface in the high strength Al alloys (Fig. 4).

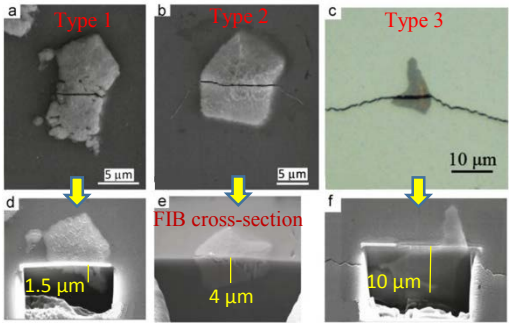

Fig. 1 Three types of fatigue cracks from particles in an AA2024 T351 alloy.

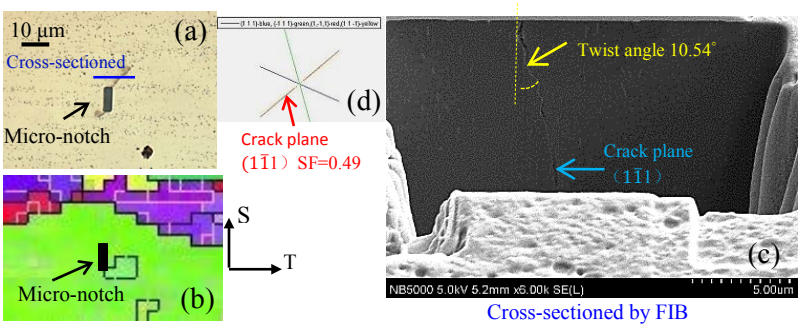

Fig. 2 (a) mimic type3 (10x12x3 μm^3) micro-notch using FIB; (b) EBSD mapping of the area in (a); (c) cross-section of crack plane showing the twist angle, and (d) four intersection lines between {111} planes and surface.

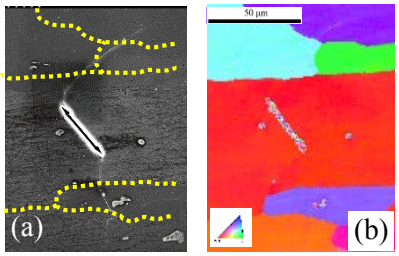

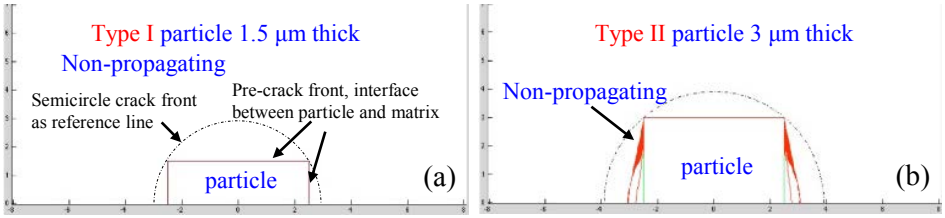

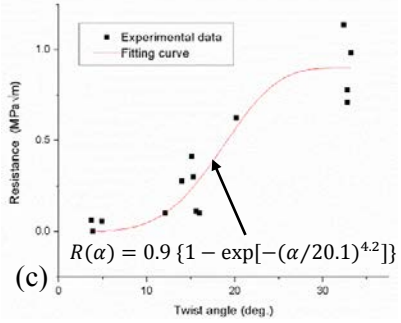

Fig. 3 (a) fatigue crack initiated from a micro-notch fabricated using FIB (b) EBSD mapping around notch and (c) Resistance to fatigue crack growth across GBs vs. twist angle of crack at GBs quantified by tracking crack propagation.

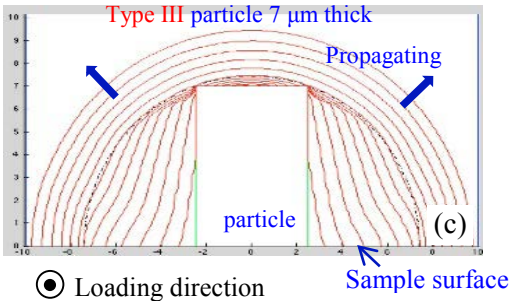

Fig. 4 Simulated growth behaviors of three types of micro-cracks from particles with three different characteristic thicknesses in AA2024 T351, (a) type-1 crack: non-propagating; (b) type-2 crack: non-propagating; and (c) type-3 crack: propagating. The results are consistent with the experimental observations.

Entropic Softening of Graphene

Ryan Nicholl
ryan.j.nicholl@vanderbilt.edu
Prof. Kirill Bolotin, Vanderbilt University

The stiffness of a material is predominantly the result of one of two forces, interatomic or entropic. The stretching of bulk materials is usually governed by the properties of its crystal lattice. As a result of these interatomic forces the materials tend to be relatively hard. Low dimensional systems, like DNA or polymer chains, have high susceptibility to Brownian motion and thermal fluctuations, making them easy to crumple. Any applied force simply un-crumples without stretching the bonds in the material. The mechanics of these materials are therefore entropic in nature, yielding much softer materials. Two-dimensional systems like graphene offer an ideal platform to study the overlap between "hard" and "soft" materials. On one hand, graphene is a crystalline material that has a very high in-plane stiffness of 340 Nm^{-1} [1] due to its strong covalent bonding. On the other hand, the low dimensionality of suspended graphene membranes allows fluctuations to play a dominating role in determining its mechanical properties.

Here we show the first evidence for entropic softening in an atomically thin two-dimensional graphene system. By measuring the geometrical profile of graphene optically under electrostatic loads we can extract its mechanical characteristics. The in-plane stiffness of graphene ranged between 50-340 Nm^{-1} for measured built-in stress between 0.02-0.14 Nm^{-1}.

This result may warrant a re-evaluation of current understanding within the field of graphene mechanics or pave the way to new advances in novel 2D material based NEMS devices for next generation applications.

[1] C. Lee, X.Wei, J.W. Kysar, and J. Hone, "Measurement of the elastic properties and intrinsic strength of monolayer graphene." Science (New York, N.Y.), vol. 321, no. 5887, pp. 385–8, Jul. 2008, ISSN: 1095-9203. DOI: 10.1126/science.1157996.

Structure modification of TiO_2 nanoparticles for photocatalysis

Mengkun Tian

University of Tennessee, Knoxville, TN, USA

Abstract: The photo-catalytic properties of TiO_2 are much more effective in nanoparticles than in the bulk form due to the particles' large surface area which directly interacts with the environment. However, the large band gap of TiO_2 limits the absorption of solar energy. Here we show the modifications of the band gap of TiO_2 by doping elements, reducing oxygen content at the surface, creating defects, inducing a new phase and modifying the TiO_6 octahedra of TiO_2. We used monochromated analytical TEM /STEM and nano-beam electron diffraction to characterize the properties of all these TiO_2 nanoparticles and finally compared the effect of band gap shifting from different modifications of TiO_2.

PHASE STABILITY AND ULTRAFAST RESPONSE OF VANADIUM DIOXIDE NANOPARTICLES

R. E. Marvel,[1] C. L. McGahan,[1] A. Boulesbaa,[2] S. T. Retterer[2] and R. F. Haglund, Jr.[1]
Department of Physics and Astronomy, Vanderbilt University, Nashville, TN
Center for Nanophase Materials Sciences, Oak Ridge National Laboratory, Oak Ridge, TN

Size and interface effects strongly influence the properties and existence of many materials on the nanometer scale. Beyond quantum confinement and strain affects, phase diagrams of many materials are altered at the nanoscale, in some cases even eliminating phases. The shifts in phase stability become especially important for metal oxides that exhibit phase diagrams with many components, narrow phase space stability windows and distinctive properties between components.

The vanadium oxygen system exhibits nearly twenty oxides, eight of which have metal insulator transitions (MIT); vanadium dioxide (VO_2) has a room temperature phase transition (67°C) with a large change in resistance (five orders of magnitude). The transition occurs on femtosecond time scales and is accompanied by a large change in the dielectric function, making it a promising material for high-speed silicon-based photonic devices [(a), (b)]. These applications can be realized by fabricating nanometer-scale patches on Si photonic structures using electron beam lithography. Typically, a deposited amorphous VO_x film is annealed to initiate solid phase crystallization, producing VO_2 films exhibiting the MIT.

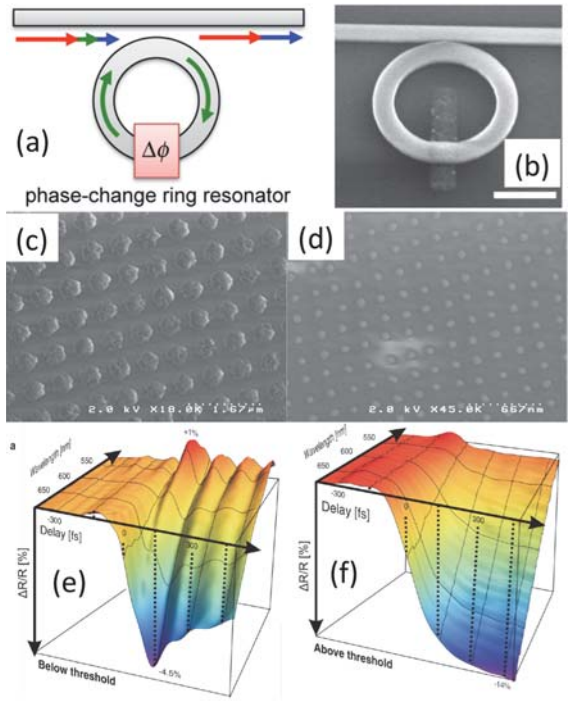

(a) Schematic of hybrid Si-VO_2 ring resonator and (b) SEM showing VO_2 patch [1]. Nanoparticle arrays (c) 400 nm and (d) 100 nm diameter. Femtosecond white-light reflectivity on VO_2 film showing (e) coherent phonon response in monoclinic phase and (f) incoherent response above threshold for monoclinic-to-rutile phase transition [2].

We report results of recent studies at Vanderbilt and the Center for Nanophase Materials Sciences addressed to (1) the stability of vanadium dioxide thin films and nanostructures at nanometer length scales, and (2) the femtosecond response of the nanostructures as a function of size, pulse duration and laser intensity. For example, sapphire and TiO_2 both exhibit good lattice matches with VO_2 while silicon does not; does this affect stability? Surface atoms significantly affect phase stability for nanoparticles in the sub 20 nm range; does this also apply to nanoparticles on substrates? How broad are the windows of phase stability and how are they affected by substrate choice and size? And perhaps most critically, how are these properties affected by repetitive femtosecond excitation?

[1] "An all-optical, reconfigurable, ultra-compact silicon ring resonator controlled by a semiconductor-to-metal transition," J. D. Ryckman, K. A. Hallman, R. E. Marvel, R. F. Haglund, Jr. and S. M. Weiss. *Optics Express* **21** (9), 10753-10763 (2013).

[2] "Tracking the evolution of the electronic and structural properties of VO_2 during the ultrafast photoinduced insulator-metal transition," S. Wall, L. Foglia, D. Wegkamp, J. Stähler, M. Wolf, K. Appavoo, J. Nag and R. F. Haglund, Jr., *Physical Review B* **87**, 115126 (2013).

Spontaneous pillar-matrix nanostructure and interface strain in epitaxial $La_{2/3}Sr_{1/2}MnO_3$：ZrO_2 thin films

Yuze Gao[1,2], Guixin Cao[3,4], Kepeng Song[5], Kui Du[5], Jincang Zhang[1].

[1]*Department of Physics, Shanghai University, Shanghai 200444, PR China*
[2]*Max Planck Institute for Solid State Research, Heisenbergstrasse 1, Stuttgart D-70569, Germany*
[3]*Center for Nanophase Materials Sciences, Oak Ridge National Laboratory, Oak Ridge, TN 37831, USA*
[4]*Department of Materials Science and Engineering, University of Tennessee, Knoxville, TN 37996, USA*
[5]*Shenyang National Laboratory for Materials Science, Institute of Metal Research, Chinese Academy of Science, Shenyang 110016, Liaoning, PR China*

Abstract

We report the experimental fabrication of 3D ZrO_2 nanopillars embedded in a matrix of $La_{2/3}Sr_{1/3}MnO_3$ (LSMO) in epitaxial $(LSMO)_{1-x}$：$(ZrO_2)_x$ (x=0, 0.2 and 0.3) nanocomposite films. A narrow pillar size with diameter of 4.0 ± 0.6 nm for x = 0.2 and 5.0 ± 0.6 nm for x = 0.3 is observed by aberration-corrected scanning transmission electron microscopy (STEM). The transport properties are tunable through control of the vertical strain at the interface between ZrO_2 pillars and LSMO matrix. Our findings expand the ability to tune functional properties of nanocomposites by appropriate choice of matrix/pillar materials and nanopillar distribution. The scanning tunneling microscope (STM) experiments were conducted recently on these films at CNMS, and we also present STM observation about the possible bistable state of the pillars.

Direct Deposition of Ferroelectric PZT Films on Glass and Polymer Substrates

S. J. Brewer[1], T. C. Field[1], P. C. Joshi[2], and N. Bassiri-Gharb[1,3]
[1]G.W. Woodruff School of Mechanical Engineering, Georgia Institute of Technology
Atlanta, GA 30332-0405, USA
[2]Materials Science and Technology Division, Oak Ridge National Laboratory
Oak Ridge, TN 37831-6083, USA
[3]School of Materials Science and Engineering, Georgia Institute of Technology
Atlanta, GA 30332-0245, USA

Ferroelectric thin films enable myriad applications in science and industry, such as use in precision positioners and optics, MEMS sensors and actuators, non-volatile memories, and energy harvesting systems. However, current processing of ferroelectric thin films, such as PZT, relies on high-temperature annealing (~650 to 700°C), thereby limiting substrates on which these films can be successfully deposited. As technological applications transition to lower weight and volume devices, complete integration with CMOS technology becomes imperative for further miniaturization, thereby rendering processing techniques that enable such integration essential.

Pulsed thermal processing (PTP) attempts to resolve this discrepancy by employing multiple high-voltage pulses from a Xenon lamp for 100 to 1500 microseconds, resulting in reduced temperature saturation required to anneal ferroelectric thin films as well as a distinct temperature difference between the film and substrate. Here we demonstrate its viability as a processing method for *in-situ* crystallization of ferroelectric thin films while maintaining the integrity of substrates and materials in CMOS fabrication. Specifically, we report direct crystallization of $PbZr_{0.53}Ti_{0.47}O_3$ (PZT) thin films on soda-lime glass and polyimide substrates. The polyimide substrates were processed both mounted on glass slides for ease of handling as well as on standalone polyimer substrates. All substrates were coated with 20 nm of sputtered Ti followed by 120 nm of sputtered Pt. This stack was chosen based on the similar choice of bottom electrode stack used in platinized Si substrates, routinely employed in processing of ferroelectric thin films. Approximately 50 nm of PZT precursor solution film were deposited by spin coating. Each of three layers was subsequently pyrolyzed at approximately 375°C for 1 minute. The final anneal of the film was performed using the PTP method at Oak Ridge National Lab for various time and voltage increments.

X-ray diffraction (XRD) analysis of the films shows strong peaks corresponding to the (111) perovskite crystallographic phase. Scanning electron microscopy (SEM) imaging of the same samples confirms crystalline grain structure of 50 to 100 nm average size. Films on polyimide typically display smaller average grain size than those on SiO_2. Film thickness of all films is approximately 25 nm. Single frequency and band excitation piezoresponse force microscopy (PFM) characterization conducted at CNMS report well developed butterfly loops, hysteresis curves with good saturation, and phase switching by 180°, consistent with presence of a ferroelectric phase. Films on both SiO_2 and polyimide substrates show localized switching behavior at a coercive voltage of 5 to 15V. Coercive voltages are typically lower in films on SiO_2 (~5 V), while films on polyamide switched around 10 to 15 V, most likely due to average grain size effects (polymer smaller than glass). Areas on the films on both substrates probed by PFM typically showed greater than 50% ferroelectrically active material, with some films on Kapton showing up to 95% or greater ferroelectrically active areas. Based on these XRD and PFM results, local regions showing promising ferroelectric behavior have been identified in the design of experiments with narrow processing ranges for pulse voltage, pulse duration, and pulse count. These narrow processing windows resulting in ferroelectric thin films suggest that further optimization of the PTP method could be a viable alternative to traditional high-temperature annealing and offer a CMOS-compatible method for direct deposition of ferroelectric thin films.

Domain structure, domain wall contributions, and nonlinear extrinsic contributions to the response will also be discussed as observed via band excitation PFM in order further elucidate the viability of direct deposition of ferroelectric PZT films on glass and polymer substrates.

Study of Ionic Dynamics in Nanostructured Ceria through Lateral Electrochemical Measurements and Finite Element Modeling

J. Ding[1], E. Strelcov[2], S. Kalinin[2] and N. Bassiri-Gharb[1,3]
[1]Department of Materials Science and Engineering, Georgia Institute of Technology, Atlanta, GA, 30332
[2]Institute for Functional Imaging of Materials and Center for Nanophase Materials Science, Oak Ridge National Laboratory, Oak Ridge, TN, 37831
[3]G. W. Woodruff School of Mechanical Engineering, Georgia Institute of Technology, Atlanta, GA, 30332

Ionic transport underpins fundamental functionalities of many technological devices such as lithium ion batteries, fuel cells, and gas sensors. In order to understand the fundamental science of the transport phenomena at the basis of the electrochemical functionalities, it is vital to separate the assorted ionic/electronic dynamics within lengthscales approaching if not similar to those the processes occur. To address this challenge, time-resolved Kelvin Probe Force Microscopy (tr-KPFM) is used to measure time evolution of surface potential profiles with ~10 ms temporal resolution and submicron spatial resolution. Nanostructured ceria (NC) is used as a model structure for the proof of concept studies. While being extensively used as a mixed ionic-electronic conductor (MIEC) in solid oxide fuel cells, catalytic devices and gas sensors, the origin of NC conductive behavior is still controversial: anisotropic bulk conduction, as well as proton-based conduction facilitated by either surface water adsorption or by surface defects as catalytic sites have been previously reported as contributing to the MIEC behavior in NC.

NC (60 nm thick) was prepared by physical vapor deposition (PVD) on quartz substrates. External bias (30V) was applied to ceria via photolithography patterned Cr/Pt electrodes, which were deposited on top of the NC layer. The surface potential profiles were studied by tr-KPFM, and the local (lateral) transport phenomena and charge distribution corresponding to each transportation species were simulated in COMSOL finite element modeling.

The surface potential response of NC to external bias pulses was initially an “S” shape, linearizing during polarization (bias-on) stage, and the potential gradually decreases during relaxation (bias-off) stage. This polarization and relaxation behavior is consistent with moving charges of protons and hydroxyl groups driven by electric field and concentration gradient, which are present in the water layer adsorbed on the ceria surface. The H^+ and OH^- groups are expected to result from water dissociation under applied bias, in a process facilitated by surface defects such as oxygen vacancies. Strong electrochemical behavior was found in proximity of biased electrode at high temperature and/or high humidity, which would be consistent with charge injection at TPB. The coupling between surface potential evolution and concentration of charge carriers over time was solved self-consistently in COMSOL finite element modeling. Optimized parameters including diffusivity of both moving charges and charge injection term were obtained as a function of environment conditions, through fitting of the theoretical curves to the experimental data.

Non-Volatile Ferroelectric Memories from CdS Nanoparticles-P(VDF-TrFE) Nanocomposite Films

Saman Salemizadeh Parizi, Daniela Caruntu, and Gabriel Caruntu

Department of Chemistry and Science of Advanced Materials (SAM) Program, Central Michigan University, Mt. Pleasant, MI 48858, USA

Ferroelectric capacitors are attractive candidates for data storage applications due to the polarization effect which can be used to encode information by using Boolean algebra. However, the read out process in ferroelectric capacitors is destructive since ferroelectrics are wide band gap insulating materials [1]. Combining ferroelectric materials with a semiconductor is a promising approach to design biphasic structures with complementary electronic properties such as ferroelectric polarization and (semi)conductivity [1-2]. Such functions will enable a device to function as a rectifying diode being therefore suitable for non-volatile data storage [3]. In this work, we present a solution-based approach to fabricate nanocomposite materials based on CdS nanoparticles encased into a ferroelectric polymer matrix, such as poly[(vinylidenefluoride-co-trifluoroethylene] P(VDF-TrFE). To this end, the as-synthesized semiconductor CdS nanoparticles were stabilized in a polar solution containing polymer molecules upon a simple surface functionalization process. Preliminary results show high quality biphasic nanocomposite films with well dispersed nanoparticles in polymeric matrix. The electronic properties of neat P(VDF-TrFE) and CdS NPs-P(VDF-TrFE) nanocomposite were determined by combining measurements with a ferroelectric tester with piezoresponse force microscopy (PFM), Kelvin probe force microscopy (KPFM) and conductive atomic force microscopy (CAFM). The CdS NPs-P(VDF-TrFE) nanocomposite perform well in a non-destructive read out process which can be used in non-volatile data storage applications.

References:

1. Kamal Asadi, Dago M. De Leeuw, Bert De Boer, and Paul W. M. Blom, *Nature Mater*. 2008, **7**, 547-550.

2. E. Y. Tsymbal and A. Gruverman, *Nature Mater*. 2013, **12**, 617-621.

3. Zheng Wen, Chen Li, Di Wu, Aidong Li and Naiben Ming, *Nature Mater*. 2013, **12**, 602-604.

Quantum transport simulations in carbon nanoring devices with low-energy phonon scattering

Mark A. Jack (Florida A&M University, Physics Department, Tallahassee, FL 32307)

The ability of a nanomaterial to conduct charge is essential for many nanodevice applications. While suitable nanomaterials should have acceptable electron transport properties in the absence of disorder, numerous studies have shown that disorder (including phononic or plasmonic effects) can disrupt or block electric current in nanomaterials. Phonons for example distort the lattice and appear as scattering centers to electrons, leading to electrical resistance and heating. An accurate theoretical account of both electron-phonon and electron-plasmon coupling in carbon nanotube-, carbon nanoring- and graphene nanoribbon-based structures is of the utmost importance in order to properly predict the performance of these new nanodevices. Our objective is to understand how disorder, as caused by the inelastic scattering of charge carriers on defects, phonons and plasmons, impacts quantum coherence signatures in charge transport in a carbon nanotorus device.

A multi-scale continuum approach developed by a collaborator (M. Leamy, Georgia Institute of Technology) forms the basis for reduced-order phonon modeling of carbon nanostructures. The device Green's function, G_d, derived with a non-equilibrium Green's function method (NEGF) will now function as key input to determine all transport observables. The NEGF algorithm is set up in such a way that the transmission function T(E) may be calculated at a single energy E by inverting the Hamiltonian matrix to obtain the transport Green's function G_d. Integrated observables such as the source-drain current ISD for example can then be calculated by integrating over the transmission function values for a predefined energy range. First results when incorporating the effects of low-energy phonon modes with an effective description of electron-phonon coupling will be discussed.

Using the parallel sparse matrix library *PETSc,* PETSc provides tools for dividing the memory and work required in inverting the Hamiltonian matrix across multiple compute cores or nodes to compute G_d. PETSc also provides several backend solvers for finding the inverse in parallel by a variety of methods, iterative and direct. The results for different energy levels are calculated with a second layer of parallelism to obtain integrated observables. Because the inversion at each energy step dominates the run time and memory use of the code, it is important that the code scales well, in terms of memory use and processing time, to larger systems of greater experimental relevance. Several different solution methods and libraries were compared for their scalability and efficiency, including the shared-memory direct dense solver from the *Intel MKL,* the *MUltifrontal Massively Parallel direct Solver MUMPS,* and the standard iterative sparse solver bundled with PETSc, based on the *Generalized Minimum RESiduals (GMRES)* algorithm. The XSEDE resource *'Stampede'* at the Texas Advanced Computing Center as well as regional computer cluster resources in Florida *(SSERCA, Florida State University)* are used for development and benchmarking, while OLCF computational facilities *'Titan'* and *'NICS/Beacon'* at Oak Ridge National Laboratory are used for physics production runs.

Modeling of a pH responsive weak polyelectrolyte brush using SCFT

Jyoti Prakash Mahalik, Rajeev Kumar and Bobby Sumpter
Center for Nanophase Materials Sciences, ORNL
mahalikjp@ornl.gov

I. Introduction

We compared and contrasted two models for pH responsive polyelectrolyte brush: Analytical [1], and Numerical SCFT [2]. Both the models were used to determine the properties of a real polyelectrolyte brush [3]. The neutron reflectivty profile of the final model agrees well with the experimental profile.

II. Background

Collective response of a large number of polymers grafted on a surface produces amplified response to a stimulus as compared to a single polymer chain [4]. This amplified signal can be harnessed for many applications such as glucose detector, artificial membranes, and nanotemplating [5]. Different polymers respond to different kind of stimulus by expanding or contracting to the magnitude and/or direction of the stimulus. The pH responsive weak polyelectrolytes expand if the pH of the medium is higher than the pka of the polymer. Modeling the real polymer brush poses challenge since it requires sophisticated models to capture all the right physical features of the actual system as well as simple enough to do the computation in reasonable amount of time. We use a combination of a simple analytical model and a sophisticated numerical SCFT model to determine the parameters of a real polyelectrolyte brush. Both the analytic and numerical models are compared and contrasted to determine the advantage and drawback of both the models. Computation using analytical model is faster but it lacks some important features of the real system such as entropy of mixing of the solvent. The numerical model is relatively slower but captures the right physical features. For the real system [3], the analytical model was used to get an initial estimate of the parameters, followed by refining the polyelectrolyte brush parameters using numerical SCFT. The neutron scattering profile obtained using this modeling technique agrees well with the experimental data.

References

[1] E. B. Zhulina and O. V. Borisov. Poisson-boltzmann theory of ph-sensitive (annealing) polyelectrolyte brush. Langmuir, 27(17):10615–10633, 2011.

[2] R. Kumar, B. G. Sumpter, and S. M. Kilbey. Charge regulation and local dielectric function in planar polyelectrolyte brushes. Journal of Chemical Physics, 136(23), 2012.

[3] C. Deodhar, E. Soto-Cantu, D. Uhrig, P. Bonnesen, B. S. Lokitz, J. F. Ankner, and S. M. Kilbey. Hydra- tion in weak polyelectrolyte brushes. Acs Macro Letters, 2(5):398–402, 2013.

[4] M. P. Weir and A. J. Parnell. Water soluble responsive polymer brushes. Polymers, 3(4):2107–2132, 2011.

[5] S. J. Peng and B. Bhushan. Smart polymer brushes and their emerging applications. Rsc Advances, 2(23):8557– 8578, 2012.

Controlling the Topology of Polymers to Tune Their Properties

Mi Zhou[1,2], Heng Wang[1], Xiaolong Jiang[1], Kunlun Hong[2], Xin Qian[1]

[1]College of Materials Science and Engineering, Zhejiang University of Technology, Hangzhou, Zhejiang 310012

[2]Center for Nanophase Materials Science, Oak Ridge National Laboratory, Oak Ridge Tennessee 37831

In the past decade, topological complex polymers have received many attentions due to their characteristic structures. Such structural features offer many opportunities to control their properties and functions both in bulk and in solution. As a result, these materials show potentials in a wide range of applications. But the structures and the properties relationship of topological complex polymers are still not well understood. In this presentation, we designed and synthesized several series of topological polymers by controlled/"living" polymerization and supermolecular assembly. These polymers show the unique aggregation behaviors, which impart their physical properties including rheology, thermo-responsiveness, compatibility, and crystallinity.

New CO_2 Responsive Macromolecular Nanomaterials

Balaka Barkakaty
Center for Nanophase Materials Sciences, Oak Ridge National Laboratory, Oak Ridge, TN

Increasing atmospheric concentrations of CO_2, a heat-trapping gas is pushing the world into a dangerous climatic condition. Reducing green-house gas emissions resulting from the combustion of fossil fuels requires new routes to capture and utilize CO_2. Furthermore, stimuli-responsive polymers have attracted significant interest due to their tremendous potential in various applications, such as controlled drug release and gene delivery, biomimetic materials, biosensors, "intelligent" coatings and "smart" surfaces or surfactants.

This poster focusses on the development of new CO_2 responsive macromolecular nanomaterials. A new polymer was synthesized by functionalization of poly(vinyldimethylazalactone) (PVDMA) with a novel benzyl alcohol derivative bearing a cyclic amidine group, "4-(N-methyltetrahydropyrimidine)benzyl alcohol" (MTHPBA). The new polymer has shown high efficiency and selectivity for the capture and release of CO_2 under ambient conditions. The CO_2 fixing efficiency of this polymer from a dilute CO_2 source, such as a flue gas type mixture (20% CO_2, 80% N_2) was higher than the CO_2 fixing efficiency of previously reported amidine based polymers from 99% CO_2 source. The CO_2 capture and release of polymer films containing poly(glycidylmethacrylate)-*block*-PVDMA modified with MTHPBA were investigated by fourier transform infrared spectroscopy (FTIR), quartz crystal microbalance (QCM) and neutron reflectivity measurements. Morphological studies via microscopy techniques confirmed a three dimensional film structure leading to high surface area. In addition, it was discovered that the CO_2 capture and release process on these nano-structured film might have potential applications for reversible capture and release of proteins using CO_2 as a reversible stimuli. Furthermore, this talk will also highlight the development of a new multi-environment chamber at the Spallation Neutron Source Liquid Reflectometer.

Synthesizing Deuterated Soft Materials

Peter V. Bonnesen, Kunlun Hong, Jun Yang,

Center for Nanophase Materials Sciences,
Oak Ridge National Laboratory, Oak Ridge TN 37831

Abstract: Substitution of protium in organic and polymeric materials with deuterium enhances contrast in neutron scattering, and provides a way to elucidate the structures and dynamics of many soft matter systems that is generally not accessible by other techniques. Accordingly, the CNMS has been developing a variety of deuterated monomers, polymers, and other synthons to be used in the construction of partially- and fully-deuterated soft materials. An additional benefit of synthesizing deuterated soft materials is to assess the impact deuteration has on a) polymeric conformation and dynamics in solution, at surface and interfaces, and in other confinement settings, b) on their optoelectronic properties, and c) on their non-covalent interaction. In this presentation we show examples of our efforts.

Acknowledgement: This work was performed at the Center for Nanophase Materials Sciences at Oak Ridge National Laboratory, supported by Scientific User Facilities Division, Office of Basic Energy Sciences, U.S. Department of Energy.

Temperature Gradient Interaction Chromatography: An inside look at the heterogeneity of multi-graft polymers

Chelsea N. Widener (Wesleyan College, Macon, GA 30467)
Deanna L. Pickel and David W. Uhrig (Oak Ridge National Laboratory, Oak Ridge, TN 37830)

Size exclusion chromatography (SEC) is a well-established method for the characterization of synthesized polymers despite the heterogeneity present in such samples. SEC separates polymers based on hydrodynamic volume. This becomes problematic when dealing with branched polymers. Recently, temperature gradient interaction chromatography (TGIC) has risen to prominence. TGIC separates polymers based on degree of polymerization and has the ability to detect heterogeneity present in architecturally complex polymer samples and resolve variants within them much more efficiently. We seek to further our understanding of the heterogeneity of a synthesized multi-graft polystyrene sample. In order to accomplish this objective, we first develop a new TGIC method that is better suited to our polymer sample. We then perform off-line 2-D chromatography using TGIC to fractionate the sample and SEC with multiple detectors to characterize the collected fractions. We were able to detect nine species, eight of which correspond to the polystyrene backbone with 0 to 7 pairs of polystyrene arms.

Manipulating Nanoscale Morphology by P3HT/PLA Molecular Bottlebrushes: Synthesis, Aggregation and Self-Assembly

Suk-kyun Ahn

Center for Nanophase Materials Sciences, Oak Ridge National Laboratory, Oak Ridge, TN 37831

Molecular bottlebrushes are highly tunable molecular scaffolds which provide interesting opportunities for creating nanostructured materials via self-assembly. Here, precision synthesis, characterization and nanoscale assembly of molecular bottlebrushes comprising poly(3-hexylthiophene) (P3HT) and poly(D,L-lactide) (PLA) as polymeric side-chains are presented. A series of bottlebrush random copolymers having different compositions of P3HT and PLA were synthesized by grafting through approach using ring-opening metathesis polymerization (ROMP). Melt-state morphologies of these bottlebrush copolymers investigated by scattering (X-ray) and imaging (AFM and TEM) methods revealed microphase-separated structures with domain size of 15-20 nm, which is desirable for organic photovoltaics (OPVs) applications. Ordering of nanostructures in these bottlebrush random copolymers was further tuned by changing the composition of P3HT and PLA side-chains. Thus, well-defined molecular bottlebrushes can serve as an interesting molecular scaffold to manipulate morphologies of P3HT containing copolymers and to access useful nanostructures for OPVs.

Dynamics of Confined Flexible and Unentangled Polymer Melts in Highly Adsorbing Cylindrical Pores

Jan-Michael Carrillo[1] and Bobby Sumpter[2,3]

[1]National Center for Computational Sciences, Oak Ridge National Laboratory, Oak Ridge, Tennessee 37831, USA
[2]Center for Nanophase Materials Sciences, Oak Ridge National Laboratory, Oak Ridge, Tennessee 37831, USA
[3]Computer Science and Mathematics Division, Oak Ridge National Laboratory, Oak Ridge, Tennessee 37831, USA

We performed coarse-grained molecular dynamics simulations to study the effect of the confinement of flexible and unentangled polymer chains in cylindrical pores. The results are compared with the recent neutron spin echo (NSE) experiments by Krutyeva and co-workers (Phys. Rev. Lett. 2013, 110, 108303), where anodized aluminum oxide (AAO) pores were infiltrated with polydimethyl-siloxane (PDMS) chains (PDMS). The NSE experiments were designed to probe the interphase layer, which is hypothesized to have polymer chain dynamic properties between those of a glassy layer and the bulk. There is excellent agreement in the values obtained for the normalized coherent single chain dynamic structure factor, $\frac{S(Q,\Delta t)}{S(Q,0)}$ between experiments and simulations. The experimentally inaccessible mean squared displacement (MSD) of the confined monomers, calculated as a function of radial distance from the pore surface was obtained in the simulations and show a gradual increase of the MSD from the adsorbed but mobile layer to that similar to the bulk. This is akin to the hypothesized interphase layer. Additionally, the simulations provide information about the static polymer chain properties such as the mean-squared radius of gyration $\langle R_g^2 \rangle$ and the average shape anisotropy $\langle \kappa^2 \rangle$. These two properties indicate that the chains form a pancake-like conformation near the surface and a bulk-like conformation near the center of the confining cylinder. Direct visualization of the polymers in the simulation confirm the pancake-like conformation of the adsorbed chains and the presence of trains, loops and tails in the region between the adsorbed chains and the chains not in contact with the surface. Despite the presence of these different conformations, the average form factor of the confined chains still follows the Debye function which describes linear ideal chains and is in agreement with small angle neutron scattering (SANS) experiments.

Molecular Engineering of 3-Alkylthiophene Polymers

Youjun He, Jihua Chen, Kai Xiao, Ming Shao, Jong Keum, Kunlun Hong

Center For Nanophase Materials Sciences, Oak Ridge National laboratory, Oak Ridge TN 37831

Abstract: The optoelectronic properties of a conjugated polymer film prepared from its solution depend on many factors, including the solvent quality, the rate of solvent evaporation, and other processing conditions. But the most important factor is the molecular structures of the polymers. However, until now, such structure-property-performance relationships are not well understood yet. To address these questions, we are utilizing poly(3-alkylthiophene) derivatives as a model system to understand how the molecular structures of conjugated polymers evolved and their relationship with their morphologies and optoelectronic properties. We also discuss other approaches to tune the optoelectronic properties.

Acknowledgement: This work was performed at the Center for Nanophase Materials Sciences at Oak Ridge National Laboratory, supported by Scientific User Facilities Division, Office of Basic Energy Sciences, US Department of Energy. GI-WAXS and GI-SAXS data were obtained from Advanced Photon Source, Argonne National Laboratory.

Overview of the CNMS User Proposal Process and Keys to Success

Tony Haynes and Viviane Schwartz
CNMS User Program Office

A primary mission of the Center for Nanophase Materials Sciences (CNMS) is to provide access to state-of-the-art nanoscience research capabilities, expertise, and equipment to a diverse user community in order to deliver cutting-edge nanoscience research that otherwise would not be possible. Access to CNMS is granted to researchers through a proposal submission and review process that is based on peer review by leading researchers from outside of Oak Ridge National Laboratory. This presentation will introduce prospective CNMS users to the user proposal submission and review process. We will discuss the review steps and criteria, sources of information to aid in proposal development, and tips for writing successful user proposals. The aim of the presentation is to enable attendees, and in particular prospective new users, to produce higher quality user proposals with improved chances for success.

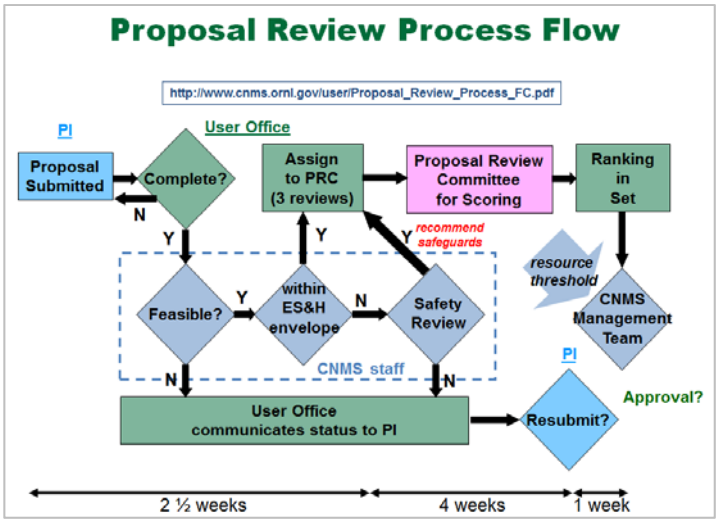

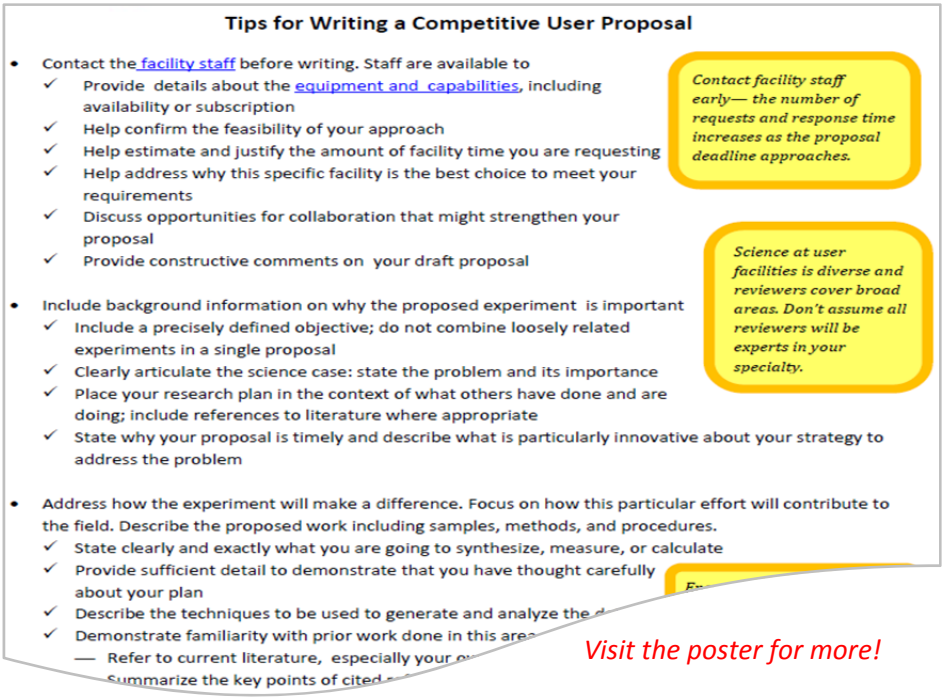

Optically Tunable Spin-exchange Energy at Donor:Acceptor Interfaces in Organic Solar Cells

Mingxing Li[1], Hongfeng Wang[1], Lei He[1], Hengxing Xu[1], Zheng Gai[2] and Bin Hu[1]

[1]Department of Materials Science and Engineering, University of Tennessee, Knoxville, TN 37996, USA
[2]Center for Nanophase Materials Science, Oak Ridge National Laboratory, Oak Ridge, TN 37831, USA

Spin-exchange energy is a critical parameter in controlling spin-dependent optic, electronic, and magnetic properties in organic materials. Here we report optically tunable spin-exchange energy by studying the line-shape characteristics in magnetic field effect of photocurrent developed from intermolecular charge-transfer states based on donor:acceptor (P3HT:PCBM) system. Specifically, we divide magnetic field effect of photocurrent into hyperfine (at low field < 10 mT) and spin-exchange (at high field > 10 mT) regimes. We observe that increasing photoexcitation intensity can lead to a significant line-shape narrowing in magnetic field effect of photocurrent occurring at the spin-exchange regime. We analyze that the line-shape characteristics is essentially determined by the changing rate of magnetic field-dependent singlet/triplet ratio when a magnetic field perturbs the singlet-triplet transition through spin mixing. Based on our analysis, the line-shape narrowing results indicate that the spin-exchange energy at D:A interfaces can be optically changed by changing photoexcitation intensity through the interactions between intermolecular charge-transfer states. Therefore, our experimental results demonstrate an optical approach to change the spin-exchange energy through the interactions between intermolecular charge-transfer states at donor:acceptor interface in organic materials.

MICROFLUIDIC MODULES FOR ISOLATION OF RECOMBINANT CYTOKINE FROM BACTERIAL LYSATES

Larry J. Millet, Scott T. Retterer and Mitchel J. Doktycz
Biosciences Division and The Center for Nanophase Materials Sciences,
Oak Ridge National Laboratory, Oak Ridge, TN 37831, USA

This work reports the development of microfluidic modules for on-chip purification of microreactor-synthesized recombinant biopharmaceuticals. Recently, reactors for cell-free protein synthesis have been demonstrated over a range of scales from liters [1] to femtoliters [2]. We have demonstrated microscale reactors for cell-free protein translation [3] and enzymatic reactions [4]. Here we present the fabrication and testing of microfluidic modules that incorporate (1) microporous barriers for retaining chromatography beads, and (2) bifurcating channels for lateral distribution of fluid samples over the high surface area chromatography bed. Silicon masters are created through oxide deposition followed by reactive ion etching using a modified Bosch process. Size exclusion and ion exchange modules are made through replicate molding of polydimethylsiloxane (PDMS), plasma bonding, and loading the device with sized chromatography beads.

Our results demonstrate the characterization and implementation of chromatography-based microfluidic devices. Typical steps for protein purification include ion exchange and desalting. The size exclusion module shown in Figure 1 is used for desalting protein products. Column efficiency is determined by measuring elution peaks of small molecules; elution peaks for red 40 (MW = 496.42 g/mol) are shown across a range of pressure head heights with corresponding flow rates. Figure 2 summarizes elution volumes and peak symmetries [5]. An ion exchange module packed with diethylaminoethanol (DEAE) sepharose beads (Figure 3) permits on-chip concentration of proteins in microfluidics as demonstrated by the increase in fluorescence of ion exchange beads during enhanced green fluorescent protein (EGFP) capture (0:00-0:45 hr:min) and elution (0:51-0:54 hr:min) (Figure 4). The post elution image (0:57 hr:min) shows no residual fluorescence. Inset graph (elution image (0:54)) shows a characteristic peak of EGFP fluorescence during elution off of these ion exchange devices, elution data for each 5 µl fraction (150-220) is shown. Figure 5 shows protein concentration (Bradford assay) results of flow-through collection and elution fractions from a microfluidic ion exchange concentration of *E. coli* cell extract spiked with human granulocyte-macrophage colony-stimulating factor (GM-CSF). The presence of GM-CSF was confirmed through SDS-PAGE gel electrophoresis (Figure 6) and ELISA. We envision that by coupling on-chip microfluidic cleanup modules with cell-free protein synthesis reactors, the deployment of scaled up cytokine reactors for on demand synthesis and delivery of biopharmaceuticals will be possible.

REFERENCES:

1. “Microscale to manufacturing scale-up of cell-free cytokine production--a new approach for shortening protein production development timelines” Zawada JF, Yin G, Steiner AR, Yang J, Naresh A, Roy SM, Gold DS, Heinsohn HG, Murray CJ, Biotechnol Bioeng., 108, 1570 (2011).
2. “Cell-free protein synthesis in femtoliter microchambers for arraying ultra-high density protein spots,” Kim SH, Yoshizawa S, Takeuchi S, Fujii T, Fourmy D, uTAS T.2.31, 2197 (2012).
3. "Continuous Protein Production in Nanoporous, Picolitre Volume Containers," P. Siuti, S. T. Retterer, and M. J. Doktycz, Lab on a Chip 11, 3523 (2011).
4. “Enzyme reactions in nanoporous, picoliter volume containers,” Siuti P, Retterer ST, Choi CK, Doktycz MJ. Anal Chem. 17, 1092 (2012).
5. GE Healthcare Application note 28-9372-07 AA (2010), www.gelifesciences.com

X-ray and neutron studies on hard $L1_0$ FePt(001)/soft CoFeB bilayers

Sin-Yong Jo[1], Hyeok-Cheol Choi[1], Chun-Yeol You[1], Haile Ambaye[2], Valeria Lauter[2], Jong Kahk Keum[2], Raymond R. Unocic[2], Kyujoon Lee[3], Myung-Hwa Jung[3], J. Y. Gu[4], Ki-Yeon Kim[5*]

[1]Department of Physics, Inha University, Incheon 402-751, Republic of Korea
[2]Oak-Ridge National Laboratory, Oak-Ridge, TN 37831, USA
[3]Department of Physics, Sogang University, Seoul 121-742, Republic of Korea
[4]Department of Physics and Astronomy, California State University-Long Beach, CA 90840, USA
[5]Neutron Science Division, KAERI, Daejeon 303-353, Republic of Korea

It has been known that chemically ordered $L1_0$ FePt(001) film have a very large perpendicular magnetic anisotropy (PMA) (theoretically predicted anisotropy constant K_{eff} =7 ×10^6 J/m^3) and bcc CoFeB(001) layer is a prerequisite to get a very large tunneling magnetoresistance (TMR) ratio (~600% at RT) in CoFeB/MgO/CoFeB magnetic tunnel junction structures. [1, 2] Both materials have separately caught much attention of scientists in each research field so far. To realize the next-generation ultrahigh density magnetic recording, several requirements such as very large TMR, PMA, high thermal stability, low switching current density and high signal to noise ratio should be simultaneously satisfied. We aim to see how the hard $L1_0$ FePt(001) /soft CoFeB exchange coupling affects the magnetic property of the CoFeB layer with several thickness (2, 5, 10 nm) by carrying out structural and magnetic measurements. Experimental results and analysis on polarized neutron reflectivity from Magnetism reflectometer at SNS and x-ray reflectivity and diffraction at CNMS will be presented.

References

[1]. O. A. Ovanov, L. V. Solina, and V. A. Demshina, Phys. Met. Metallogr. **35**, 81 (1973).
[2]. S. Ikeda, J. Hayakawa, Y. Ashizawa, Y. M. Lee, K. Miura, H. Hasegawa, M. Tsunoda, F. Matsukura, and H. Ohno, Appl. Phys. Lett. **93**, 082508 (2008).

Electro-Optical Properties of Self-assembled Metal-Chalcogenide Nanoparticles

Christopher B. Jacobs,[1] Gyoung Gug Jang,[2] David E. Graham,[2] Pooran C. Joshi,[3] Ji-Won Moon,[2] Ilia N. Ivanov[1]

[1]Center for Nanophase Materials Sciences, Oak Ridge National Laboratory, Oak Ridge, TN, 37931
[2]Biosciences Division, Oak Ridge National Laboratory, Oak Ridge, TN, 37931
[3]Materials Science and Technology Division, Oak Ridge National Laboratory, Oak Ridge, TN, 37931

Nanoparticles of inorganic semiconductors have enhanced optical and electronic properties, compared to bulk semi-conductors, and thus have gained momentum in both electronics and optoelectronic devices, such as sensors, field-effect transistors, light-emitting diodes and lasers. The band gap of semiconductor nanoparticles is defined by quantum confinement effects and increases for smaller nanoparticles. The control of the nanoparticle size can yield tunable electronic structures and luminescent properties. For example, 5 nm CdS nanoparticles have a band gap of 2.57 eV, while the band gap of bulk CdS is 2.42 eV.[1,2] While semiconducting nanoparticles are a promising material, the typical synthesis methods require high temperatures, controlled atmospheres and hazardous and highly reactive reagents, which lead to high production cost. Low cost synthesis methods have been developed. However, there typically is a trade-off between cost and the nanoparticle quality, often reduced by wide size distributions, crystalline defects, and poorly controlled surface chemistry. Nanofermentation is a technique for low-temperature synthesis of nanoparticles using anaerobic *Thermoanaerobacter* sp. X513 bacteria.[3] However, since nucleation takes place at the bacterial cell wall, the optical and electronic properties of nanoparticles are altered by non-specifically bound proteins and other chemicals present in the bacterial environment. The development of low-temperature chemical methods to remove these biological and chemical contaminants from the nanoparticle surface, and control the nanoparticle surface chemistry in order to stabilize aqueous suspensions and improve the optical and electronic properties are at the center of this effort. A multi-step chemical treatment has been developed to remove ~10 % of the mass from the surface of 5 nm CdS nanoparticles and to improve the stability of aqueous suspensions. After treatment, the nanoparticles showed an optical band gap similar to the reported values for 5 nm CdS nanoparticles, about 2.57 eV. Targeted ligation of the nanoparticles enhanced the self-assembly process and led to improved charge transport through the nanoparticle networks, which was evaluated using broad frequency impedance spectroscopy. By coupling nanofermentation synthesis with the low-temperature post-processing procedures the production of inexpensive metal-chalcogenide nanoparticles can be realized.

This research was conducted in part at the Center for Nanophase Materials Science (CNMS) and the Spallation Neutron Source (SNS) which are sponsored at Oak Ridge National Laboratory, by the Scientific User Facility Division, Office of Basic Energy Sciences, U.S. Department of Energy. Research is sponsored by the U.S. Department of Energy, Office of Energy Efficiency and Renewable Energy, Advanced Manufacturing Office, under contract DE-AC05-00OR22725 with UT-Battelle, LLC.

References:

1. R. Maity, K. K. Chattopadhyay. Journal of Nanoparticle Research. 2006, 8, 1, 125-130
2. Lee,H., Mohammed,I., Belmahi,M., Assouar,M., Rinnert,H., Alnot,M. Materials. 2010, 3, 2069-2086
3. Moon,J.W., Ivanov,I.N., Duty,C.E., Love,L.J., Rondinone,A.J., Wang,W., Li,Y.L., Madden,A.S., Mosher,J.J., Hu,M.Z., Suresh,A.K. Rawn,C.J., Jung,H., Lauf,R.J., Phelps,T.J. Journal of Industrial Microbiology & Biotechnology. 2013, 40, 11, 1263-1271

Tailoring of a metastable material: α-$FeSi_2$ thin film

Guixin Cao[1], D. J. Singh[2], Xiaoguang Zhang[1], German Samolyuk[2], Liang Qiao[1], G.M. Stocks[2], and Zheng Gai [1,*]

[1]Center for Nanophase Materials Sciences, Oak Ridge National Laboratory, Oak Ridge, TN 37831

[2]Materials Science and Technology Division, Oak Ridge National Laboratory, Oak Ridge, TN 37831-6056

Abstract

A metastable phase α-$FeSi_2$ was epitaxially stabilized on silicon substrate using pulsed laser deposition. While the bulk material of α-$FeSi_2$ is metallic and nonmagnetic, nonmetallic and ferromagnetic behaviors were tailored on the thin film. The transport renders two different conducting states with a strong crossover at 50 K accompanied by an onset of ferromagnetism as well as a substantial magnetocaloric effect and magnetoresistance. These experimental results are discussed in terms of the unusual electronic structure of α-$FeSi_2$ obtained within density functional calculations and Boltzmann transport calculations with and without strain. Our findings provide an example of a tailored material with rich physical properties for practical applications and shed light on achieving ferromagnetic semiconductors through the structure tailoring.

* Corresponding author, Email: gaiz@ornl.gov

Unusual strain–lattice behavior in Sr-doped La_2CuO_4 thin film

Jaekwang Lee[1], Lu Jiang[2], Tricia Meyer[2], Ho Nyung Lee[2], and Mina Yoon[1]

[1]Center for Nanophase Materials Sciences, Oak Ridge National Laboratory,
Oak Ridge, TN 37831, USA.
[2]Materials Science and Technology Division, Oak Ridge National Laboratory,
Oak Ridge, TN 37831, USA.

Lattice strain is known to remarkably modify the electronic and structural properties of a number of 3*d* transition metal oxides, as they are highly susceptible to changes in interatomic bond lengths and bond strengths. Recently, contrary to the traditional concept that oxygen deficiency in a simple perovskite increases the lattice volume, an unusual lattice constant change has been observed in Sr-doped La_2CuO_4 thin films under biaxial strain. Using first-principles density-functional calculations, we explore the influence of biaxial strain on the oxygen vacancy formation energy ($E_{formation}$) and the lattice constant change of Sr-doped La_2CuO_4. We find that oxygen vacancy prefers an equatorial site to an apical site based on oxygen vacancy formation energy, leading to the shrinkage of *c*-axis lattice parameters as shown in the figure below. We also find that $E_{formation}$ decreases as biaxial tensile strain increases, allowing oxygen ions to migrate more easily. Consequently, we expect that this strain engineering can be a promising approach to enhance the kinetics of the oxygen reduction reaction for efficient solid oxide fuel cells operating at low temperature.

Theory part of the research was conducted at the Center for Nanophase Materials Sciences, which is sponsored at Oak Ridge National Laboratory by the Scientific User Facilities Divions, Office of Basic Energy Sciences, U.S. Department of Energy.

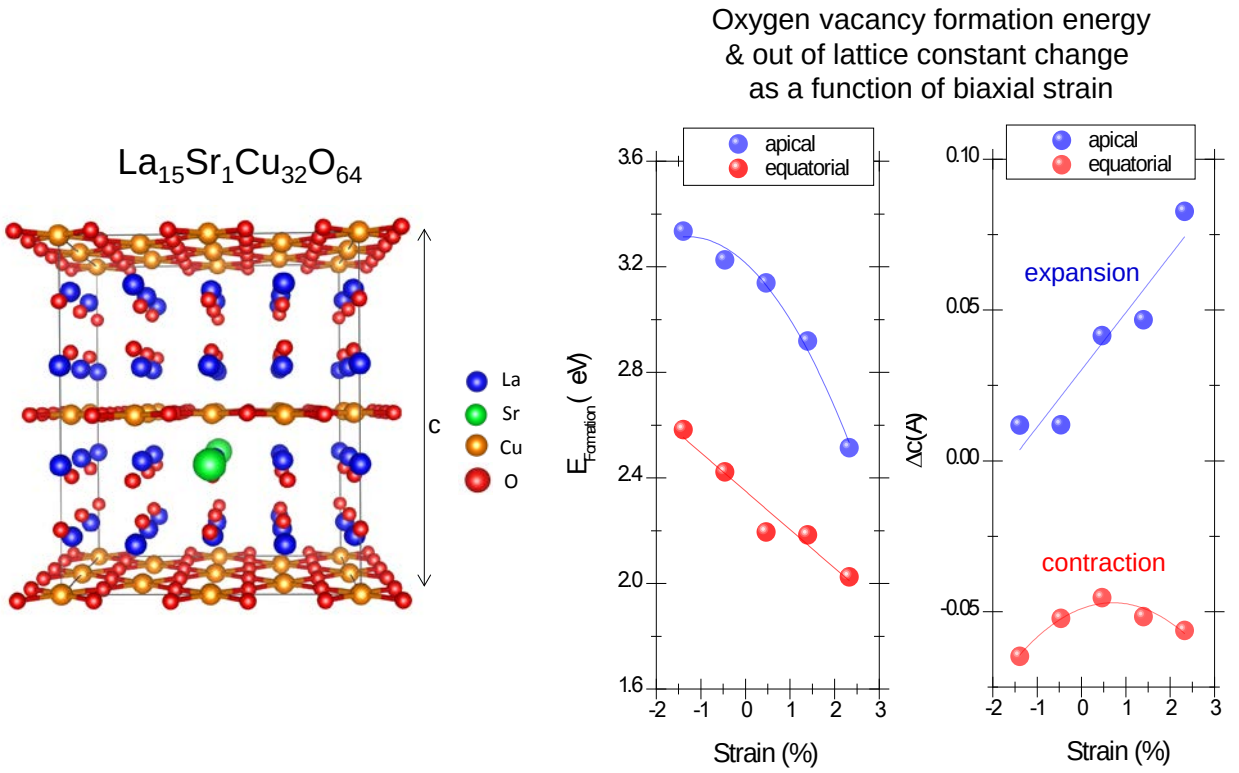

Discovery, Understanding and Validation of Functional Materials using Novel Computational Methods

Panchapakesan Ganesh
Center for Nanophase Materials Sciences, Oak Ridge National Laboratory, Oak Ridge, TN

We will present research activities in a wide range of areas in bulk, surfaces of low-dimensional materials and interfaces. Examples will include (1) understanding behavior of the newly discovered intercalation pseudocapacitance (2) a new approach to understand superionic Li-ion conduction in thiophosphate-based solid electrolytes, (3) predicting magnetism in low dimensional layered materials, (4) predicting superconducting T_c in mono-layer FeSe and relating it with local strain/chalcogen-height (5) role of defects/nanostructuring in controlling the electronic properties of oxide surfaces and interfaces and (6) interfacial behavior of metal-supported charge transfer salts. Research has been carried out using a wide range of electronic structure methods, including DFT and beyond-DFT methods. Cluster-expansion, Monte Carlo, Basin Hopping, high-throughput methods etc. are a few other computational techniques that have been used in conjunction with electronic structure methods to solve some of these scientific problems. Our poster will present the key science problem, our novel approach and our solution in each of these areas of research above. The tools/methodologies are expected to be useful for similar types of problems in other systems.

Controlled Molecular Growth via Metal-ion Induced Orbital Hybridization of Metal Phthalocyanine on Deactivated Si Surfaces

Bing Huang[1], Changwon Park[1], Sean Wagner[2], Jiagui Feng[2], Pengpeng Zhang[2], and Mina Yoon[1]

[1]*Center for Nanophase Materials Sciences, Oak Ridge National Laboratory, Oak Ridge, Tennessee 37831, U.S.A*

[2]*Department of Physics and Astronomy, Michigan State University, East Lansing, Michigan 48823, U.S.A*

A highly selective mechanism for tuning the molecule-substrate interaction has been a long sought after goal in order to direct the formation of long-ranged ordered molecular growth. Insulating surfaces often offer weak van der Waals interaction, while the high density of states near the Fermi energy of metallic surfaces easily induces orbital hybridization of low selectivity with molecular adsorbates. Combining scanning tunneling microscopy and density functional theory, we show that by changing the coordinated transition metal ion in phthalocyanine molecules deposited on the deactivated Si surface, we can selectively tune orbital hybridization via *p-d* orbital selection rules, which alters the molecule-substrate interaction and, consequently, the molecular growth. This mechanism offers a means for realizing controlled long-ranged ordered molecular growth which could be applied to other high-symmetric semiconducting surfaces.

Theory part of the work was supported by theme research at the Center for Nanophase Materials Sciences, which is sponsored at Oak Ridge National Laboratory by the Scientific User Facilities Division, Office of Basic Energy Sciences, U.S. Department of Energy.

Understanding the Role of Ultrasmall Nanoparticles as Nanoscale Building Blocks for Mesoscale Architectures

M. Mahjouri-Samani[1], M. Tian[3], K. Wang[1], A. A. Puretzky[1], C. M. Rouleau[1], G. Eres[2], M. Yoon[1], K. L. More[1], M. Chi[1], G. Duscher[2,3], D. B. Geohegan[1]

1) Center for Nanophase Materials Sciences, Oak Ridge National Laboratory, Oak Ridge, TN
2) Materials Science and Technology Division, Oak Ridge National Laboratory, Oak Ridge, TN
3) Dept. of Materials Science and Engineering, University of Tennessee, Knoxville, TN
*M. Mahjouri-Samani, mahjourisamm@ornl.gov, 865-241-0731

The formation of mesoscale architectures with preferred crystalline phases are a fundamental challenge in fabrication of functional devices. Determining how nm-sized building blocks form higher order structures is central to understanding the growth of nanoparticles and nanowires, and their assemblies, using nonequilibrium synthesis techniques. Pulsed, nonequilibrium growth and processing approaches involving ns-lasers are developed to supply the necessary kinetic energy required to explore the synthesis of nanostructures with metastable phases and structures that are inaccessible using traditional synthetic methods.

Ultrasmall nanoparticles (UNPs, ~ 3 nm) synthesized in pulsed laser vaporization (PLV) are investigated as "building blocks" in the growth of nano and mesoscale architectures with different crystalline phases. Here we primarily study the synthesis conditions, size distribution, and atomic structure of TiO_2 UNPs as a test material due to its extraordinary optical and photocatalytic properties. Temporally- and spatially resolved gated-ICCD imaging, spectroscopy and ion probes are employed as in situ diagnostics to understand and control the plume expansion conditions for synthesis of various TiO_2 UNPs. TEM and EELS are described to characterize the atomic structure, stoichiometry, and surface states of individual UNPs under various deposition conditions. In Situ and Ex-situ annealing experiments are used to understand how UNPs are integrated into larger nanostructures and thin films. These findings provide an insight into the controlled growth of nanoarchitectures with desired structures and functionalities.

For instance, when deposited at d = 5 cm, in 200 mTorr O_2, the 'amorphous' TiO_2 UNPs become integrated into columnar, branched, anatase nanostructures at substrate temperatures as low as 400 °C with 7-nm crystalline domains. At deposition temperatures of 500 and 600 °C, nanobelts of ~20 nm diameter of an interesting TiO_2 (B) phase are instead observed. At higher temperatures (>700 °C), close-packed crystalline anatase nanorods of ~50 nm diameter are formed. To understand the incorporation process, in situ TEM measurements of as-deposited TiO_2 UNPs were performed during annealing in vacuum. Consistent with the deposition results, UNPs began to sinter at 400C, forming crystalline nanoparticles of ~ 20 nm diameter at 600 °C, and larger (50 nm diameter) crystalline domains at 800 °C.

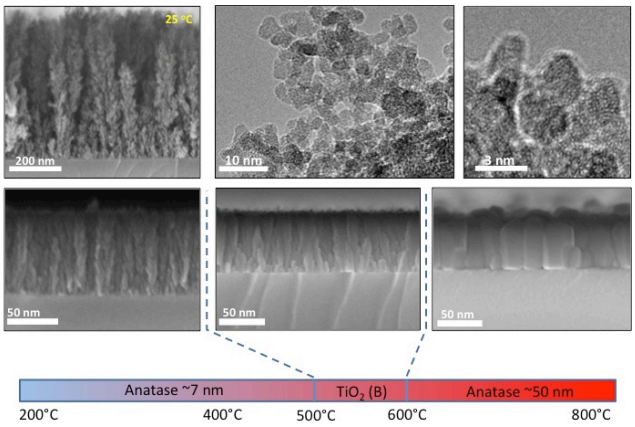

Figure1. (top row) SEM and TEM images of TiO_2 nanoparticles (~3 nm) assembled into fractal structures at room temperature. (bottom row) SEM images of the mesoscale structures formed by incorporation of the UNPs at different temperatures.

Synthesis science was supported by the Materials Sciences and Engineering Division, Office of Basic Energy Sciences, U.S. Department of Energy. A portion of the research was conducted at the Center for Nanophase Materials Sciences, which is sponsored at Oak Ridge National Laboratory by the Scientific User Facilities Division, Office of Basic Energy Sciences, U. S. Department of Energy.

Two-dimensional Layered Materials of ZnX and CdX

Jia Zhou, Jingsong Huang, Bobby G. Sumpter
Center for Nanophase Materials Sciences, Oak Ridge National Laboratory
zhouj1@ornl.gov

The discovery of graphene, a single atomic layer of graphite, has created enormous excitement in the last decade by revealing a wealth of novel physics including two-dimensional (2D) gas of massless Dirac fermions, ambipolar electric field effect, room-temperature quantum Hall effect, breakdown of the Born-Oppenheimer approximation, and quantum capacitance. It has also triggered a boom for 2D layered materials beyond graphene such as silicene, germanene, SiC, hexagonal BN, AlN, transition metal dichalcogenides (e.g. MoS_2, WS_2), and group V metal chalcogenides (e.g. Sb_2Te_3, Bi_2Se_3).

In addition to the 2D layered materials that are addressed in great detail, scientists also keep their eyes open for other possible candidates. In this regard, the II-VI binary chalcogenide compounds ZnX and CdX (X = S, Se, Te) deserve a devoted account. Semiconducting ZnX and CdX have been drawing tremendous interest for broad applications, including transistor, heterojunction diodes, photoconductors, and photovoltaic devices, owing to their outstanding electronic and optical properties. 3D bulk structures of ZnX and CdX exist in both zinc blende (ZB) and wurtzite (WZ) phases. Experimental advances in the last two decades have shown that the manipulation of physical dimensions provides an efficient way to tune the electronic and optical properties of ZnX and CdX.

The II-VI binary chalcogenide compounds ZnX and CdX may be considered isovalent with the IV-IV (e.g. graphene and silicene) and III-V materials (e.g. hexagonal BN and AlN). Given the similarity of their valence electron count, it is legitimate to ask whether free-standing 2D sheets of ZnX and CdX that feature graphene-like honeycomb lattices can be made. Such free-standing sheets with clean surfaces are different from the 2D nanocrystals typically grown by colloidal synthesis in that the latter are coated with organic ligands (or surfactants), which stabilize the nanocrystals, control their size and shape, and affect their properties by passivating the surface electronic states. Interestingly, the 3D bulk structures of ZnX and CdX are indeed characterized by "layers" of six-membered rings with alternating Zn or Cd and X atoms. However, unlike the aforementioned vdW solids, the neighboring "layers" are covalently bonded, thus making it challenging to prepare their freestanding 2D sheets directly by exfoliation.

During the last decade, various 2D lamellar inorganic-organic hybrid structures $[M_nX_n(L)_m]$ (where M = Zn or Cd, L = alkylamine ligand, n = 1 – 2, and m = 0.5 or 1 depending on L) have been synthesized by solvothermal and soft colloidal template techniques. These lamellar structures may be viewed as being obtained by "breaking" the 3D lattice with organic alkylamines into separate inorganic honeycomb slabs, with the number of layers in each ZnX or CdX slab depending on the reactants and reaction temperatures. These 2D lamellar structures can be then exfoliated by sonication in appropriate organic solvents into isolated 2D nanosheets, with each ZnX or CdX slab coated by alkylamine ligands. Recently, a genuine freestanding double-layer honeycomb lattice of ZnSe has been synthesized by exfoliating its lamellar hybrid intermediate followed by removing the alkylamine ligand with heating. The freestanding 2D sheet of ZnSe has been tested for photoelectrochemical solar water splitting, exhibiting a photocurrent density 4-10 times higher than those of its ligand-coated hybrid layers, 8 times higher than quantum dots, and nearly 200 times higher than that of its 3D bulk.

In this theoretical work, freestanding single- to few-layer sheets of ZnX and CdX, each possessing a pseudo honeycomb lattice, are considered by cutting along all possible lattice planes of the bulk ZB and WZ phases. Using density functional theory, we have systematically studied their geometric structures, energetics, and electronic properties. Based on the present work, we envision that the freestanding 2D layered sheets of ZnX and CdX are potential synthesis targets, which may offer tunable band gaps depending on their structural features including surface corrugations, stacking motifs, and number of layers.

REFERENCES

[1] Zhou, J.; Huang, J.; Sumpter, B. G.; Kent, P. R. C.; Terrones, H.; Smith, S. C.,. J. Phys. Chem. C 2013, 117 (48), 25817-25825.

[2] Zhou, J.; Huang, J.; Sumpter, B. G.; Kent, P. R. C.; Xie, Y.; Terrones, H.; Smith, S. C.,. J. Phys. Chem. C 2014, DOI: 10.1021/jp504299e.

Growth and Optical properties of Two-Dimensional Transition Metal Dichalcogenides: WS_2 and WSe_2 Monolayers

Kai Wang,[1] Masoud Mahjouri-Samani, [1] Ming-Wei Lin, [1] Mengkun Tian, [2] Abdelaziz Boulesbaa, [1] Alexander Puretzky, [1] Christopher Rouleau, [1] Gerd Duscher, [2] Kai Xiao, [1] David Geohegan[1]

[1]Center for Nanophase Materials Sciences, Oak Ridge National Laboratory, Oak Ridge, Tennessee 37831,USA
[2]Department of Materials Science and Engineering, University of Tennessee, Knoxville, Tennessee, 37996, USA
Email: wangk@ornl.gov

Two-dimensional materials have attracted great attention because of their unique properties and potential applications in functional electronic and optoelectronic devices. Among them, layered transition metal dichalcogenides (TMDCs), notably MoS_2, $MoSe_2$, WS_2 and WSe_2, feature a native direct-energy gap in the visible and near-infrared frequency range when scaled down to a monolayer, making them appealing materials for light-emitters and biosensors. So far, intensive studies have been focused on monolayer MoS_2, including growth, intrinsic and modulated chemophysical properties and various device functionalities. Compared to monolayer MoS_2, monolayer WS_2 and WSe_2 exhibit much stronger room-temperature photoluminescence and spin-orbit coupling but have received less attention.

Here, we report the synthesis of WS_2 and WSe_2 by two approaches, namely, low-pressure chemical vapor deposition (LPCVD) and high pressure chemical vapor deposition (HPCVD). Their structural and optical properties were characterized via comprehensive techniques, including atomic-resolution scanning transmission electron microscopy and electron energy loss spectroscopy, and mapping by micro-photoluminescence, Raman, and absorption spectroscopy. Additionally, field-effect transistors (FET) based on WS_2 monolayers were fabricated to investigate the transport properties. High photoluminescence at room-temperature in LPCVD-grown WS_2 and WSe_2 monolayers, together with the high mobility extracted from the FET devices, indicate that our monolayers are of high-crystalline quality. The CVD-grown tungsten chalcogenide monolayers promise potential applications in flexible optoelectronics, such as photodetectors and solar cells.

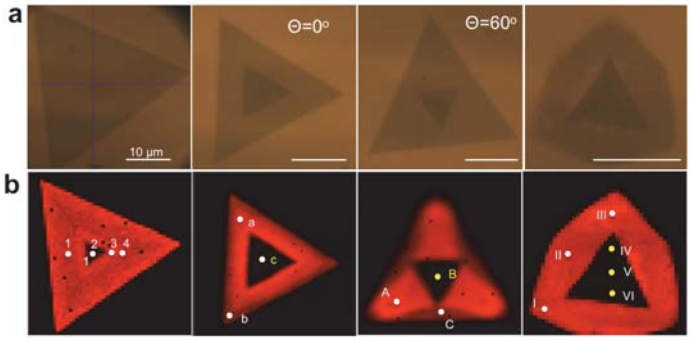

Figure. (a) Optical images of monolayer WS_2 and twisted bilayers; (b) PL mapping of four WS_2 flakes shown in (a).

Synthesis science was supported by the Materials Sciences and Engineering Division, Office of Basic Energy Sciences, U.S. Department of Energy. A portion of the research was conducted at the Center for Nanophase Materials Sciences, which is sponsored at Oak Ridge National Laboratory by the Scientific User Facilities Division, Office of Basic Energy Sciences, U.S. Department of Energy.

Theoretical discovery of two-dimensional SiP alloys for energy conversion applications

Bing Huang, Mina Yoon, and Bobby Sumpter

Center for Nanophase Materials Sciences, Oak Ridge National Laboratory, Oak Ridge, Tennessee 37831, USA

Two-dimensional materials have great advantages over conventional bulk materials for various applications. The search of new earth-abundant 2D materials for energy conversion is of great interests, unfortunately, we do not have good candidates yet. Silicene and black phosphorus have recently attracted great attentions as new kind of 2D materials, but we do not have any knowledge of the possible stable 2D SiP alloys between them. In this study, we use the global structural search method to theoretically investigate the stable SiP structures with different stoichiometry and we find some SiP phases are very suitable for energy conversion applications, like photovoltaics and solid-state lighting. Our research opens a door for accelerating the discovery of novel earth-abundant materials for energy applications.

This work was supported by theme research at the Center for Nanophase Materials Sciences, which is sponsored at Oak Ridge National Laboratory by the Scientific User Facilities Division, Office of Basic Energy Sciences, U.S. Department of Energy.

Ultrafast spectroscopy and microscopy of exciton dynamics in two-dimensional materials and heterostructures

Abdelaziz Boulesbaa*, Kai Wang, Masoud Mahjouri-Samani, Christopher Rouleau, Kai Xiao, Bing Huang, Mina Yoon, Bobby Sumpter, Alexander Puretzky, and David Geohegan

Center for Nanophase Materials Sciences, Oak Ridge National Laboratory

*boulesbaaa@ornl.gov

Here we describe capabilities and measurements at the CNMS on transient absorption spectroscopy (TAS) and microscopy of two-dimensional (2D) nanomaterials and their heterostructures, in order to understand the ultrafast dynamics of charge and energy propagation relevant to optoelectronics. Two-dimensional layered materials provide an ideal testbed to explore interfacial interactions and assembly, as they are computationally tractable, semitransparent, and amenable to optical and electron spectroscopies. In a TAS experiment, one laser pulse creates an exciton in the 2D material and after a controlled time-delay, a second weak but spectrally broad laser pulse measures the change in the absorption spectrum of the system – from which fundamental excitonic properties (e.g., lifetimes, binding energy, diffusion, dissociation) and effects of interfacial interactions (e.g., from substrates, adsorbates, quantum dots, etc.) can be inferred. Our TASM experiments provide sub-50 femtosecond temporal resolution, and cover the spectral domain from UV to NIR for both excitation and probe. We are currently developing microscope-based approaches for transient pump-probe absorption and reflection spectroscopy using 40-fs pulses of tunable laser light and photogenerated white light continuum. To understand the ultrafast photogeneration and separation of carriers at interfaces crucial to optoelectronic applications, two microscopes will probe both interband (vis-UV) and intraband (IR) absorption of light in order to reveal the generation and dynamics of excitons within ~μm spatial regions in 2D crystalline nanosheets, polymers, quantum dots, and their heterostructures.

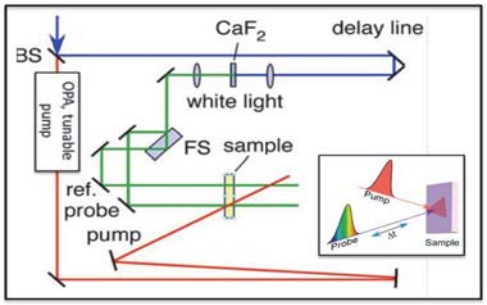

Schematic of sub-50 fs resolution pump-probe spectroscopy setup at CNMS used to understand exciton dynamics in 2D layered materials and heterostructures.

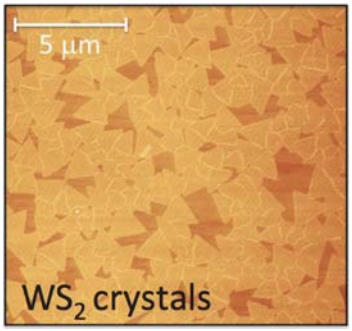

AFM of ensemble of monolayer WS_2 crystals on sapphire grown by CVD used for TAS expts.

Here we will focus on ultrafast TASM experiments to reveal exciton dynamics in tungsten disulfide (WS_2) monolayers resulting from excitation with different photon energies. Our results suggest that photoexcited excitons relax through different pathways depending on the excitation energy. Furthermore, we examined the charge and/or energy exchange between photoexcited 2D monolayers and semiconductor quantum dots (0D). The ability to control the dynamics of excitons at the interface of 2D materials and other confined nanostructures, such as semiconductor quantum dots may open the perspective for new applications in photosensing and photovoltaics.

This research was conducted at the Center for Nanophase Materials Sciences, which is sponsored at Oak Ridge National Laboratory by the Scientific User Facilities Division, Office of Basic Energy Sciences, U.S. Department of Energy.

Adsorption of a Hydrogen Atom on a Graphene Flake Examined with Quantum Trajectory/Electronic Structure Dynamics

Lei Wang and Sophya Garashchuk
Department of Chemistry and Biochemistry,
University of South Carolina, Columbia, SC 29208
Jacek Jakowski
National Institute of Computational Sciences,
University of Tennessee, Oak Ridge, TN 37831
Bobby G. Sumpter
Center for Nanophase Materials Sciences and Computer Science and Mathematics Division, Oak Ridge National Laboratory, Oak Ridge, TN 37831

Abstract

Adsorption of atomic hydrogen colliding with $C_{37}H_{15}$, a planar 'flake' of graphene, is examined using a hybrid quantum trajectory/electronic structure (QTES) dynamics for the values of the collision energies below 2.0 eV. The entire system of 53 atoms is represented by a quantum trajectory ensemble. The quantum correction on dynamics is included for the adsorbing hydrogen. The electronic structure is computed on-the-fly using the Density Functional Tight Binding (DFTB) method. The highest probability of adsorption is obtained for the kinetic energy of incident hydrogen in the range from 0.1 to 0.9 eV. Adsorption mechanism involves transfer of the collision energy to the graphene flake and projection of the carbon atom of the forming CH bond, accompanying sp^3 hybridization of orbitals. The QTES-DFTB simulations with and without the quantum correction show that localization of the proton wavefunction and details of the mixed quantum/classical description of light and heavy nuclei greatly influence the adsorption probabilities.

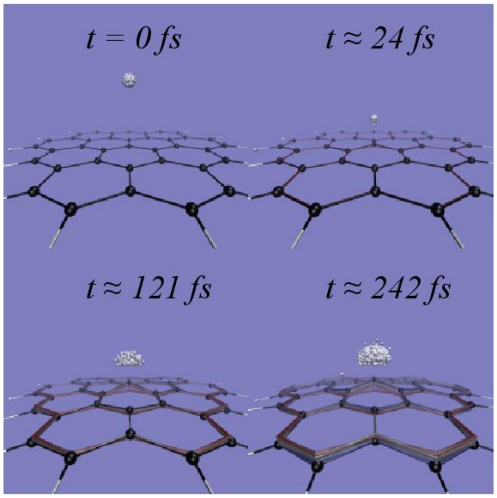

FIG 1: A quantum hydrogen (represented as a swarm of particles) in collision course with the carbon atom of the graphene flake. The relative displacement of carbon network (comparing to t = 0 fs) in response to interaction with incoming hydrogen is shown as silver/gray bonds (past frames).

Garashchuk, S.; Jakowski, J.; Wang, L.; Sumpter, B. G. A Quantum Trajectory-Electronic Structure Approach for Exploring Nuclear Effects in the Dynamics of Nanomaterials, *J. Chem. Theory Comput.* **2013**, 9, 5221–5235.

Thickness Dependence of Electrical Transport in Few-Layer Two-Dimensional Crystals

Ming-Wei Lin[1], Ivan Kravchenko[1], Jason Fowlkes[1], Jiaqiang Yan[2], Xufan Li[1], Alexander A. Puretzky[1], Christopher M. Rouleau[1], David Mandrus[2], David Geohegan[1], and Kai Xiao[1*]

[1]*Center for Nanophase Materials Sciences, Oak Ridge National Laboratory*
[2]*Department of Materials Science and Engineering, University of Tennessee, Knoxville*

I. INTRODUCTION

Two dimensional (2D) layered materials beyond graphene have attracted much attention recently for their diverse electrical and optical properties. Molybdenum disulfide (MoS_2) with direct bandgap 1.8eV of single layer has emerged an alternative of graphene and been widely studied for applications. Several mechanisms[1,2] have been proposed to explain the correlation between mobility and thickness change. However, the transition temperature of mobility with thickness has not been studied thoroughly and mechanism remains unclear. In addition, MoS_2 has been fabricated as phototransistors[3] for application, paving a way to explore more light sensitive 2D layered materials.

II. MAIN RESULTS

The single and few-layer MoS_2 flakes were deposited onto Si/SiO_2 substrates using exfoliation method as shown in AFM images (Figure 1 top). The MoS_2 field effect transistors (FETs) were fabricated using e-beam lithography, followed by metal deposition with Ti (5nm)/Au (30nm) shown also in Figure 1 top. Typical transport characteristics with temperature were measured in vacuum and mobility was extracted from the linear region of those curves. The mobility of MoS_2 FET exceeds $100 cm^2V^{-1}s^{-1}$ at low temperatures. Based on the calculated mobility for MoS_2 devices with different thickness, we found that the transition temperature of mobility increases as thickness increases (Figure 1 center), which is possibly attributed to the strong effect of Coulomb scattering or weakened in-plane electron-phonon interaction. The metal-insulator transition behavior was observed below 7-nm-thick MoS_2 (Figure 1 bottom). In addition, 2D layered materials such as WSe_2 and $MoSe_2$ have shown highly sensitive to the light (Figure 1 bottom), providing the potential applications for photodetectors or optoelectronic devices.

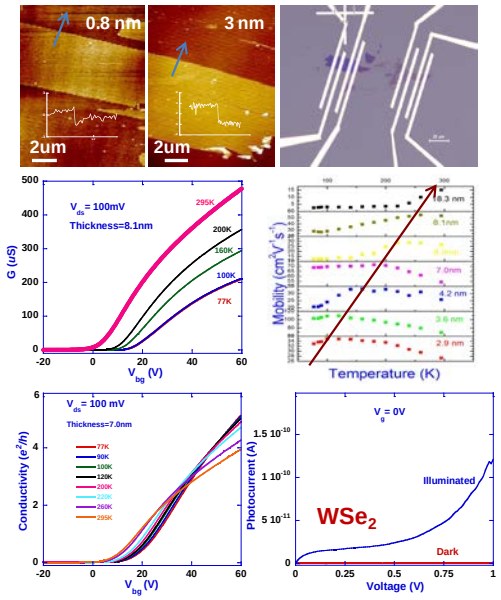

Figure 1. (top) The AFM images and micrograph show the thickness of MoS_2 flakes by exfoliation and device fabrication by e-beam lithography, respectively. (center) The transport curves with temperatures of MoS_2 FET on the left and the correlation between the transition temperature of mobility and MoS_2 thickness on the right. (bottom) The metal-insulator transition at 7-nm-thick MoS_2 device on the left and photocurrent of WSe_2 device when illuminated with white light on the right.

Acknowledgement: This research was conducted at the Center for Nanophase Materials Sciences, which is sponsored at Oak Ridge National Laboratory by the Scientific User Facilities Division, Office of Basic Energy Sciences, U.S. Department of Energy. M.W.L and X.F.L acknowledge the support by LDRD.

REFERENCES

[1] Radisavljevic, B. and A. Kis, *Mobility engineering and a metal–insulator transition in monolayer MoS_2*. Nat Mater, 2013. **12**(9): p. 815-820.
[2] Qiu, H., et al., *Hopping transport through defect-induced localized states in molybdenum disulphide*. Nat Commun, 2013. **4**.
[3] Yin, Z., et al., *Single-Layer MoS_2 Phototransistors*. ACS Nano, 2011. **6**(1): p. 74-80.